# Cutting - edge Neurosurgical Technology: Working Towards New Surgical Strategies In Pediatric Neuro-oncology

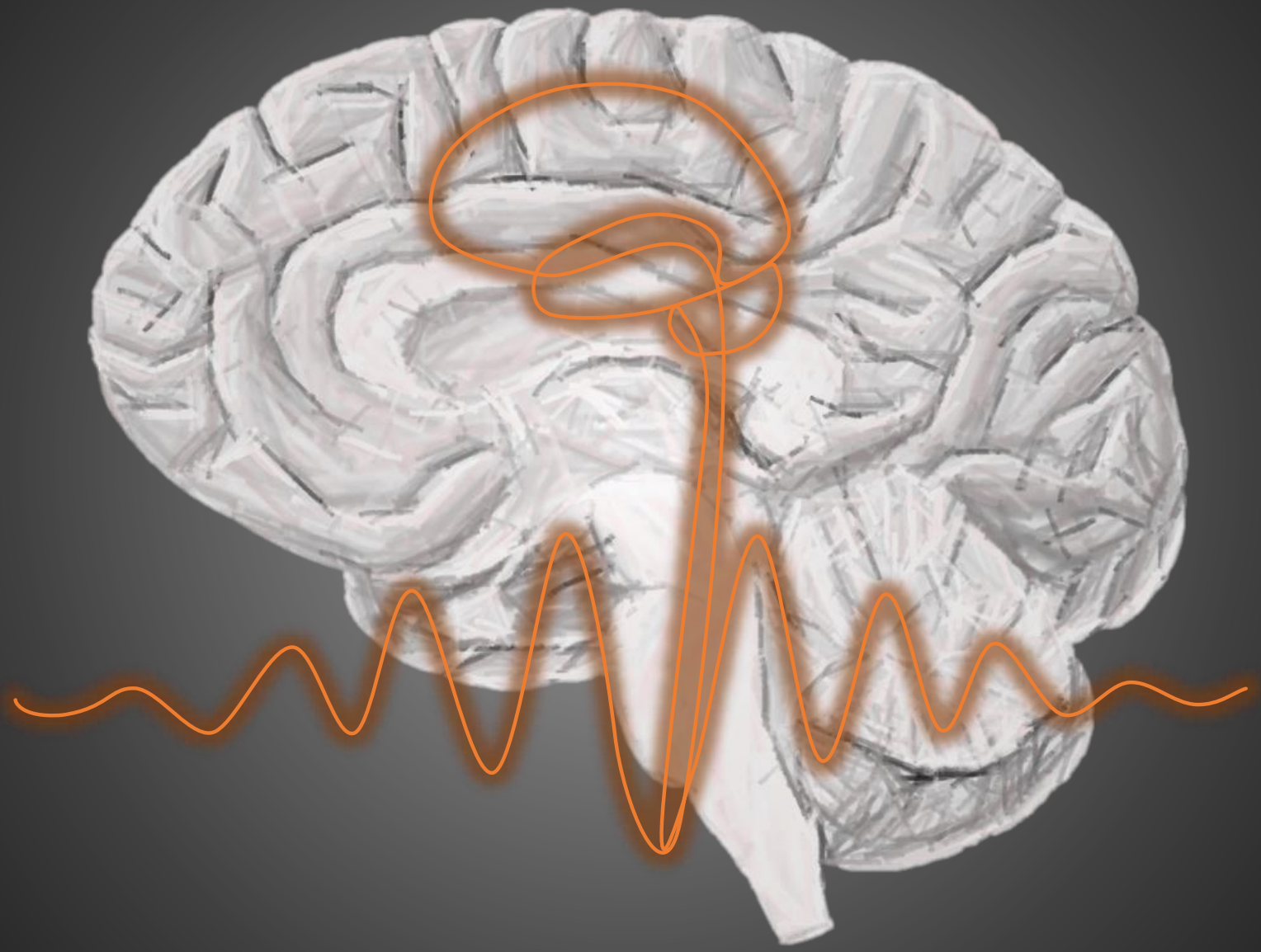

K. Klein Gunnewiek

Master Thesis Technical Medicine

Medical Imaging and Interventions

2023

Master Thesis

# Cutting-edge Neurosurgical Technology: Working Towards New Surgical Strategies in Pediatric Neuro-oncology

**K. Klein Gunnewiek**

A thesis submitted in partial fulfillment
of the requirements for the degree of Master of Science

in

Technical Medicine
Master track: Medical Imaging and Interventions
Faculty of Science and Technology
University of Twente

September 2023

Princess máxima center
pediatric oncology

UNIVERSITY OF TWENTE.

# Graduation Committee

| | |
|---|---|
| **Chairman:** | Prof. dr. ir. B. ten Haken<br>Magnetic Detection & Imaging<br>Faculty of Science and Technology<br>University of Twente, Enschede |
| **Clinical Supervisor:** | dr. K.M. van Baarsen<br>Pediatric Neurosurgery<br>Department of Neuro-oncology<br>Princess Máxima Center for Pediatric Oncology, Utrecht |
| **Technical Supervisor:** | dr. ir. W.M. Brink<br>Magnetic Detection & Imaging<br>Faculty of Science and Technology<br>University of Twente, Enschede |
| **Process Supervisor:** | dr. M. Groenier<br>Technical Medicine<br>Faculty of Science and Technology<br>University of Twente, Enschede |
| **External Member:** | dr. ir. A.M. Leferink<br>Applied Stem Cell Technologies<br>Faculty of Science and Technology<br>University of Twente, Enschede |

# Acknowledgement

# Abstract

**Purpose:** Gross surgical resection of pediatric brain tumors remains difficult due to difficult visualization of tumor tissue boundaries. Therefore, several novel technical modalities have been introduced to the neurosurgical operating theatre. Ideally, every technical modality is optimally implemented in the surgical workflow to make the surgical procedure more efficient, effective and safer. Additional intraoperative information can both support and complicate the surgical workflow. This study focuses on identifying the optimal usage of technical modalities. Besides, this study determines the diagnostic value of navigated intraoperative ultrasound (iUS) in visualizing tumor and residual tumor.

**Methods:** In the first part of this study, a survey research was conducted to determine the usability of intraoperative technical modalities. Every modality was given a Likert-score and technical problems and best practices were identified to propose guidelines for optimal modality usage. In the second part of the study, the diagnostic value of navigated iUS was determined as compared to intraoperative MRI (iMRI). Segmentations were created in iUS and iMR images from before and after tumor debulking. The quantitative metrics for segmentation analysis were Dice similarity coefficient (DSC), Hausdorff distance (HD) 95$^{th}$ percentile, and absolute volumetric differences. Besides, the sensitivity and specificity of iUS in detecting residual tumor were determined based on clinical assessment.

**Results:** Based on the survey results, differences in modality usage between prone and supine patient positioning were found. Two guidelines have been proposed, however the multifactorial character of every individual procedure complicates generalization of modality usage. Intraoperative image acquisition showed to have benefit in most procedures. Navigated iUS showed a high sensitivity (100%) and specificity (80%) in detecting residual tumor. A moderate DSC of 0.61 (IQR: 0.17), a median HD 95$^{th}$ percentile of 5.84 mm (IQR: 2.56 mm), and a median absolute volume difference of 0.82 cm$^3$ (IQR: 1.87 cm$^3$) were found for post resection tumor volume. For pre-resection tumor visualization, a good DSC of 0.71 (IQR: 0.11), a median HD 95$^{th}$ percentile of 4.61 mm (2.06 mm), a high volumetric correlation with iMRI (R=0.996) and median absolute volume difference of 1.28 cm$^3$ (IQR: 2.50 cm$^3$) were found.

**Conclusion:** This study showed the differences in optimal technical modality implementation between prone and supine procedures. Moreover, this study demonstrated that navigated iUS has good diagnostic value in detecting tumor tissue during surgery. It was found that navigated iUS showed to be a good alternative if the current gold standard iMRI is not available.

# Table of Contents

**I Introduction** 1

Research aim 1

Research objectives 2

**II Clinical Background** 3

I. Pediatric brain tumors 3

II. Clinical presentation and pathophysiology 3

III. Surgical management of tumors 5

**III Technical Background** 9

I. Technical OR modalities of the Neuro OR suite 9

II. Technical background intraoperative Ultrasound 19

**IV Evaluation of advanced surgical techniques in Neuro OR Suite** 23

General findings 26

I. Planning 27

II. Intraoperative Acquisition 29

III. Navigation 32

IV. Visualization 34

**V Illustrative intraoperative ultrasound cases in pediatric oncological neurosurgery** 45

**VI Diagnostic value of navigated intraoperative ultrasound in pediatric oncological neurosurgery** 51

**VII General discussion** 71

**VIII General conclusions** 73

**IX Bibliography** 74

**X Appendices** 80

# List of Abbreviations

| Abbreviation: | Definition: |
|---|---|
| AEA | Acoustic Enhancement Artifact |
| CR | Contrast Ratio |
| CSF | Cerebral Spinal Fluid |
| DICOM | Digital Imaging and Communications in Medicine |
| DSC | Dice Similarity Coefficient |
| EM | Electromagnetic |
| EoR | Extent of Resection |
| FoR | Frame of Reference |
| FOV | Field of View |
| GTR | Gross Total Resection |
| HD | Hausdorff Distance |
| HUD | Heads-up Display |
| IGS | Image Guided Surgery |
| iMRI | Intraoperative Magnetic Resonance Imaging |
| iNM | Intraoperative Neuromonitoring |
| IQR | Interquartile Range |
| iUS | Intraoperative Ultrasound |
| iUS1 | Navigated Intraoperative Ultrasound swipe made before dura opening |
| iUS3 | Navigated Intraoperative Ultrasound swipe made after tumor debulking |
| MEPS | Motor Evoked Potentials |
| MRI | Magnetic Resonance Imaging |
| OR | Operating Room |
| SD | Standard Deviation |
| SR | Surgical Resection |
| SSEPS | Somatosensory Evoked Potentials |
| T1-w/ T2-w | T1-weighted/ T2-weighted |

# I

# Introduction

Pediatric central nervous system tumors are the second most occurring cancers in children, with a described incidence rate of 5.67 per 100,000 person-years [1]. Brain tumors are known for having a poor prognosis and are the most common cause of death among all types of childhood cancers [1]. Gross surgical resection of tumor tissue without inducing major neurological deficits, remains the main treatment option in most brain cancer types [2]–[4]. Enlarging the extent of resection (EoR) is associated with prolonged survival, described for both the adult and pediatric patient population [5]–[8]. Therefore, surgeons are striving to achieve a gross total resection (GTR).

Gross total tumor resection is often hard to achieve, because intraoperative definition of tumor-tissue boundaries remains a challenge. Tumor tissue might be very similar to normal brain tissue under the surgical microscope. The surgeon always has to find the optimum between maximal tumor reduction and preservation of neurological function. To support the surgeon in achieving a gross total resection more effectively, efficiently and safely, several novel technical modalities have been added to the neurosurgical armamentarium.

In November 2022, the Princess Máxima Center for pediatric oncology in Utrecht has opened a high-tech hybrid Neuro OR suite. The wide range of modalities to choose from during surgery massively increased, which led to an increase in complexity. Complexity requires attention, investment, experience and knowledge. Introduction of new modalities does not automatically lead to optimal implementation and integration in an existing working environment and could even become a burden on the surgical procedure. Therefore, the aim is to improve and innovate current surgical treatment options for pediatric brain tumors.

## Research aim

The aim of this thesis is to establish a basis for research focusing on improvement and innovation of the technical modalities involved in pediatric neurosurgery in the hybrid Neuro OR suite. This suite facilitates the connection between advanced technology and neurosurgery. Techniques as intraoperative magnetic resonance imaging (iMRI) and intraoperative ultrasound (iUS) are available during surgery, creating many new possibilities to explore novel surgical strategies.

These new possibilities potentially improve both short and long-term patient outcomes. In the short-term, the recent advancements could potentially prevent children from undergoing additional surgical procedures. In the long-term, we hope to improve prognosis and possibly curate all children with brain tumors. Besides, we hope to decrease surgical sequelae and improve overall quality of life.

## Research objectives

This thesis is divided into two parts. The first part covers the usage of all technical modalities in the novel Neuro OR Suite. The aim is to work towards improving surgical treatment with advanced technology. Therefore, research objectives of the first part are defined as follows:

i. To identify the role of individual technical OR modalities
ii. To identify practical challenges and explore best practices of technical OR modality usage
iii. To define initial guidelines in deploying new technical modalities in the Neuro OR suite effectively

During the first part of this thesis, the role of intraoperative ultrasound was identified and the modality showed potential in optimizing the surgical workflow. Therefore, the second part of this thesis focuses on the role of intraoperative ultrasound in neurosurgical procedures within the pediatric population. The research objectives defined for this second part are:

i. To show the potential of unnavigated intraoperative ultrasound in pediatric neurosurgery.
ii. To quantify the diagnostic value of navigated intraoperative ultrasound in detecting brain tumors before tumor debulking as compared to preoperative MRI.
iii. To find the sensitivity and specificity of navigated intraoperative ultrasound in detecting residual tumor tissue as compared to intraoperative MRI.
iv. To quantify the diagnostic value of navigated intraoperative ultrasound in detecting residual tumor tissue as compared to intraoperative MRI.

The ultimate goal of this thesis is to contribute to better understanding and implementation of technical modalities that support the treatment of pediatric brain tumors to achieve the mission of the Princess Máxima Center: '*To cure every child with cancer, with optimal quality of life*'.

# II

# Clinical Background

## I. Pediatric brain tumors

Pediatric central nervous system tumors are the second most occurring cancers in children, with a described incidence rate of 5.67 per 100,000 person-years [1], [9], [10]. Brain tumors are known for having a poor prognosis and are the most common cause of death among all types of childhood cancers [1]. One in four children with a brain tumor does not survive the disease.[9] The clinical presentation of the disease depends on different factors, like location and size of the tumor, age of the child and rate of tumor progression. Supratentorial brain tumors are more prevalent in children aged between 0 and 3 years and older than 10 years. Children from 0 to 14 years have a higher incidence of embryonal tumors, whereas children from 15 to 19 years have more glial tumors. [1]

## II. Clinical presentation and pathophysiology

The clinical presentation depends on the age of the patient and location of the tumor.[11] Pediatric brain tumors are often more centrally located than brain tumors in the adult population. The peripherally located tumors in the adult population cause localized neurological deficits due to mass effect or cortical stimulation of tumor metabolites. Centrally located tumors pose a mass effect often causing obstruction of the flow of cerebral spinal fluid (CSF), this results in a rise of intracranial pressure leading to more non-localizing symptoms. [1], [11] The most frequent signs and symptoms of pediatric brain tumors that are reported at diagnosis are nonspecific like headaches, nausea and vomiting, which are reported in one third of the patient population. These symptoms can often be ascribed to an increased intracranial pressure, but are absent in more than half of children with brain tumors.[11] Depending on the location, more specific signs like abnormal gait and coordination, cranial nerve deficits and papilledema may be observed. Below, nonspecific and specific clinical symptoms are described for different tumor locations, where the brain tumors are divided into three categories: infratentorial tumors, central tumors and supratentorial hemispheric tumors. The location of the tumor highly affects the quality of life. Moreover, the surgical approach depends on the location of the tumor.

### Infratentorial tumors

Fifty percent of all pediatric brain tumors are located in the posterior fossa, of which pilocytic astrocytomas and medulloblastomas have the highest incidence.[1], [12], [13] Pilocytic astrocytomas are the most common type of low grade gliomas, comprising 17% of all pediatric brain tumors. Medulloblastoma is the most common malignant tumor, comprising 20% of all pediatric brain tumors. Tumors may grow extensively before being noticed, due to the elasticity of the brain. Signs and symptoms may arise once a tumor poses a larger mass effect on the surrounding tissues. In the posterior fossa these are the cerebellar tonsils, the brainstem and the fourth ventricle, see left image of figure 2.1 [14]. If a tumor grows in the fourth ventricle, the four CSF passages: aqueduct of Silvius, two lateral apertures of Luschka, and the medial aperture of Magendie may be obstructed.

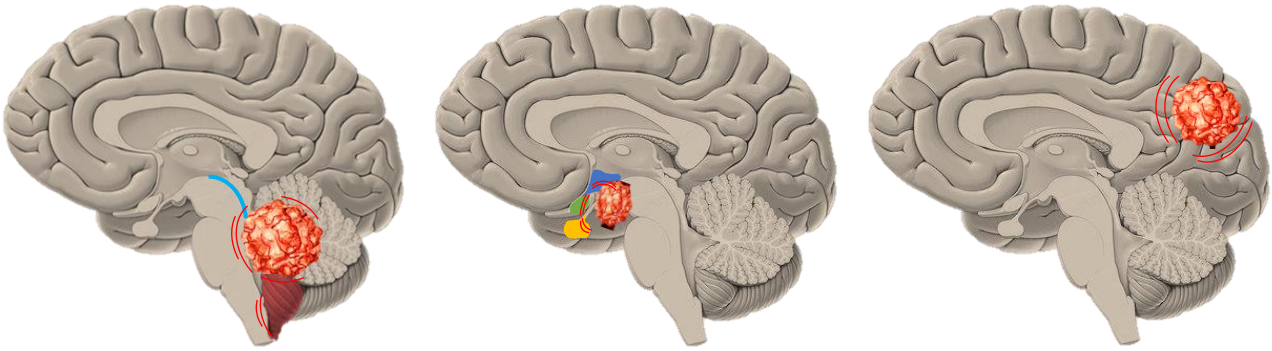

*Figure 2.1: Schematic visualization of three different tumor locations. Left image: tumor in the posterior fossa causing an obstruction hydrocephalus by blocking the Aqueduct of Sylvius (blue). The pressure built up and mass-effect of the tumor can cause the cerebellar tonsils to herniate through the foramen magnum (red). Middle image: central tumor in the suprasellar region exerting forces on the optic chiasm (green), pituitary gland and stalk (yellow) and the hypothalamus (blue). Right image: supratentorial convexity tumor causing stimulation and/or dysfunction of the local cerebral cortex resulting in focal neurological deficits. Modified image from Kenhub.com [12].*

This impedes CSF to flow from the cerebrum to the medulla, while CSF is continously being produced. This results in an intracranial pressure increase leading to obstruction hydrocephalus. A large tumor mass effect and pressure builtup may cause a severe condition called cerebellar tonsillar herniation, see left image of figure 2.1. Because of the pressure builtup, the cerebellar tonsils may be partially pushed through the foramen magnum posing great pressure on the medulla oblongata. Clinically, these patients are in a critical condition with signs of neck pain, dizziness and fatigue. Symptoms can worsen and eventually lead to coma, respiratory arrest and death. [15] Therefore, it is of great importance to directly intervene by inserting an external ventricle drain, to reduce the intracranial pressure. Other less life-threatening symptoms of posterior fossa tumors include cranial nerve deficits, e.g. facialis paresis, and gait and coordination abnormalities.

### Central tumors

Central brain tumors are located in the suprasellar, intraventricular, hypothalamic and thalamic regions and account for about 20% of the brain tumors in the pediatric population.[11], [13] Craniopharyngioma is an embryonic tumor in the suprasellar region specific to the pediatric population, comprising 5 to 10% of all pediatric tumors. [1] The signs and symptoms of centrally located tumors are related to the neighboring structures to which the tumor exerts a mass-effect upon. In the middle image of figure 2.1, a tumor in de suprasellar region is shown. In this region the pituitary gland and stalk (yellow), the hypothalamus (blue) and the optic chiasm (green) are situated. Forces exerted on this area may lead to dysfunction of the structures and pose endocrinological problems caused by diabetes insipidus and panhypopituitarism. Besides, ophthalmological problems are caused by compressive optic neuropathy. These symptoms include abnormal eye movements, squint and reduced visual acuity, which are reported in about one in five children with a central tumor [11]. Hypothalamic disorders result in behavioral and eating disorders, like obesity. Also central tumors can cause obstruction hydrocephalus, e.g. if the tumor compresses the foramen of Monroe.

### Supratentorial hemispheric tumors

Supratentorial hemispheric tumors encompass all intracranial neoplasms in the periphery of the cerebrum and account for about 30% of all pediatric brain tumors. The clinical presentation of these tumors is comparable to adult brain tumors. Seizures are most common (38%) for these tumors, followed by focal neurological signs (17%), hemiplegia is reported in 10% of cases. The specific nature of the seizures and focal deficits is caused by

cortical stimulation and hints towards the location of the tumor. Unspecified symptoms of raised intra cranial pressure are among the most commonly reported (47%). [11]

## III. Surgical management of tumors

The first main treatment option in management of pediatric brain tumors remains gross surgical resection of the tumor. Signs and symptoms related to raised intracranial pressure and compression of neurological structures can be stabilized or resolved by immediate pressure reduction. Surgery directly leads to a relieve of symptoms, but does not always curate the disease. The extent of resection (EoR) describes the amount of tumor tissue that could be surgically removed. Studies show that a higher EoR is associated with prolonged survival for high grade tumors and curation for low grade tumors. [5]–[8]

Surgical resection of a brain tumor is often a complex and intricate task to complete. Unlike other oncological surgical disciplines, a brain tumor cannot be excised by cutting in healthy functional tissue. Therefore, the surgeon needs to remove the tumor volume from the inside, working towards the boundaries. This is accomplished with several microsurgical instruments, used to mobilize the tumor at the boundaries and reduce the bulk of the tumor; a visual representation of this procedure is presented in figure 2.2 [16]. As depicted in the illustration, a craniotomy is performed at the location of the planned surgical trajectory. The size of the craniotomy restricts the surgeon from obtaining a broad anatomical overview, thus forcing the surgeon to navigate upon smaller visible structures.[17] The location of the craniotomy and the surgical approach depend on the location of the tumor. Below, four surgical approaches are further elaborated upon: convexity tumor, midline suboccipital, pterional, and interhemispheric transcallosal approaches.

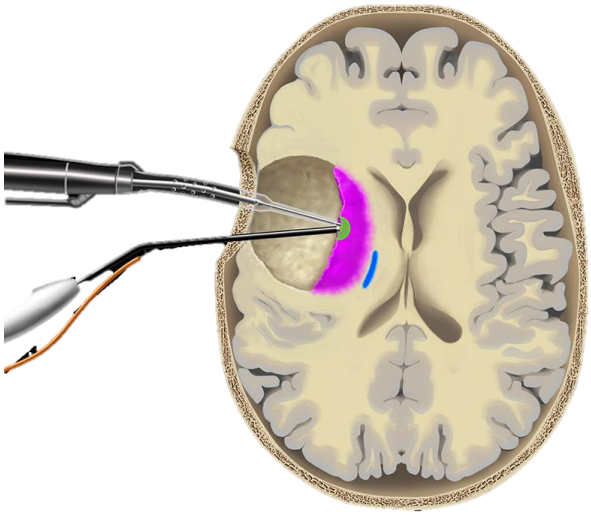

*Figure 2.2: Schematic visualization of tumor debulking procedure. The tumor is removed from the inside using microsurgical instruments. The image shows the surgical approach for a convexity tumor. Image is retrieved from Neurosurgery Wiki. [16]*

### Convexity tumor approach

For supratentorial convexity tumors, a craniotomy is performed at the point closest to the surface of the tumor or where the surgical trajectory will not damage eloquent areas. The patient is positioned accordingly, with the craniotomy oriented upward. Figure 2.2 illustrates a case where a craniotomy is made in close proximity to the tumor. The size of the craniotomy is sufficiently large to provide a comprehensive view of the entire extent of the tumor. Superficially located tumors are the most accessible without posing a significant risk of causing major neurological deficits.

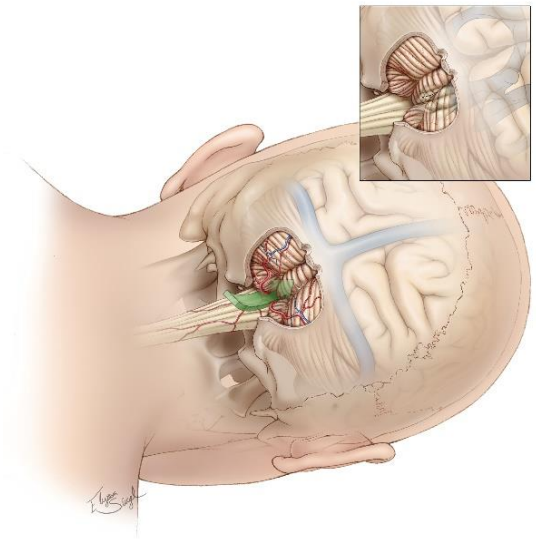

*Figure 2.3: Schematic visualization of midline suboccipital approach. The green arrow shows the telovelar approach to access the fourth ventricle. Image is retrieved from Neurosurgicalatlas.com [18].*

## Midline suboccipital approach

All posterior fossa tumors are approached via a craniotomy in the midline suboccipital region. In our center, the patient is always positioned in prone position with the neck flexed to gain optimal access to the suboccipital region. A craniotomy is made below the sagittal sinus, sometimes a part of the Atlas C1 vertebra is removed to enlarge the surgical entry (left image of figure 2.3 [18]). A telovelar approach is common to gain access to tumors in the fourth ventricle (shown in green). During surgery, manipulation of the brain stem could cause sudden blood pressure alterations or bradycardia. These potential complications need to be taken into consideration for determining the EoR in these procedures. [19]

## Interhemispheric transcallosal approach

Depending on the location of central tumors, a surgical access can be created via the corpus callosum or via the skull base. For a interhemispheric transcallosal approach, a craniotomy in the sagittal midline is created. The patient's head is tilted to the right, so gravity will help in gaining access. The falx cerebri can be used to support the dominant left hemisphere, while the right hemisphere shifts downwards creating an anatomical access to the corpus callosum, (see right image of figure 2.3 [20]). The deeper the lesion is situated, the more the maneuverability of the surgical instruments is restricted. Therefore, only a small part of the anatomy is accessible, increasing the complexity of finding and debulking the tumor. The orientation in the cavity is based on the morphology of the structures that create anatomical contours in the lateral ventricle. A small incision in the corpus callosum will not directly result in major neurological complications. However the deep nuclei and the limbic system structures are very delicate that may cause severe complications if damaged. [21]

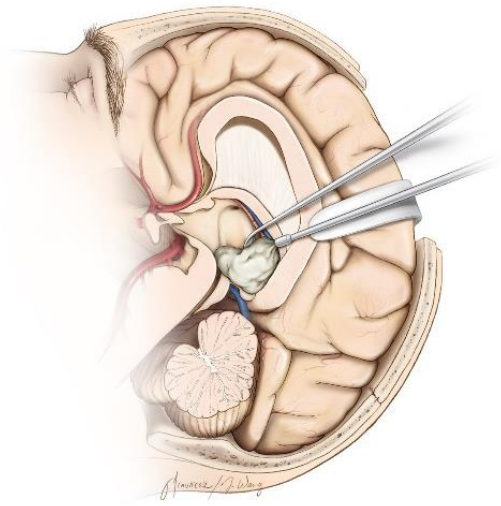

*Figure 2.4: Right image: interhemispheric transcallosal approach with surgical instruments removing a deeply seated tumor. Image is retrieved from Neurosurgicalatlas.com [20].*

## Pterional approach

Another approach to access central tumors is via the skull base, this approach is called pterional (around the pterion, see left image of figure 2.4 [22]). Deeply seated suprasellar tumors can be accessed via this approach. The size of the craniotomy is typically largest for pterional approaches. Also in this approach, the range of motion decreases with increasing depth, complicating the tumor debulking process.[17] Although this approach is rather anatomically guided by following the anatomical space between the skull base and the frontal lobe. Eventually the optic chiasm and internal carotid arteries become exposed (see right image of figure 2.4 [22]). These eloquent structures play an important role in guiding the surgeon towards the tumor location, but will also complicate the procedure. It is of utmost importance that these structures remain intact, so the surgeon will always refrain from excessively mobilizing these structures. Besides the limited range of motion, the line of sight is also limited. This complicates the procedure and could result in unintentionally leaving a tumor remnant in situ.

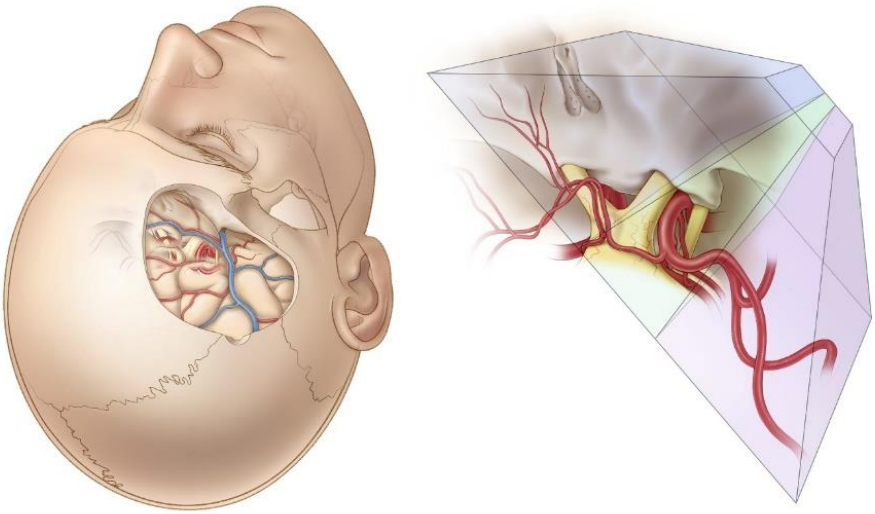

*Figure 2.4: Schematic visualization of pterional approach. Left image: shows large craniotomy around pterion, exposing the frontal lobe and skull base. Right image: shows exposure of the second and third cranial nerves and the internal carotid arteries, after following the anatomical route along the skull base. Image is retrieved from Neurosurgicalatlas.com [22].*

## Postoperative neurological complications

In oncological neurosurgery, the surgeon constantly needs to determine whether additional tumor can be safely resected. The balance between additional resection and the risk for neurological deficits needs to be constantly evaluated, depending on the location and extension of the tumor. Based on the optimal balance, the surgeon adopts a more or less aggressive approach in removing tumor tissue. The postoperative neurological complications that may arise can pose a significant impact on the quality of life of the patient.

Convexity tumors are better accessible and are more often located in non-eloquent areas, decreasing the risk for postoperative neurological complications. If complications occur, focal neurological deficits and seizures ascribed to the tumor location are reported. [23]

Central tumors are more difficult to resect, because of the depth of the tumor and the close vicinity of eloquent structures. Vasospasms may occur, affecting overall perfusion of the brain. Moreover, the optical tract could be damaged resulting in postoperative ophthalmological complications. Endocrinological complications may arise if the hypothalamus and/or pituitary gland are affected. Especially in resecting a low grade tumor, radical resection is key for curation, but could induce severe complications that have a major impact on the patient's quality of life. [5], [23]

Regarding posterior fossa tumors, the location of tumor adhesion is important for the EoR. GTR is not possible if the tumor is attached to the brainstem, the potential risk of damaging the brainstem does not outweigh the oncological benefit of removing the last remnant. Furthermore, cranial nerves can be impacted, potentially causing conditions such as paresis of the facial nerve, for instance. Facial nerve paresis is most prevalent for tumors in the posterior fossa, of which a significant part is still existent after 30 days. [23] Moreover, manipulation of the cerebellum could result in cerebellar mutism syndrome after surgery. [23][24]

In some cases, the described neurological complications may have been preexistent and caused by the tumor. However, in some cases preexistent complications progress or new complications arise due to surgery. Some of the complications may be transient, but others will be permanent, thereby changing the patient's life irreversibly. It is therefore of great importance to always strive for the optimal EoR, balancing between prognosis and quality of life. Every additional source of information regarding the tumor-tissue boundary could potentially benefit the surgical outcome. In recent years, many new technologies have been introduced to the neurosurgical operating theatre, aiming to optimize the surgical outcomes by maximizing the EoR and minimizing postoperative complications.

# III

# Technical Background

In November 2022 the Princess Máxima Center for pediatric oncology opened a novel Neuro OR suite dedicated to neurosurgical procedures. With the opening of the OR suite, numerous novel intraoperative technical modalities were introduced. These modalities all have different roles in the procedure and have different applications. In this chapter a more elaborate technical background regarding these modalities is provided in two sections.

In the first section, the eleven technical modalities of the neuro OR suite are explained and background information is provided. The role of these technical modalities is evaluated in a survey study described in Chapter IV. The first section provides an overview to understand the details of the different modalities.

In the second section, a more detailed explanation of navigated intraoperative ultrasound (iUS) is provided. The section covers the role of iUS in neurosurgery, the fundamental physical principles of iUS, and how it is integrated with neuronavigation. This background knowledge is necessary for understanding Chapters V and VI.

## I. Technical OR modalities of the Neuro OR suite

A schematic overview of the Neuro OR suite is provided in figure 3.1. The suite consist of an operating room (left in image) and a MRI scanning room (right in image). Most modalities are positioned around the OR table. For clarity, the eleven OR modalities are divided into four categories: 'Planning', 'Acquisition', 'Navigation', and 'Visualization', see also the description of figure 3.1.

### Planning

Before the start of every procedure, a surgical plan is made based on the preoperative imaging data. The imaging data usually consists of different T1- and T2-weighted Magnetic Resonance Imaging (MRI) sequences. These images are used to plan the surgical approach, to determine the location and volume of the tumor and to identify eloquent structures. The plan and the images are used during the procedure to help the surgeon work towards the planned surgical goal. In the OR, the plans can be adjusted and new images can be added with the network based central information hub (Buzz, Brainlab, Munich), depicted in figure 3.1 in yellow. Eventually, the plan and images can be used for neuronavigation. The two modalities that are involved in preparing the procedure before incision are image fusion and image registration.

#### *Image Fusion*

Before, during and after surgery, additional imaging helps in evaluating the anatomical situation. The anatomy is constantly changing as tumor debulking progresses. The images that are acquired with iUS or different MRI

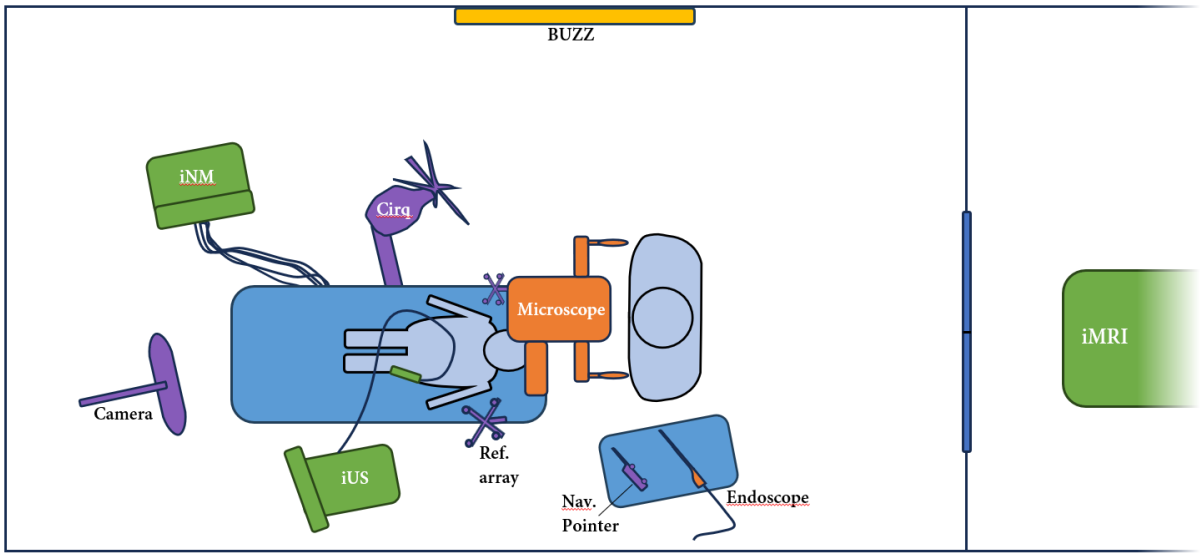


*Figure 3.1: Schematic overview of Neuro OR suite with the iMRI scanning room separated from the operating room. The operating table is visualized in the middle of the image in blue. The modalities are categorized in Planning (yellow), Acquisition (green), Navigation (purple), and Visualization (orange). The overview shows the position of all modalities in the OR. Depending on the procedure, only a selection of these modalities is used.*

sequences. To assess the debulking progress, slice-to-slice comparison of these images is important. In order to compare the images per slice, the images need to be transformed to the same reference space. Finding this transformation is done with the modality image fusion.

The modality image fusion is based on global image transformation, which means that the transformation affects the image in all points equally. An image is a collection of three dimensional points (voxels) with an intensity value, which can therefore also be transformed in its entirety to another spacing. [25] Imagine having two different images of the same patient, scanned at different time points, visualized in Figure 3.2 with green and purple. One image is used as a parent (purple), and the other as a child (green). The child image needs to be transformed the parent image based on rigid image transformation. In rigid image transformation, a 4x4 transformation matrix describes the rotation, scaling and translation that is needed to transform every point (x, y, z) in the child image to (x',y',z') in the parent image, as described in equation 3.1. In this equation, the letters *a* and *t* describe the scaling/rotation and translation, respectively.

$$\begin{bmatrix} x' \\ y' \\ z' \\ 1 \end{bmatrix} = \begin{bmatrix} a_{11} & a_{12} & a_{13} & t_x \\ a_{21} & a_{22} & a_{23} & t_y \\ a_{31} & a_{32} & a_{33} & t_z \\ 0 & 0 & 0 & 1 \end{bmatrix} \begin{bmatrix} x \\ y \\ z \\ 1 \end{bmatrix} \qquad (3.1)$$

Before the transformation can be calculated, the transformation matrix needs to be determined. The software in the image fusion modality finds the optimal fit of the two images by maximizing the mutual information of corresponding voxel intensities. [26] The software performs multiple iterations to converge towards the optimal fusion of the two images. Once the result is accepted, a transformation matrix is stored by the system.

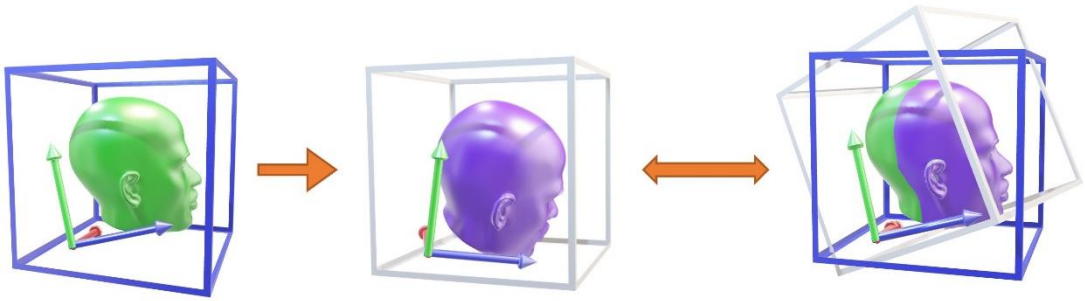

*Figure 3.2: Schematic visualization of image fusion. Two images, green and purple, are scanned in two different orientations. Image fusion finds the transformation matrix that transforms the green image to the purple image spacing, positioning both heads at the same position.*

By applying the transformation matrix, the child image is transformed to same reference space as the parent image, as shown in the right image of figure 3.2. Additionally planned objects or trajectories are also transformed accordingly, allowing for better interpretation of the surgical plan.

Once multiple image fusions have been performed, multiple transformation matrices are created. These transformation matrices can be easily combined by matrix multiplication. This creates one transformation matrix that provides the same results by applying all transformation matrices on the images consecutively. By using one matrix that describes the total transformation, less computational power and time is required. Moreover, transformation matrices can be easily inverted to get the backwards transformation; i.e. bringing the parent image to the child image reference spacing.

### *Image registration*

To couple the plans and transformed images to the intraoperative situation, the images need to be registered to the patient. Before the images can be registered, the Image Guided Surgery (IGS) setup needs to be prepared, as shown in figure 3.3. The patient's head needs to be fixed in a head frame, to which the optical reference array is mounted afterwards. This ensures that the position of the patient's head with respect to the reference array is constant for the entire procedure. Determining this relative position and relating this to the preoperative imaging is called image registration. Two common methods are available to perform this image registration.

The first registration method is based upon surface matching. For surface matching, the surgeon needs to define a number of anatomical landmarks, (e.g. nasion and lateral canthus), with a navigation pointer. Then, the surgeon defines the facial surface by scanning it with the navigated pointer. The software tracks the position of the pointer during this registration and creates a surface. This surface needs to be matched optimally with the surface of the skin on MRI, which is automatically retrieved from the imaging data. This registration method can be done optically (as shown in figure 3.3) and electromagnetically. Electromagnetic (EM) IGS is preferred when the head cannot be fixed in a frame, hence the setup is different. An adhesive array with fiducials is placed on the patient's forehead and an EM field generator and detector is positioned near the surgical field. An EM stylus is used similar to the navigation pointer in figure 3.3. The position of the stylus can be tracked and image registration based on surface matching can be performed in a similar fashion. In both optical and EM IGS, the surface matching method is more prone to errors. The registration accuracy depends on the quality of the scan

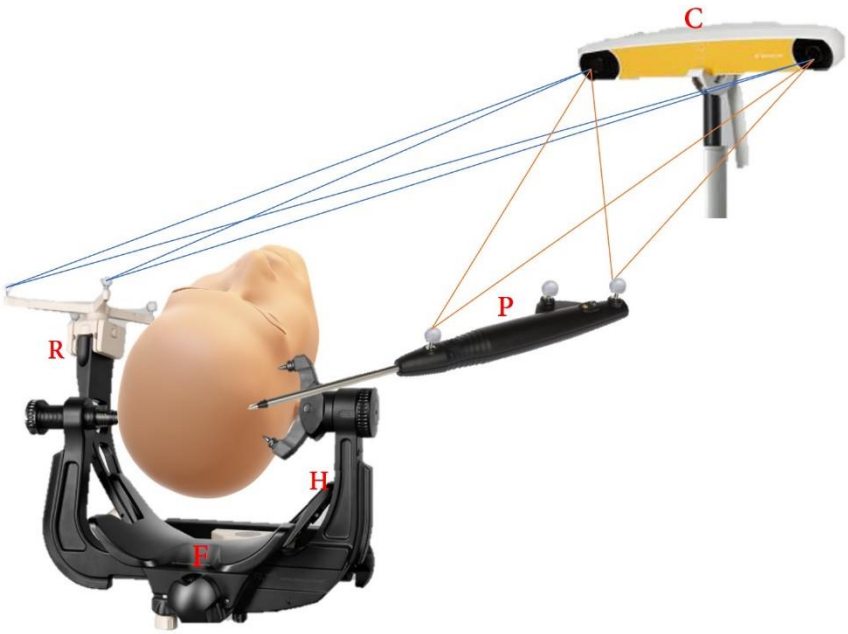


*Figure 3.3: Setup of optical image guided surgery. The patient's head is fixed in a headframe (H). The optical reference array (R) is mounted to the frame, ensuring a fixed position with respect to the head. A fiducial array (F) is placed when iMRI automatic registration is used. The navigation pointer (P) is used for tracking the location of the tip in the patient's head. The stereotactic camera (C) detects both the optical reference array and the navigation pointer, allowing visualization of the pointer's tip in the preoperative imaging.*

and the quality of the surface registration. The spatial accuracy tend to decrease with increasing distance from the registered surface. [27]

The second registration method is more accurate, as it is based on automatic registration with fiducials. The fiducials are incorporated in fiducial array which has a fixed position in the IGS setup, see figure 3.3. This array contains thirteen fiducials that are hyperintense on T1 weighted MRI. The fiducials have a specific configuration which can be automatically detected by the algorithm. The fiducials are schematically shown in purple in both images of figure 3.4. Since the fiducials are always in the same orientation and at the same position from the optical reference array, the software is able to automatically detect the fiducials and create a transformation matrix. This matrix describes the relation between the MR images (left image, fig. 3.4) and the physical IGS setup (right image, fig. 3.4). By using a navigation pointer, the position of the pointer relative to the reference array can be determined by the stereotactic camera. This allows the surgeon to find the location of the tip of the pointer in the MR image.

For all registration methods, the surgeon needs to validate the accuracy of the registration by checking several positions with the pointer. Once validated, IGS is ready to be used intraoperatively.

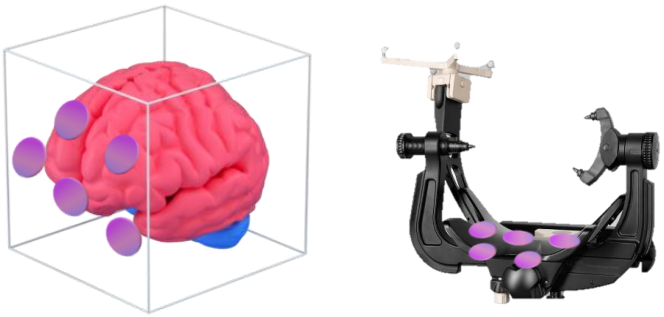

*Figure 3.4: Schematic overview of automatic registration based on iMRI. The fiducials (purple) in the fiducial frame are scanned and recognized by the registration software (left image). The registration is automatically done, because the reference array frame is always at a fixed position from the fiducial frame (right image).*

## Intraoperative Acquisition

Every neurosurgical procedure will result in changes of the anatomy and function of the brain. During a tumor debulking procedure, the optimal balance between extent of tumor resection and preservation of neurological function needs to be found. However, finding the optimal balance is difficult, because the anatomy is constantly changing due to surgery. To obtain more information regarding the changed anatomy and potential functional alterations, intraoperative acquisition techniques are introduced to the Neuro OR Suite. These acquisition techniques are based on measuring signals to create either images or obtain functional information. The additional information allows for monitoring the optimal balance between tumor removal and neurological outcomes, assuring effectivity, efficiency and safety during the procedure. In this section, two image acquisition techniques and a signal acquisition technique are explained. As shown in green in figure 3.1, iUS and iNM are available in the OR and can be freely positioned around the surgical field. Due to the strong magnetic field of the iMRI machine, it is necessary for the machine to be positioned in a separate room, as shown in figure 3.1.

### *Intraoperative Magnetic Resonance Imaging*

The most complex and innovative modality in the surgical workflow is the intraoperative MRI (iMRI). iMRI has two major roles in the intraoperative setting, namely for neuronavigation and for diagnostic purposes. The iMRI can be used to automatically register the imaging data with the real-world surgical setting. Second, iMRI can visualize residual tumor tissue, local ischemia or hemorrhages while surgery is still ongoing. This allows the OR team to assess whether the surgical goal has been reached.[28], [29]

In order to scan the patient intraoperatively, the patient needs to be transferred to the MRI table while being draped in sterile covers. This is a potential hazardous situation, where potentially hidden metal instruments can accidentally be drawn into the strong magnetic field of the MRI system. Therefore, strict precautions need to be taken during this transfer. [30]

Since the patient's head is still fixed in the head frame while scanning, it is not possible to employ a conventional close-fitting 32 channel head coil. Instead, two 1 channel flexible surface coils are positioned along the anterior and posterior side of the patient's head, as shown in figure 3.5. The posterior coil is placed between the patient's head and the fiducial frame. The anterior coil is placed on top of the sterile covers that cover the surgical field. It is important to note that the coils are freely movable between the scanning session, but will remain in place during a scanning session.

*Figure 3.5: Two flexible surface coils are placed anteriorly and posteriorly of the patients head, respectively. The posteriorly positioned coil will remain in place during the entire procedure, whereas the anteriorly placed coil is removed between scanning sessions. This allows for intraoperative MRI acquisition while the patient's head is fixed in a head frame.*

After coil positioning and patient transfer, a conventional imaging protocol is started. The protocol consists of T1 weighted, T2 weighted, T1 weighted gadolinium enhanced and diffusion weighted imaging. For further acquisition specifications, see Appendix 6C. The T1 and T2 weighted images are used by the surgeon to identify residual tumor tissue and obtain an update regarding the anatomy. The diffusion images are used to identify potential areas of ischemia. Depending on the procedure, additional sequences like fluid attenuated inversion recovery (FLAIR) or diffusion kurtosis imaging may be added to the imaging protocol.

### *Intraoperative Ultrasound*

The second acquisition technique to visualize the surgical field is intraoperative ultrasound (iUS). Setting up iUS acquisition requires little additional preparation, other than assuring sterility. The ultrasound transducer can either be sterilized, or draped in a sterile cover. Once sterile, the transducer can be directly placed on the cortical surface, dura or in a fluid-filled cavity. Depending on the field of interest, different imaging parameters need to be adjusted in order to obtain the optimal image quality.

Although iUS and iMRI have a common purpose, iUS has several advantages as compared to iMRI. A great advantage of iUS over iMRI is that iUS allows for real-time image acquisition. Second, iUS is a flexible and portable modality which can be easily used during surgery. This limits the need for potentially hazardous exploration of the resection cavity. The third benefit is the fact that iUS operates independently of any image-to-patient registration. Not all children are eligible to have their head fixed in the head frame, due to the presence of fontanelles at a young age. In this case, iMRI cannot be used to navigate upon, whereas iUS can be deployed without the need for image registration. [31]

On the contrary, iUS images are more difficult to interpret than conventional MR images. iUS images can be acquired in any image orientation, which is more difficult to interpret than the conventional orientation of image planes chosen in MRI.[32] To improve the interpretability, the transducer can be navigated during the procedure, allowing for integration of iUS images with MR images. Moreover, navigated iUS could update IGS to compensate for brain shift induced inaccuracies.[33]–[36] The integration of iUS with IGS is further explained in the second section of this chapter.

### *Intraoperative neuromonitoring*

Intraoperative neuromonitoring (iNM) is a modality capable of acquiring functional information intraoperatively. Nerve conductivity can be monitored during the surgery as a measure of the degree of nerve integrity. Electrodes are positioned at different locations to stimulate and measure the amplitude and latency of action potentials intraoperatively. Motor-evoked potentials (MEPs) are monitored for assessment of the descending cortico-spinal tracts. The motor cortex can be transcranially stimulated with electrodes over the scalp. The potentials can be recorded from needle electrodes which are placed sub-dermally in different muscle groups.[37] Somatosensory-evoked potentials (SSEPs) are monitored for the assessment of the dorsal pathways. Electrodes are placed near the posterior tibial nerve and the median nerve for stimulation. The signals can be recorded by electrodes placed in the scalp at the sensory cortex. SSEPs are continuously monitored, whereas MEPs are only stimulated occasionally.[37] Besides, cranial nerves can be monitored during infratentorial tumor debulking procedures. During these procedures, resection close to the brainstem is necessary, risking cranial nerve damage. To monitor the facial nerve intraoperatively, several needle electrodes are placed in the face to measure potentials by monopolar stimulation of the facial nerve in the posterior fossa. Signal changes during surgery may indicate injury of cranial or spinal nerves, even before any clinical symptoms would be present after surgery. This allows the surgeon to stop removing tissue without the risk of inducing neurological deficits. [37]

## Visualization

Neurosurgery is known for working through a narrow corridor while working with small and delicate structures. The human eye is not capable of focusing on such small structures for a long period of time. Therefore, magnification of the surgical field has improved the surgical achievements. Besides, illumination of the surgical field through a small corridor has also become indispensable in neurosurgery. The visualization techniques are meant to extend and improve the surgeon's vision. In figure 3.1 the visualization modalities are shown in orange.

### *Microscope*

The most important technical modality is the surgical microscope, shown in figure 3.7. The microscope allows the surgeon to zoom in on the small delicate structures of the brain and illuminate the surgical 'keyhole'. These major advantages have made the microscope indispensable in most of the microsurgical procedures for several decades. By using the microscope, more complex surgical goals can be achieved. [38]

### *Endoscope*

Besides the microscope, the endoscope plays an important role in minimal invasive surgery. An endoscope consists of different channels for illumination, camera and surgical instruments. It allows the surgeon to operate through a smaller hole while illuminating the surgical area. Endoscopy has some advantages compared to surgical microscopes: 1) increased light intensity, 2) extended viewing angle, and 3) high details of small structures in close-up. [17] The tool is often used for biopsies of intraventricular lesions or third ventriculostomies. This is desirable since a small and deep surgical corridor is needed, for which a small incision suffices. However, an important drawback of the endoscope is the inability of having two free hands. One hand will always stabilize the trocar, while the other can operate one instrument at a time. Moreover, once the endoscope is inserted, the field of view is small. This complicates the interpretation as compared to the surgical

microscope. The interpretability may be improved by integrating the endoscope with IGS. This improves positioning of the endoscope and the interpretation of the camera view.

### *Head-up display*

A new visualization technique is the Head-up display (HUD). This tool is an integrated visualization technique in the microscope based on IGS information. HUD allows information from the surgical plan to be superimposed in the microscopic view. This applies to objects like segmentations and reconstructed white matter tracts. The segmentations can be visualized as outlines, which allows the surgeon to see the planned objects at the corresponding location in the microscopic view. The outlines are actively updated when the microscope is moved, or the zoom is adjusted. An example of the HUD is shown in figure 3.9. The surgeon can intraoperatively see the contours of the tumor and the preoperatively reconstructed white matter tracts.

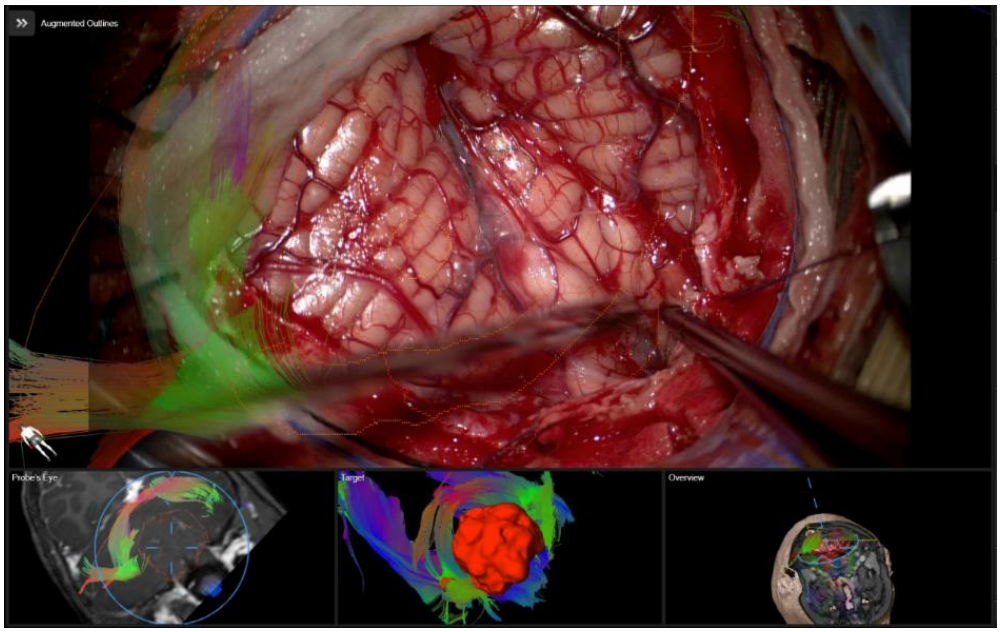


*Figure 3.6: Visualization of HUD and navigated microscope. In the top image, the vision through the microscope is visible. The surgeon sees the surgical field, the instruments and the projected objects; which represent white matter tracts and outlines. Below, the images on the left an right show the location of the microscope in the preoperative imaging. The middle image shows a three-dimensional visualization of the planned objects.*

## Navigation

Neuronavigation is a technical modality that has already been used in neurosurgery for decades, allowing for integration of imaging within the surgical process. [39], [40] Surgeons can more safely determine the location of the incision, eloquent structures and tumor by using Image Guided Surgery (IGS) [41], [42]. The usability of IGS highly depends on the spatial accuracy, which is affected by two factors. First, the accuracy of the navigation depends on the quality of the registration, which varies depending on the method. This type of inaccuracy can already be noted at the start of the surgery. Second, the navigation accuracy can also progressively decrease during surgery, due to changes in anatomy during surgery. While the neuronavigation is still registered to the preoperative imaging, brain shift occurs because of surgical manipulation and gravity. For this reason, the navigation becomes increasingly less reliable while surgery progresses. [36] In order to restore the accuracy for both scenarios, new intraoperative imaging is required, for which iUS and iMRI are used [29], [33]–[35], [43], [44].

Image guided surgery can be both EM and optically tracked. For practical reasons, optical tracking typically used. EM tracking tends to be more impractical, since the field generator needs to be close to the surgical field. Moreover, other surgical tools might interfere with the field, disabling EM navigation. [41], [42]

For optical tracking, arrays with reflective spheres are used for the stereotactic camera to determine the location. Every surgical instrument to which an array with reflective spheres can be attached, are optically trackable. In order for this to work, the line of sight with the camera needs to be unobstructed. This is sometimes challenging given the surgical setup. The instruments, reference arrays and camera are positioned at different locations around the surgical field, as shown in figure 3.1 in purple. The instruments that are frequently used for neuronavigation are further explained below.

### *Navigation pointer*

The navigation pointer is an optically or electromagnetically tracked instrument aiding the surgeon in navigating in the surgical field by showing the exact location of the tool tip in the registered and fused MR images. The optically tracked navigation pointer is annotated in figure 3.2 with P. When the pointer is moved in the surgical field, the camera determines and tracks the position of the tip. The location of its tip is then visualized in the preoperative imaging.

### *Navigated microscope*

Similar to the navigation pointer, the microscope can be optically tracked with an array, as shown in figure 3.6. The microscope is tracked with the same reflective spheres as the other instruments. This allows the surgeon to


*Figure 3.7: Surgical microscope integrated with the neuronavigation (R).*

see the line of sight of the microscope in the MR image and the deviation from a planned trajectory. By adjusting the focus of the microscope, the depth in the MR image is adjusted. This information is used for navigation in the surgical field, without the field being manipulated physically.

### *Cirq robotic biopsy arm*

The neuronavigation could also be used for image guided biopsies. Biopsies in the vital areas of the brain, like the brainstem are very perilous. The spatial margins in the brainstem are very small and the biopsy needle should be precisely placed in the lesion to avoid fatal complications. Without the navigation, a biopsy would not be as precise and therefore not possible, since there would be no information regarding the correct position of the needle. Cirq® (Brainlab, Munich, Germany) is a highly specialized robotic arm designed to precisely biopt by image guidance. Cirq is integrated with optical IGS and allows for accurate needle placement along a planned trajectory. The robotic arm ensures that the position of the biopsy channel matches the path of trajectory. The biopsy needle is optically tracked with reflective spheres, as shown in Figure 3.8. The spheres help in defining the position and depth of the needle after insertion along the trajectory. The system will automatically warn the surgeons if the needle deviates from the trajectory. Therefore, a highly accurate image registration is required to obtain the most precise biopsy. In future, the Cirq could potentially be used for precise local drug administration.

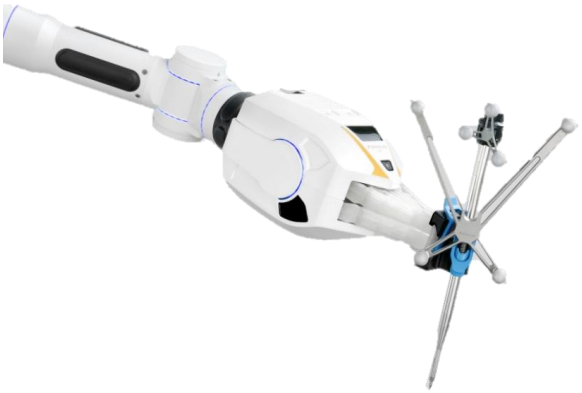

*Figure 3.8: Cirq robotic arm, navigated with reflective spheres. The biopsy needle is also navigated, allowing the surgeon to accurately localize the tip of the needle.*

# II. Technical background intraoperative Ultrasound

## Ultrasound in neurosurgery

Several techniques have been used to identify tumor tissue intraoperatively, of which intraoperative MRI (iMRI) and intraoperative ultrasound (iUS) play an increasingly important role. These techniques enable visualization of the tumor intraoperatively to be able to 1) assess whether the surgical goal is reached, 2) identify potential tumor remnants or 3) update the neuronavigation with newly acquired data. iMRI and iUS both have their advantages and disadvantages, iMRI is known to be a burden on the surgical workflow and a time- and resource-intensive modality. On the other hand, iUS is unable to create a synoptic view of the brain and the image quality is often inferior to MRI, hampering clinical interpretation.

The use of intraoperative ultrasound (iUS) in neurosurgery dates back to the early 1980s. In the first neurosurgical applications, iUS was already used for guiding the surgeon to the location of the tumor and to correct for brain shift. [44], [45] Most iUS devices are not dedicated to neurosurgical application and the spatial resolution is too low to image small delicate structures of the brain. Although the devices were significantly larger than nowadays, iUS has always shown to be a quick, versatile and non-invasive technique.

## Physics of Ultrasound

To understand the underlying principles and physical limitations of ultrasound imaging, a brief explanation of the physics of ultrasound is provided.

Ultrasound imaging is based on the physics of high frequency sound waves interacting between different tissue types. The high frequency ultrasound waves are created by applying an electric field across the surfaces of piezo-electric crystals. These crystals expand and shrink depending on the direction and amplitude of the electric field. This expansion and shrinkage forms mechanical waves that can propagate through a certain tissue type. Every tissue type has a unique acoustic impedance, which represents the resistance that a certain tissue opposes to an acoustic sound wave. If the density of a tissue type is high, it is harder for the acoustic wave to propagate; the acoustic impedance is higher. At a tissue boundary, there is an abrupt acoustic impedance difference. This difference results in a part of the acoustic wave being reflected and a part being transmitted. The greater the impedance difference at the interface, the more energy is reflected back to the transducer. This creates a larger contrast between the two tissue types. The reflected part that arrives at the transducer will mechanically deform the piezoelectric crystals that create an electric field. This electric signal and the corresponding echo time can be recorded. By acquiring different acquisition lines, an ultrasound image can be reconstructed (B-mode image). [46]

If the acoustic impedance of a structure is low, e.g. a cavity filled with fluid, few signal is reflected. This results in more signal left to interact with the interface of the bottom. The amount of signal reflected will be more at this depth compared to the surrounding tissue. Therefore, the bottom of the structure might appear brighter on imaging. This is an artefactual phenomenon called Acoustic Enhancement Artifact (AEA), which plays a major role in iUS imaging in neurosurgery. [47] AEAs at the bottom of the cavity makes distinction from hyperechoic tumor remnant difficult [34], [48], [49]. A schematic representation of this artefact is shown in the second image of figure 3.10. The green arrows represent transmitted acoustic energy waves, the orange arrows represent reflected waves. The red asterisk indicates the AEA that occurs at the bottom due to the acoustic energy that is preserved due to the superiorly located fluid filled cavity.

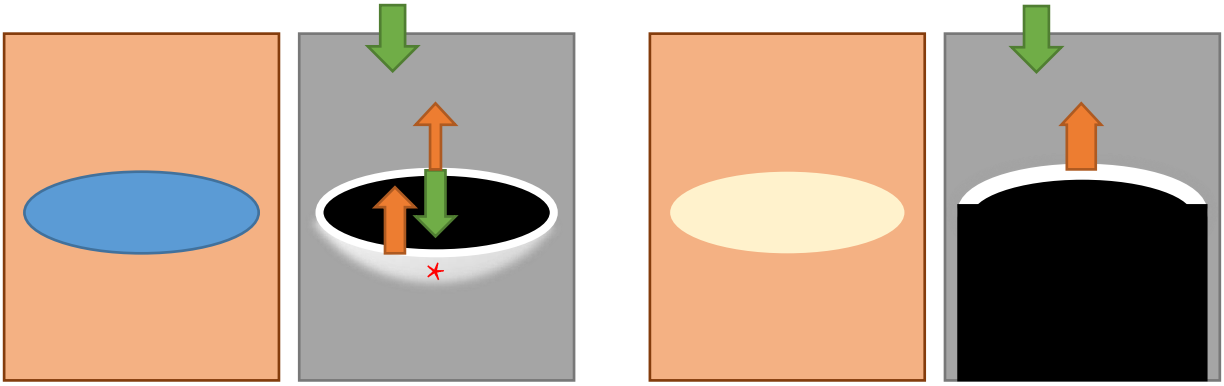

*Figure 3.10: Schematic image of two ultrasound imaging artefacts. A green and orange arrow indicate respectively acoustic transmission and reflection. The first image on the left shows a schematic representation of a fluid filled structure surrounded by other tissue. The second image shows the acoustic enhancing artifact. A fluid filled structure (blue) appears hypoechogenic, transmitting more acoustic energy. This creates a greater reflection at the interface, creating a brighter image at the bottom (*). The third image shows a schematic representation of an osseous structure surrounded by other tissue. The fourth image shows the resulting ultrasound image, representing acoustic shadowing. A bony structure reflects all acoustic energy, creating a very bright signal at the interface and a shadow below the interface.*

Another phenomenon that plays an important role in affecting the image quality of ultrasound in neurosurgery is acoustic shadowing. Calcareous tissue and osseous structures create impedance differences that are too large for sound waves to overcome, leaving no acoustic energy to be detected after the interface. This creates an acoustic shadow. Therefore, it is important to always optimize the transducer-tissue surface contact and to avoid bony or calcareous structures to be in the field of view. [47] Similar artifacts can be observed with air. Pneumocephalus is one of the most important causes of artifacts during surgery, creating an acoustic vacuum. [50] A schematic representation of a osseous structure is shown in the third image of figure 3.10. The most right image shows the schematic representation of the resulting ultrasound image. The high acoustic impedance of bone causes a large reflection of the acoustic signal, leaving no signal below the boundary of the bone.

### Navigated intraoperative ultrasound

iUS has only recently been adopted in neurosurgery, mainly because of poor image interpretability. The interpretability is often difficult for three reasons. First, the spatial resolution of iUS was typically poorer than other imaging modalities like computed tomography and MRI. The spatial resolution in ultrasound imaging is limited to the physical dimensions of the piezoelectric crystals in the transducer, the elements that send and receive the high frequency sound waves.[32], [48], [51], [52] Recent developments have allowed transducers to be smaller in size and to contain smaller piezoelectric crystals. This increased the spatial resolution and allowed the surgeon for easier placement of the transducer on the brain. Second, ultrasound imaging does not image the entire brain at once, since the FOV is smaller than in other imaging modalities. Although depth resolution has increased in recent years, the small transducer will always create the effect of a flash light in a cave, creating a diverging view starting from the transducer. Third, the real-time imaging characteristic of ultrasound can be considered both an advantage and a disadvantage. Images can be instantly made and in different planes, depending on movement and positioning of the probe. On the other hand, this increases the complexity of image interpretation. The last two interpretability challenges have been greatly diminished by integration with preoperative MR imaging via neuronavigation. [34], [53], [54]

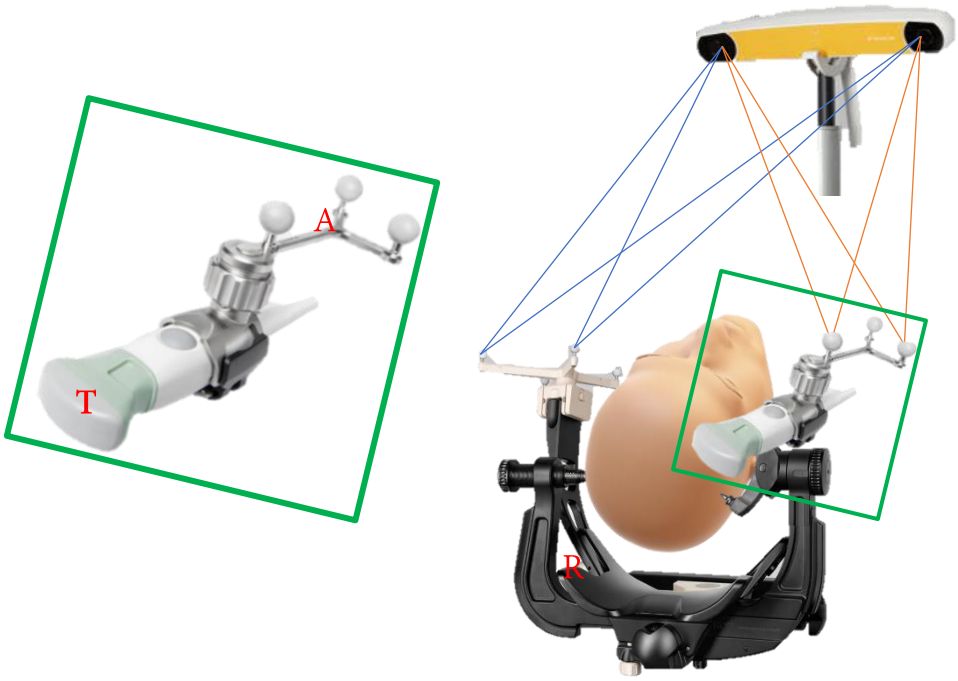


*Figure 3.11: Navigated iUS set-up. The left image shows the navigation array (A) with reflective spheres attached to the transducer (N13C5, BK Medical, Denmark). The right image shows the camera recognizing both reference array on the table (R) (blue) and the transducer (orange). The position of the transducer can be determined and the ultrasound image is overlaid on the preoperative imaging.*

As mentioned in Section I of this chapter, any surgical instrument can be navigated, as long as reflective spheres can be mounted to it. Figure 3.11 shows the reflective spheres mounted on a custom-made array (A), which is attached to the transducer. Once calibrated, the position of the transducer tip (T) is always fixed to the array (A). Once the transducer is brought in sight of the stereotactic camera, the transducer's position relative to the reference array (R) on the table is determined. An example of the set-up is shown in figure 3.11. Like the navigation pointer, the software then positions the ultrasound at the location in the preoperative image. Instead of positioning only one point, a two-dimensional ultrasound image is superimposed on the preoperative image, as shown in figure 3.12.

Another addition of navigated ultrasound, is that a volume can be composed from consecutive two-dimensional US images, by tracking the position of the ultrasound images and constructing them accordingly. This allows the surgeon to compare two scan moments in time, monitoring debulking progression. Moreover, it enables the surgeon to interpret the amount of brain shift and the accuracy of the neuronavigation. Integration with neuronavigation has led to advancements resulting in an increase of iUS applicability in neurosurgery.

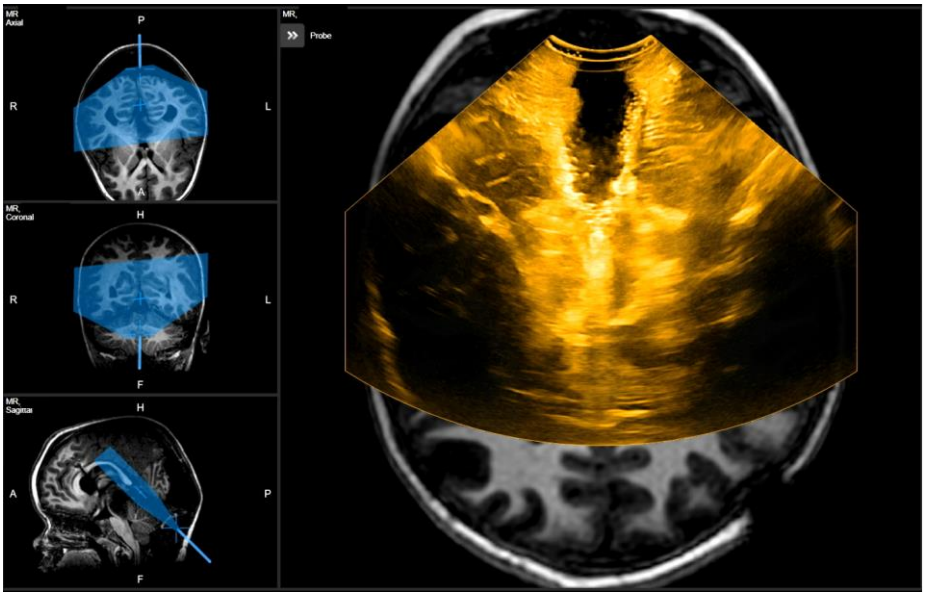


*Figure 3.12: Navigated intraoperative ultrasound overlaid on MR imaging. The column on the left shows the orientation of the ultrasound probe. The image on the right shows the overlaid ultrasound image on the MRI.*

# IV

# Evaluation of advanced surgical techniques in Neuro OR Suite

## Introduction

In November 2022, a novel operating theatre facility for pediatric neurosurgical procedures has been opened in the Princess Máxima Center for pediatric oncology (Utrecht, the Netherlands). The neuro OR suite encompasses a variety of different advanced intraoperative technical modalities, that can be divided into four different categories: 1) Planning, 2) Acquisition, 3) Visualization and 4) Navigation. Some modalities were already present in the previous OR, e.g. the surgical microscope, image guided surgery, navigation pointer, intraoperative neuromonitoring and the endoscope. New intraoperative technical modalities that required adaptation of the surgical workflow were intraoperative imaging techniques: intraoperative MRI and intraoperative US.

An optimal implementation of technical modalities in a highly complex environment is import to make the surgical workflow more efficient, effective and safer. [55] Although every neurosurgical procedure is different, similarities are found in surgical approaches and strategies. Some modalities may have the same purpose and may therefore overlap in functionality. Some modalities may show dependency, requiring other techniques to function properly. Some modalities might be superior to other techniques. Moreover, techniques can also be burden on the surgical workflow, which may lead to abandoning the technique. Therefore, observation and evaluation of the different technical modalities is necessary to assure continuous optimization of the surgical work flow and patient outcomes.

Several studies report on the difficulty of successfully implementing a new medical device in an existing highly complex environment, because of the number of factors involved [55]–[57]. Implementing a new technique in an existing highly complex environment requires several factors to be correctly addressed. Misser et al. [55] describe seven factors that play an important role in successfully implementing medical equipment: 1) processes and activities, 2) staff, 3) communication, 4) project management, 5) technology, 6) training, and 7) performance. In our center six new techniques are added in a short period of time, which makes successful implementation even more complex as compared to introduction of solely one technique.

In this research, we intend to record the individual role of the available technical modalities in the novel Neuro OR suite. All available technical modalities which were assessed in this research are explained in Chapter III.

The aim of this research is to identify the optimal usage of the new and established technical modalities for neurosurgical procedures. Other study objectives are to identify practical challenges and recommendations and to propose guidelines concerning optimal usage of OR techniques given a certain procedure.

## Methods

The procedures included in this research involve all neurosurgical tumor debulking or biopsy procedures. Other surgical procedures were not taken into consideration, since no advanced surgical techniques were required. Since the first evaluations started a month after introduction of the neuro OR suite, a learning effect will inevitably be present in our observations. However, registering these observations allowed for identification of technical problems and solutions, leading to recommendations for more optimal implementation of techniques.

A standardized questionnaire was developed to quantify the usage of OR techniques and gather user experiences, see Appendix A. This questionnaire was filled out after each procedure by the attending surgeon in charge of the surgery. The questionnaire consists of three sections. The first section requests general information about the procedure, the assessment of the technical interplay and addressing technical problems. The second section is divided into the same categories as mentioned in Chapter III: planning, acquisition, navigation and visualization.

In the second section, the following statement was posed: 'Was the technique necessary to accomplish the goal?' The questionnaire provides a Likert-scoring, ranging from 1 (strongly disagree) to 5 (strongly agree), to answer this statement for every individual technique. Besides the Likert scoring, the surgeon has the option to elaborate on the scoring in the free text fields.

The third section of the questionnaire consists of two free text fields where learnt aspects during this procedure and aspects for future procedures can be described. Eventually, the remarks on these topics are clustered and analyzed.

The results of the questionnaires are descriptively analyzed. Techniques are individually analyzed and free text field responses are clustered. The frequency of individual techniques usage is recorded with the corresponding Likert-score. Incidental observations are separately reported. This includes responses regarding technical problems and recommendations.

## Results

### Baseline characterization

A total of 68 consecutive tumor debulking and biopsy procedures were included between December 2022 and June 2023. No tumor debulking or biopsy procedures were excluded from analysis. The procedures were performed by two surgeons, accounting for 43 and 25 procedures, respectively. A total of 65 patients were included, of which 36 males and 29 females with a mean age of 9.2 ± 5.3 years. 58 patients underwent a neurosurgical tumor debulking procedure and 10 patients underwent a biopsy procedure.

Four of the debulking procedures were spinal approaches and two procedures were transsphenoidal approaches. The most frequent procedures involved lesions in the posterior fossa, n=33 (50%). The most frequent tumor grade was WHO-I, n=33 (48%), of which 17 were pilocytic astrocytomas. Planned and achieved surgical goals are defined in a surgical resection (SR) category: SR-0 (complete resection), SR-1 (rim-like residue), SR-2 (bulky residue) and SR3 (biopsy) [3]. In 87% of the procedures, the planned surgical goal was achieved. Additional baseline characteristics are shown in table 4.1.

*Table 4.1: Patient population characteristics*

| | | |
|---|---|---|
| **Number of patients:** | | 65 |
| **Number of procedures:** | | 68 |
| **Sex:** | | |
| Male: | | 36 (55.4%) |
| Female: | | 29 (44.6%) |
| **Age: mean (SD) years** | | 9.2 (5.3) |
| **OR time: mean (SD) mins** | | 389 (158) |
| **Patient positioning:** | | |
| Prone | | 34 (50.0%) |
| Supine | | 34 (50.0%) |
| **Location of Tumor:** | | |
| Intracranial | | 64 (94.1%) |
| Medulla | | 4 (5.9%) |
| **Surgical approach:** | | |
| Midline Occipital | | 33 (48.5%) |
| Pterional | | 12 (17.6%) |
| Convexity | | 10 (14.7%) |
| Interhemispheric Transcallosal | | 7 (10.3%) |
| Spinal | | 4 (5.9%) |
| Transsphenoidal | | 2 (2.9%) |
| **Surgical goal:** | | |
| **Planned** | **Achieved** | |
| SR-0 | SR-0 | 13 (19.1%) |
| SR-1 | SR-1 | 19 (27.9%) |
| SR-2 | SR-2 | 17 (25.0%) |
| SR-3 | SR-3 | 10 (14.7%) |
| SR-0 | SR-1 | 4 (5.9%) |
| SR-1 | SR-0 | 2 (2.9%) |
| SR-0 | SR-2 | 1 (1.5%) |
| SR-1 | SR-2 | 1 (1.5%) |
| SR-2 | SR-1 | 1 (1.5%) |
| **Procedures per surgeon:** | | |
| Surgeon A | | 43 (63.2%) |
| Surgeon B | | 25 (36.8%) |
| **Tumor type:** | | |
| **Low Grade Tumors:** | | **46 (67.6%)** |
| Pilocytic astrocytoma | | 17 (37.0%) |
| Low grade glioma not further specified | | 8 (17.4%) |
| Craniopharyngioma | | 5 (10.9%) |
| Ependymoma | | 2 (4.3%) |
| Germinoma | | 2 (4.3%) |
| Other | | 10 (21.7%) |
| **High Grade Tumors:** | | **17 (25.0%)** |
| Medulloblastoma | | 12 (70.6%) |
| Diffuse Midline Glioma | | 3 (17.6%) |
| Anaplastic Ependymoma | | 2 (11.8%) |
| Other | | 2 (11.8%) |
| **Non-neoplastic:** | | **1 (1.4%)** |
| **Inconclusive pathological outcome:** | | **4 (5.6%)** |

## General findings

The scoring of the individual OR modalities has been divided among four categories; planning, intraoperative acquisition, navigation and visualization. It was observed that the surgeons used and scored certain techniques differently due to variations in surgical approaches. Therefore, the results of each modality are divided by surgical approach, since patient positioning and anatomical tumor location affect procedure preparation.

In general, procedures with prone patient positioning showed to require less OR techniques to inform the surgeon. In five cases it was explicitly mentioned that tumor resection was possible without using various additional techniques. Planning techniques were frequently used, but the more dedicated techniques were less used. For instance, image fusion and registration were used in most procedures, 84% and 75% respectively. Although the neuronavigation was initialized in 75% of the cases, the navigation tools were used less frequently. Resulting in 69% and 40% of procedures for the navigation pointer and navigated microscope, respectively. These frequencies indicate that the relevance of each technique is varying. If a procedure was described as 'intuitive' and 'straight-forward', neuronavigation was not deemed necessary in retrospect.

It was observed that the intraoperative imaging modalities complicated and prolonged the procedures. iMRI affected the surgical workflow notably. Every scanning session prolonged the surgery with approximately an hour, including patient transfers. iUS had a smaller impact on the surgical workflow, prolonging it by only 5 minutes per scanning session. However, iUS showed to be more difficult to interpret due to image orientation and artifacts. Integration with the neuronavigation has improved the interpretation, but acquiring good quality images remained difficult. Good quality images were especially difficult to acquire in supine positioning due to fluids leaking from the resection cavity. Nevertheless, besides the challenges the OR team faced, the intraoperative imaging modalities provided valuable additional information. In 21% of procedures using iMRI, it was explicitly mentioned that iMRI led to additional resection. In 38% of the procedures, GTR was confirmed. In these cases, iMRI could serve as postoperative imaging. This prevented the patient from undergoing an additional MRI scanning session with anesthesia.

It should be noted that the four spinal and two transsphenoidal approaches are included in the total amount of procedures, but are not separately described in the barplot analysis. These procedures are excluded from this subanalysis because of the low amount of procedures.

The two transsphenoidal procedures were both endoscopic procedures. The Ear Nose Throat (ENT) department was always involved in these procedures to get the optimal access to the inferior part of the sella turcica. Image acquisition techniques were never used. Image fusion was used for fusing CT and MRI data for the navigation. The navigation pointer was used to orient in the sphenoidal area, and to obtain an indication of the location and size of the tumor. The endoscope, image fusion, registration and navigation pointer were all scored 5 on the Likert-scale.

The four spinal procedures all required the surgical microscope, which was always scored a 5. Additionally, x-ray imaging was used in three procedures, iUS in two procedures and image fusion in one procedures. X-ray imaging was scored a five twice and a 3 once. iUS was scored a 4 and a 5, image fusion was scored 4. X-ray imaging was used to determine which spinous process was to be removed first, which could still be challenging task. iUS played an important role in visualizing the border of the tumor transdurally, to determine the direction of laminotomy and to optimize the dural incision.

For the other technical modalities, the results are visualized below in bar plots per surgical approach. The different surgical approaches are defined as midline suboccipital, pterional, convexity, interhemispheric transcallosal and spinal. These approaches are further explained in Chapter II.

## I. Planning

### *Image Fusion*

Image fusion was used during 57 procedures, comprising 84%. The median Likert score was 5 with an interquartile range (IQR) of 1, indicating satisfaction among the surgeons (see also figure 4.1). The procedures with a lower score showed to be more intuitive and straightforward, therefore image fusion was not necessary in retrospect.

Image fusion allowed overlapping images and objects, therewith merging different plans. This allowed the surgeons to compare different image volumes. Vital structures, (residual) tumor tissue, ischemia and edema, could be identified between the different images. Moreover, the surgeons used the fused images to measure distances and plan trajectories. Besides planning, the fused images was used for navigational purposes. This supported the surgeon in interpreting the structures within the resection cavity.

In two procedures, the fusion needed to be manually adjusted to correctly initialize the fusion software. This was needed when the patient was scanned in a non-conventional position. If the patients head is tilted 90 degrees, aligning the chin with the shoulder, a coronal slice on the scan shows an sagittal view of the head. The initial position determined by the software is therefore not correct. Another aspect that affects the fusion accuracy is the spatial resolution of the scans to be fused. Any low resolution scans can potentially pollute the quality of the fusion and should be removed from the fusion tree (see appendix F).

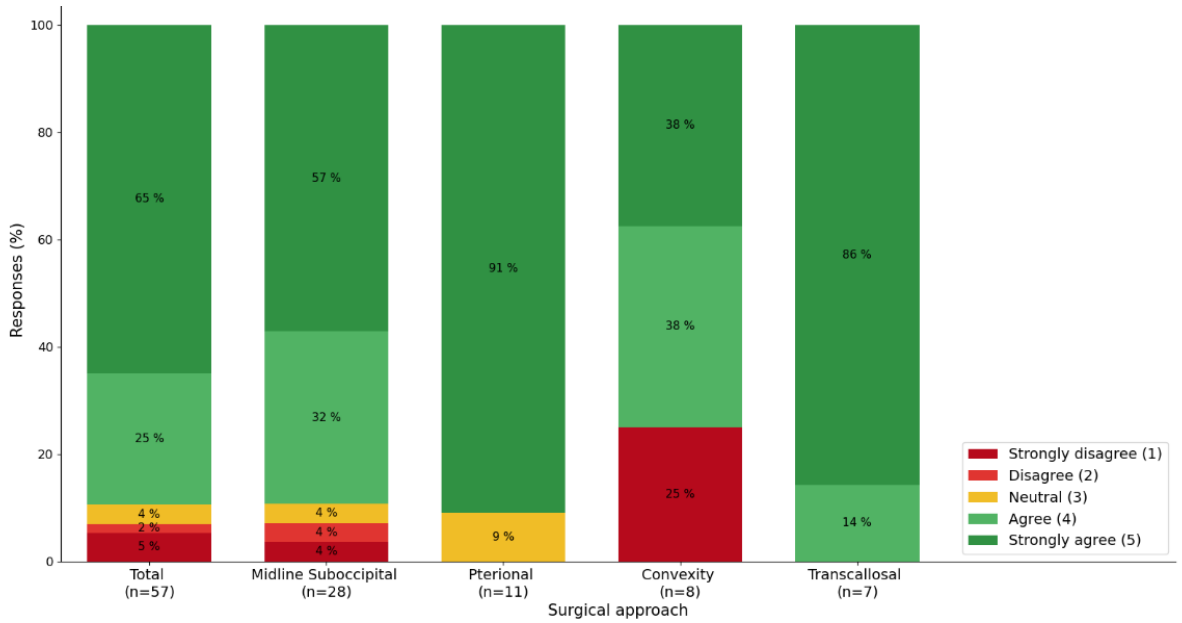


*Figure 4.1: Likert-score distribution per surgical approach for image fusion (n=57).*

### *Image Registration*

Image registration was widely utilized, comprising 51 procedures (75%). Image registration was used to initiate the image guided surgery (IGS). In general, the surgeons agreed that the technique was necessary for the procedure when the use of neuronavigation was expected. A median Likert score of 5 (IQR: 1) was found. The surgeons deemed this technique necessary to be able to use all navigated instruments, showing an important dependency for other techniques.

Three different methods were used for patient-to-image registration. The most used method was based on automatic iMRI registration (63%), followed by optical surface matching (31%) and electromagnetic registration (6%). iMRI registration is the fastest method, setting up registration within two minutes; excluding the time taken for patient transfer and scanning. The registration scan lasted approximately 90 seconds. Automatic iMRI registration was used in 91% of all posterior fossa procedures, and was never used in convexity approaches.

The presence of fontanelles in infant skulls does not allow for fixation of the head in the DORO™ headframe, so optical tracked IGS could not be used. Therefore, electromagnetic navigation was used for three patients. In nine cases (18%), the registration was initially based on surface matching and eventually re-registered based on automatic iMRI registration.

In six procedures (9%) the navigation could not be used, since the registration could not be performed successfully for three different reasons. First, in four cases the patient positioning did not allow for successful image registration. The patients that underwent a procedure in prone position with their neck flexed, often had their shoulders elevated. This resulted in a physical obstruction for the table reference array, which is mounted to the DORO™ headframe (as visualized in figure 4.9). Second, in two cases the registration could not be performed because the number of detectable MRI fiducials was not sufficient. This was caused by both poor signal detection and a insufficiently wide field of view on MRI. In one case this was resolved with a second scan. Last, in one case the registration was not set up because the DORO™ headframe was set too narrow for the fiducial array to fit.

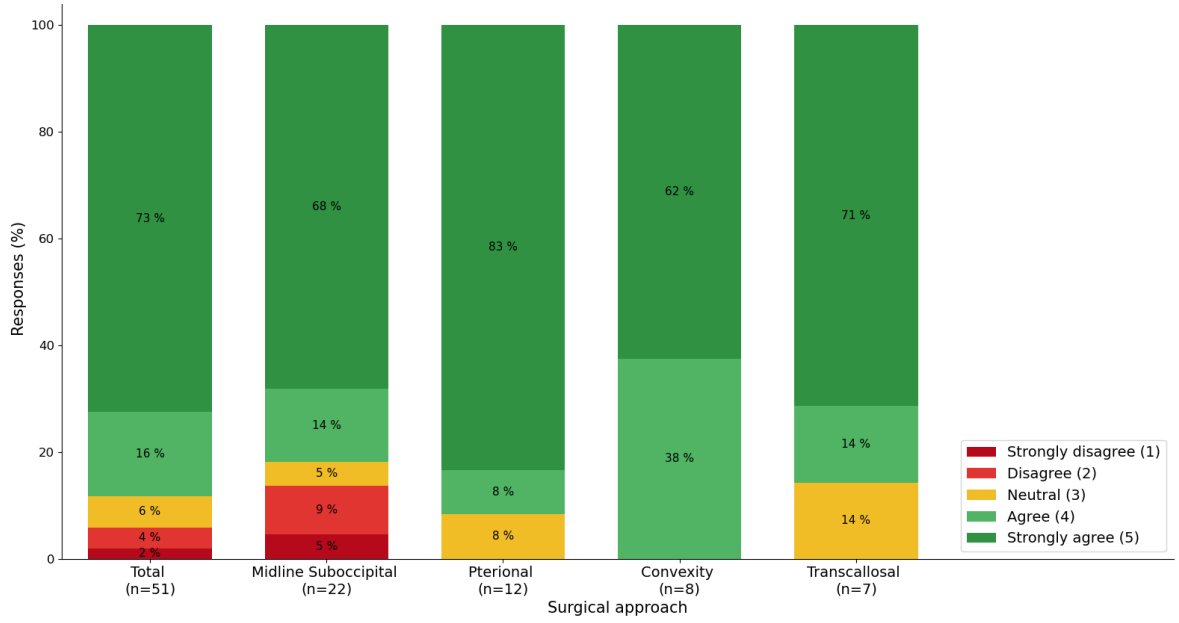


*Figure 4.1: Likert-score distribution for image registration (n=51) per surgical approach.*

## II. Intraoperative Acquisition

### *Intraoperative Magnetic Resonance Imaging (iMRI)*

Intraoperative MRI was used in 39 procedures (57%). In general, the surgeons deemed iMRI necessary for the procedure, which is expressed in a high median Likert score of 5. The surgeons used intraoperative MRI for two purposes in the surgical setting.

First, iMRI was used to visualize the most recent anatomical situation; identifying possible tumor remnants and ischemic areas. In eight cases (21%), it was explicitly mentioned that iMRI led to direct additional tumor resection, see figure 4.4. In 15 cases (38%), it was explicitly mentioned that iMRI confirmed a complete resection. In five cases (13%), iMRI showed residual tumor, but this was intentionally left behind. In these cases, additional resection would have risked posing serious neurological deficits. An additional benefit of iMRI is that the last scan session can serve as a postoperative MRI, avoiding an additional procedure requiring anesthesia. In four cases (10%) the interpretation of iMRI was difficult and ambiguous. Especially T2 weighted scans showed a hyperintense region that was larger than the residual tumor volume on T1 weighted scans. Also, the resection cavity did not show abnormal tissue under the surgical microscope, whereas iMRI showed possible tumor remnant. This made the surgeon refrain from additional resection.

Second, iMRI was used for initializing and updating the neuronavigation, for which a 3D T1-w MPRAGE image with a wide field of view (350x250x250 mm) was acquired. In nine cases (23%), a registration scan was made but was eventually not used for navigational purposes. This scan is always performed as the first sequence in the protocol, so the quality of the registration scan can already be checked while the other scans are still being made. However, if the other scans show no indication for continuation of debulking, the navigation is no longer necessary. Moreover, if there is already an iMRI automatic registration performed before the surgery, a second registration is not always necessary. The patient's head will remain fixed in the same position and therefore there are no major deviations in navigation expected.

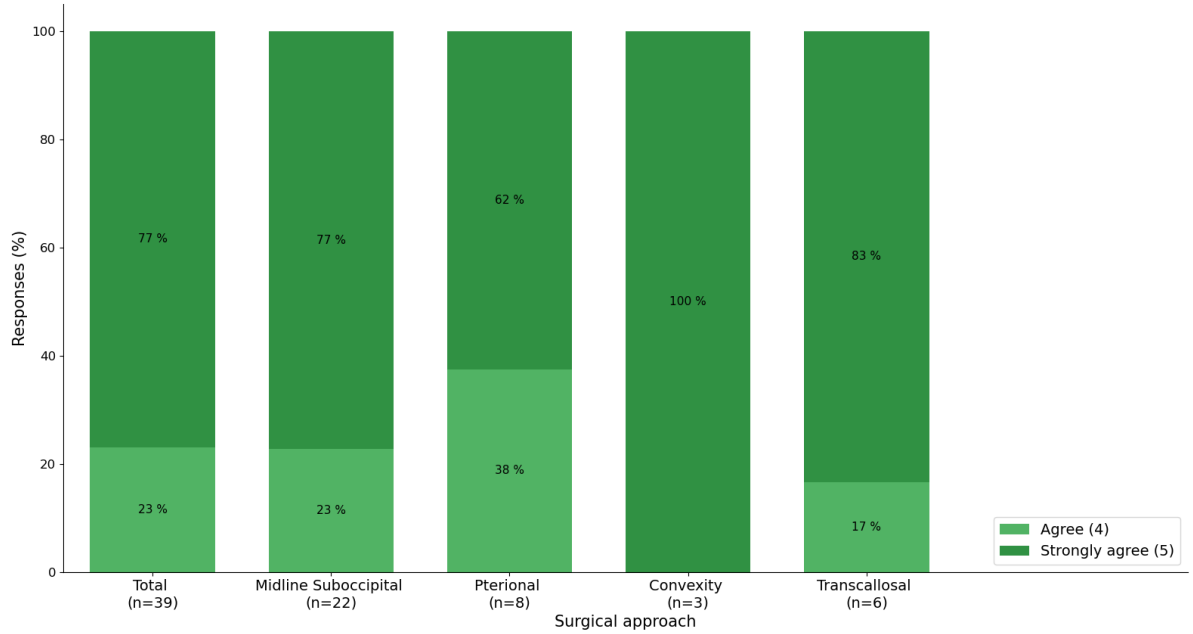


*Figure 4.3: Bar plots showing scoring of the surgeons per surgical approach. In general, the surgeons regarded iMRI as necessary in the procedures where it was used.*

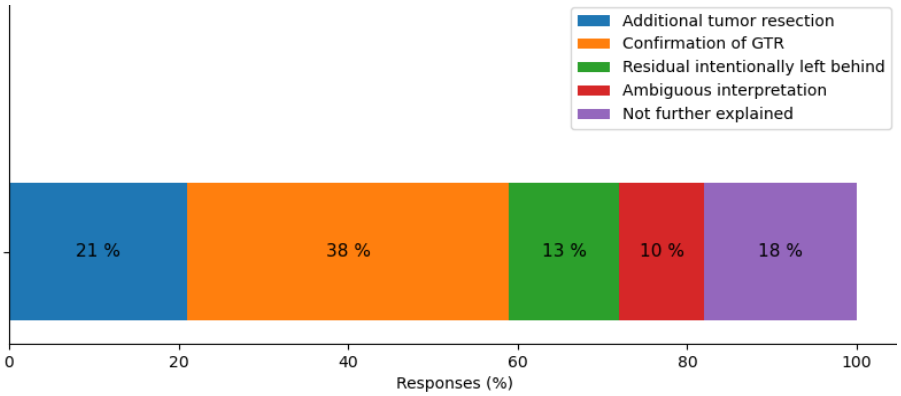


*Figure 4.4: Surgical decision making based on iMRI. Distribution of responses for iMRI in detecting residual tumor.*

To assess the presence of potential tumor remnants, 3D T1-w MPRAGE and 3D T2-w images were acquired. If the T1w and T2w images showed no residual or were inconclusive, gadolinium contrast agent was administered and an additional contrast enhanced T1-w image was acquired. However, if the T1-w and T2-w images showed a clear residual and the surgeon decided to continue resecting, the surgeon could still choose for an additional T1-w contrast image. In this case, half the dose of contrast was administrated to avoid potential neurotoxicity [58]. A more elaborate iMRI scanning protocol is included in Appendix D.

### *Intraoperative Ultrasound (iUS)*

Due to logistical causes, the ultrasound device (BK5000, BKmedical, Denmark) was only available from February 2023, and integrated with the neuronavigation from March 2023. Intraoperative ultrasound was used in 42 procedures (62%). The surgeons deemed iUS necessary in 86% of procedures involving iUS (see figure 4.5).

In 11 procedures (26%), iUS showed additional value during surgery because of three reasons. First, iUS showed the location of tumor attachment before dura opening. This allowed the surgeon to plan the trajectory towards the tumor. Second, during resection iUS showed potential residual tumor and guided the surgeon to reinspect certain areas of the resection cavity. In four cases (10%) iUS led to reinspection and further tumor debulking, before using iMRI. Third, iUS showed the magnitude of deviation of the neuronavigation during the surgery. This provided the surgeon with an estimation of the accuracy of the neuronavigation. Neuronavigation could potentially be updated based on the images acquired by iUS.

Although iMRI and iUS show an overlap in their role within the OR, both modalities show different applications. The in-plane resolution closest to the iUS transducer is twice as high as iMRI, which showed benefit during certain procedures. In two cases, iUS showed to be at least as good in visualizing residual tumor as iMRI. In one case the surgeon stated that iUS performed better than iMRI in visualizing the tumor. Also, it was mentioned that iUS was easier and quicker to use at the surgeon's desire without hindering the surgical workflow as compared to iMRI.

On the contrary, in certain procedures iUS was not contributing as compared to iMRI for three reasons. First, the image quality of iUS is highly affected by surgical changes to the tissue. Discrimination between edema, blood products and residual tumor was difficult. In three cases (7%) the surgeon did not trust the iUS image enough to rely upon due to image artifacts. Poor image quality led to difficult interpretation of the images. Obtaining good image quality was most difficult for the pterional and hemispheric transcallosal approaches. The

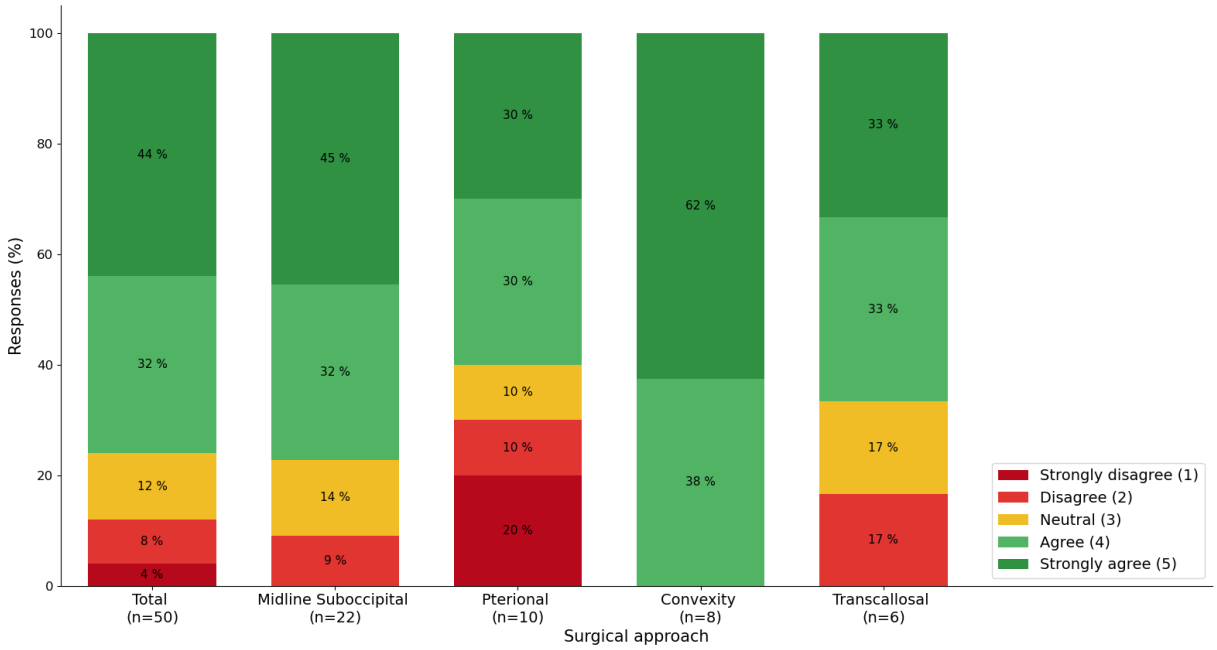


*Figure 4.5: Bar plots showing Likert-scoring of intraoperative ultrasound per surgical approach.*

patient positioning for these approaches impedes maintaining proper contact with the transducer and the tissue. In these approaches, the positioning allows fluid to easily drain from the cavity, allowing air to enter. Air also enters the cavity when surgery progresses and brain shift occurs, causing an acoustic vacuum.

Second, pediatric brain tumors are often centrally located, so iUS images need to be acquired at a greater depth. Therefore, the ultrasound frequency needs to be decreased resulting in a lower in-plane resolution. The lower resolution complicated interpretation.

Third, although iUS images are easily acquired, the dynamic character and imaging in non-conventional planes make interpretation more difficult. The integration of iUS with the neuronavigation allowed for iUS images to be overlaid on iMRI. This resulted in an increase in interpretability, which was reported in eighteen procedures involving iUS (43%). A good visual congruency with preoperative imaging was observed. This combined the best of both iMRI and iUS. The synoptic view of the brain on the preoperative MRI served as basis for orientation, whereas iUS could provide information regarding the most recent anatomical situation.

### *Intraoperative Neuromonitoring (iNM)*

In only five procedures, iNM was used (7.4%). In four procedures a Likert-score of 5 was given. The surgeons deemed the information helpful, but not essential. iNM is applied in very specific situations in which the functionality of pyramidal tracts and specific cranial nerves may be at risk intraoperatively. Deployment of this technique is highly dependent on the location of the tumor and the surgical approach. iNM was only used for posterior fossa (n=4) and convexity (n=1) tumors. The clincal neurophysiology department was always consulted. For the cases where iNM was deployed, the surgeon experienced additional value in having an extra source of information regarding perseverance of neurological function. The surgeon could rely on this information in considering additional resection, independent on other OR modalities.

## III. Navigation

### *Navigation Pointer*

The navigation pointer was used in 47 procedures (69%), with a median Likert score of 5 (IQR: 2). The additional value of the navigation pointer is highly varying among procedures. In general, the surgeons used the navigation pointer to determine the incision, to identify eloquent structures and to confirm the tumor location. It was observed that the navigation pointer was also used to identify tumor remnants. In certain procedures, this was a last check before iMRI.

If residual tumor was shown on iMRI, the navigation pointer was used to identify the part that needed to be additionally resected. Occasionally, the pointer was also used to mark some points in the navigation software, to define the resection cavity.

In 13 procedures (28%), a Likert score of 3 or lower was given because of two reasons. First, if the procedure was anatomically guided and tumor was clearly visible under the microscope, the navigation pointer was not necessary. Second, the navigation pointer was used to confirm the surgeon's expectation, which was considered helpful, but not necessary.

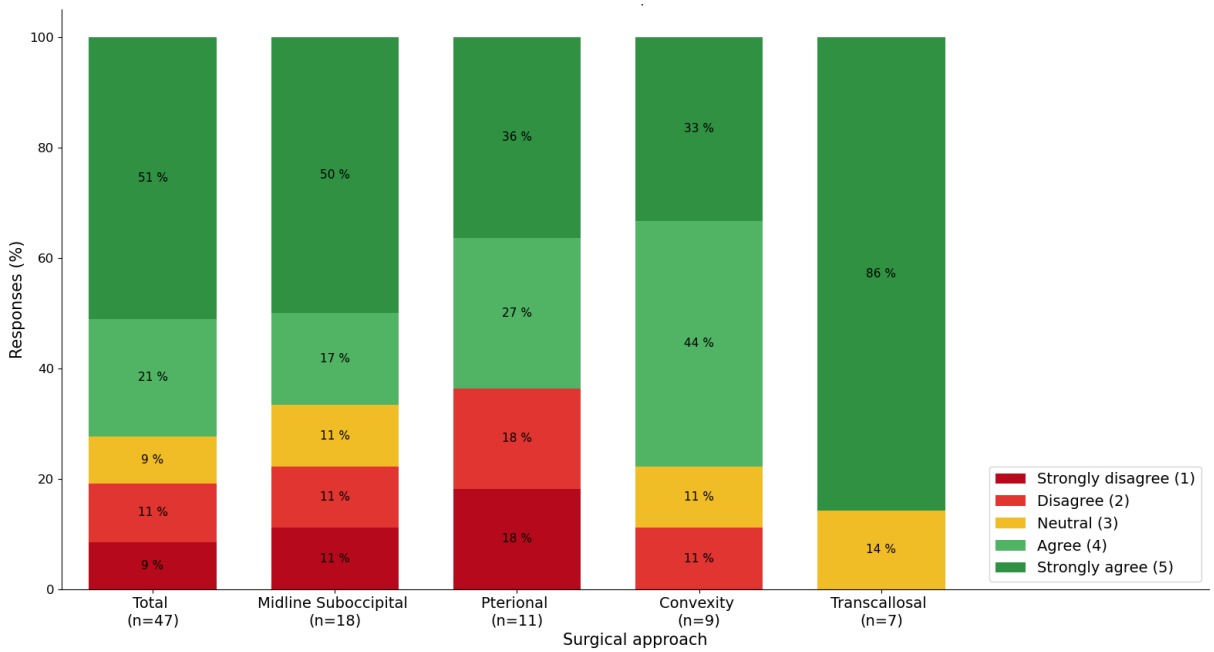


*Figure 4.6: Bar plots showing Likert-scoring of navigation pointer per surgical approach.*

### *Navigated Microscope*

The navigated microscope was used in 27 procedures (40%). The median Likert score was 3 (IQR: 3). The surgeons qualified the navigated microscope as not necessary in achieving the surgical goal in most cases. In eight of these procedures (30%), the technique was scored a 4 or 5. The role of the navigated microscope shows great overlap with the navigation pointer. The surgeons preferred to use the navigation pointer over the navigated microscope, because of the more intuitive line of sight of the navigation pointer. This line of sight

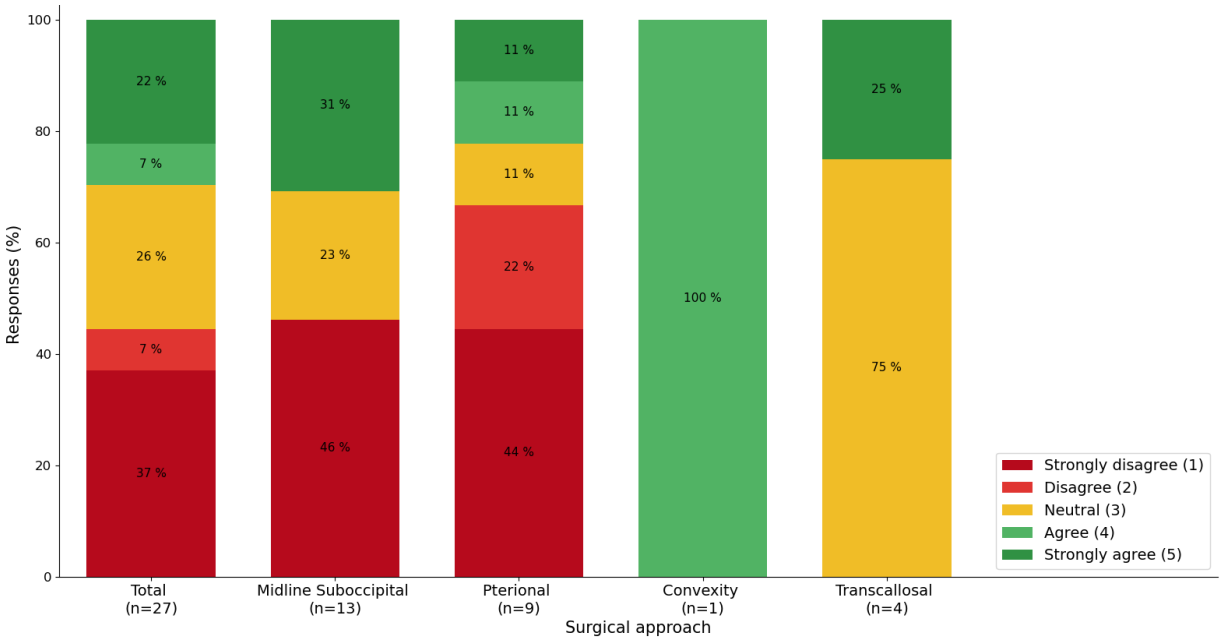


*Figure 4.7: Bar plots showing Likert-scoring of navigated microscope per surgical procedure.*

provided a better interpretation of the exact location of the tip of the instrument, since the surgeon also experienced haptic feedback when using the pointer.

On the contrary, it was occasionally experienced that the navigated microscope was typically easier for steady focus in one location, especially for deeply seated structures. This allowed the surgeon to interpret the navigation information without needing the pointer to be held in the cavity. In these procedures the navigated microscope was deemed helpful, but not necessary.

A drawback of using the navigated microscope was the position of the microscope reference array. The reflective spheres were not always visible for the camera in every microscope position. The microscope was frequently pointed away from the camera, especially for posterior fossa tumors. Moreover, the table reference array was regularly covered during surgery. This resulted in the navigation not showing the microscope's position. The technique was therefore not well integrated in the surgical workflow and was therefore often neglected.

### *Cirq*

Cirq® was used in four procedures (6%), and was deemed necessary in all four procedures. Cirq has a high dependency on three other techniques, namely: iMRI automatic registration, image fusion and stereotactic navigation. Therefore, these techniques need to work optimally in order for the Cirq to work optimally. The other techniques are therefore qualified as necessary in reaching the surgical goal, since the Cirq is required for the procedure to be performed successfully.

It was observed that correct planning of the position of the patient and the position of all parts of the neuronavigation and the Cirq robotic arm is necessary. Taking the time to correctly prepare the procedure is highly advisable, since correct positioning and registration highly affects the accuracy of the biopsy.

In the novel neuro OR suite, the Cirq can be initialized based on iMRI registration, which is safer as compared to CT fiducial based registration. For CT fiducial based registration, the patient needed to be transported to a

CT scanner outside of the OR-complex, as compared to the on-site MRI scanner. Besides, the registration based on iMRI does not require additional screws to be fixed to the skull, limiting the burden on the patient.

## IV. Visualization

### *Microscope*

In 56 procedures (82%) the surgical microscope was used. This technique is regarded as the extension of the surgeon's vision and has obtained an important role in the neurosurgical field in the last decades. This translates in the high Likert-scoring of 5 for all procedures. It is evident and expected that the surgeons are very satisfied with the microscope in all procedures, qualifying the technique indispensable. There was consensus among the surgeons that without the technique, the surgical results would not have reached the current extents of resection. The direct light source in the resection cavity and the magnifying function of the microscope are indispensable and not comparable to a surgical loupe. The microscope does not show any dependency on other techniques, if only used for illumination and magnification purposes.

### *Endoscope*

The endoscope was used in 7 procedures (10%). The endoscope has a more specialized application than the microscope as it is used for biopsies and endoscopic third ventriculostomies (ETVs). This technique is also regarded as an extension of the surgeon's vision and was scored a 5 in all procedures. Without the endoscope, the surgeons are forced to enlarge the incision, creating more space for light and tools to enter, but also increasing the risk for intra- and postoperative complications. Although the tool is navigable, the endoscope does not show any dependency on other techniques in order to function properly.

### *Head-up Display*

HUD was used in 25 procedures (37%) and was assessed with a median Likert-score of 2 (IQR: 3). There is a difference observed between the medians for the different approaches, see figure 4.8. No strong conclusions can be drawn given the low number of procedures per approach, but some observations are worth mentioning.

In 3 procedures (11%), HUD was contributing to reaching the surgical goal. This was mainly by directing the surgeon's attention to areas with potential tumor residue and for keeping an broad overview of the extent of the tumor. In 4 procedures (16%), HUD was solely confirming the surgeon's estimation of the debulking progress. In 9 procedures (36%), HUD was qualified as not necessary or was not used, because a procedure was based on microscopic vision and anatomical structures. In 4 procedures (16%), HUD could not be used because the navigation did not work properly, or the stereotactic camera was not able to detect the microscope reference array. In 5 procedures (20%), HUD was not used, because it was distracting or confusing the surgeon for four reasons. Firstly, when the contours are not accurately positioned due to brain shift. Secondly, when more than two contours are simultaneously visualized. Thirdly, when the background noise is amplified, the microscopic image would be blurred. And lastly, minor disturbances to the microscope resulted in a continuous dynamic shape change of the contour, creating a distraction for the surgeon.

HUD can be used to project both contours and navigated MR images, of which the latter is similar to what is shown in the navigation module. When the HUD was used, it was always used for visualizing contours, not for visualizing the projected preoperative MRI. The surgeons deemed the MRI image localization to be clearer on the external monitor than in the microscope.

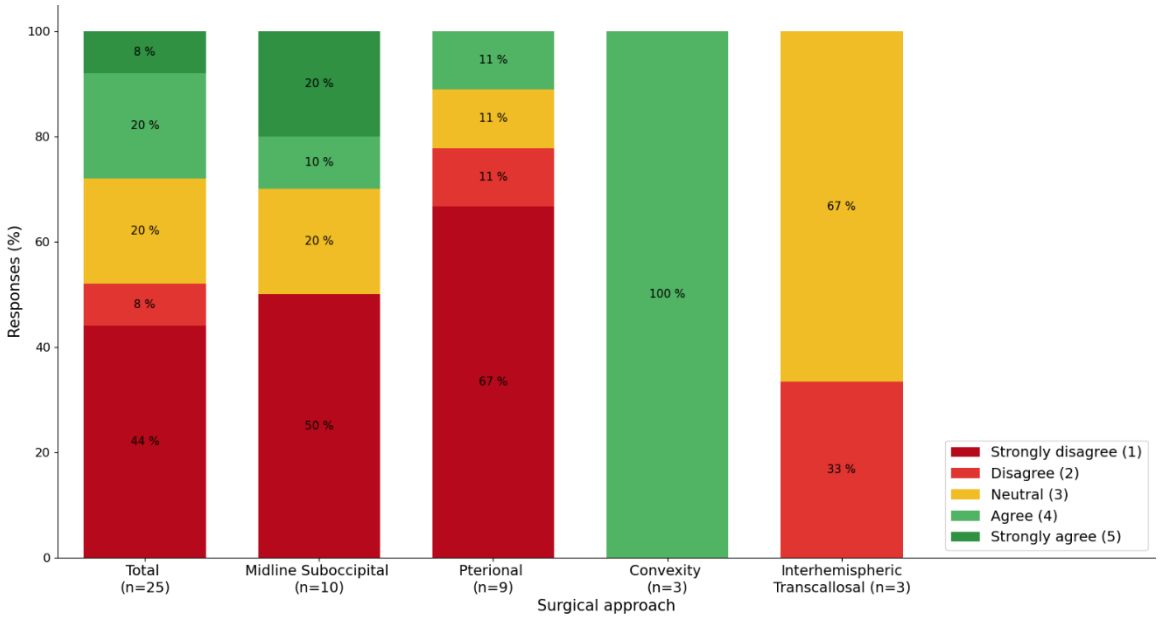


*Figure 4.8: Bar plots showing Likert-scoring of HUD per surgical procedure.*

## Technical problems

Technical problems were reported in 21 procedures (31%). The problems had a varying impact on the surgical workflow. Six different technical problems that occurred during the observation period are described below.

First, there was a problem regarding the registration in six procedures (9%). The registration could not be validated due to the inability of table reference array placement. This occurred always using iMRI automatic registration, because of the sequential character of the steps in this method. In this method, the table reference array is not placed for registration purposes, but for validation of the automatic registration. This means that the array needs to be placed after the patient is positioned, the head is fixed and the registration scan was made. If the table reference array was placed after positioning and fixation of the head, the array could be physically obstructed by the patient. In prone positioning, the shoulders of the patient were often elevated, therewith physically obstructing the placement of the array (see figure 4.9). The consequence was that the navigation could not be used, disabling the navigation pointer, navigated microscope, head-up display and navigated iUS. During these procedures, the surgeons based their decisions on the visual information from the microscope, the preoperative imaging and unnavigated iUS. By focusing more on patient positioning, the surgeons managed to avoid this registration problem.

Second, there were technical problems with the iMRI in four procedures (6%). The problems that are described regard positioning issues with the transfer table, an internal MRI software crash and poor image quality due to pneumocephalus. This affected the length of the procedure, increasing the total procedure time with 20 to 30 minutes. In two procedures, iMRI could no longer be used.

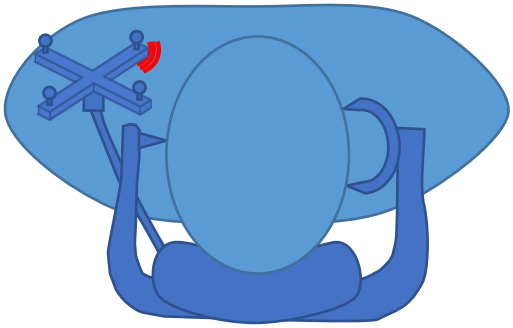

*Figure 4.9: Patient in prone position with the neck flexed and shoulders elevated caused physical obstruction of the table reference array. This hindered navigation set-up*

Third, a problem regarding the positioning of the reference arrays in posterior fossa approaches was reported in five procedures (8%). In general, the surgeons point the microscope cranially during a procedure involving prone positioning of the patient. This means pointing the microscope reference array away from the caudally positioned stereotactic camera. In this position, the reference arrays on the microscope and the table are only visible within a specific range of camera positioning. Therefore, successful tracking of the microscope is only possible if the table reference array needs to be positioned beside the patient's right ear is. This specific setup is visualized in figure 4.10. Outside the range of the camera's vision, the navigated microscope and HUD cannot be used. Besides, we observed that the navigation pointer can only be used when the microscope is moved out of the surgical field, allowing the camera to see the pointer and the table array. The need for moving these modalities intraoperatively to obtain navigation information, posed a burden on the surgical workflow. This burden resulted in neglecting the technique or in removing the table reference array since it was obstructing the work field.

Fourth, in two procedures (3%) there was a problem with the iUS, forcing the device to auto-shutdown due to an internal software error. This did not delay the procedure since this occurred when the device was not used. Restarting the device resolved these problems.

Fifth, there was a problem with the video routing system of the BUZZ. The visual output of the modalities could not be correctly displayed due to an internal bug. Besides, recording videos from displays was not possible in four procedures (6%), due to an internal software error. These problems had no impact on the procedure.

Last, there were four procedures with an incidental technical problem concerning the software, which were regarding: 1) improper image fusion, where the scans needed to be manually adjusted, 2) the network-based central information hub (BUZZ) was unresponsive, 3) the microscope video output was not recognized. These problems did not have a major impact on the procedure, other than prolonging the procedure with a maximum of ten minutes.

All in all, most problems did not have a major impact on the surgical procedure. However, the technical problems could result in complicating and prolonging the procedure. In some procedures, the involved modalities were abandoned if the burden on the process was large.

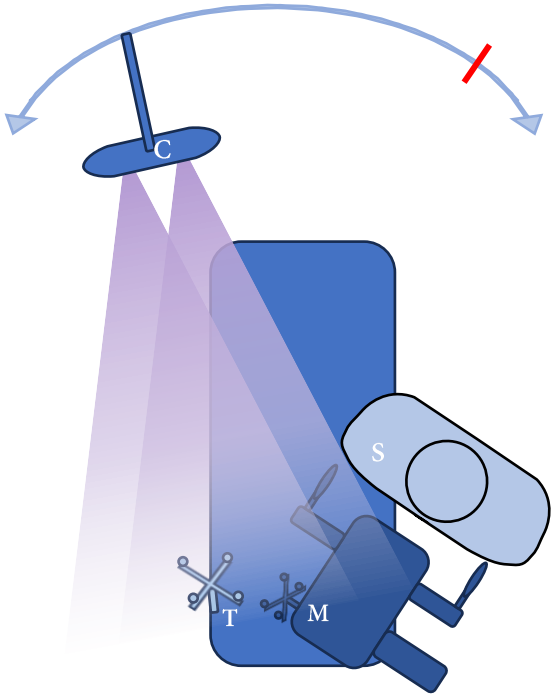


*Figure 4.10: Overhead view of navigated microscope setup for prone patient positioning. The table (T) and microscope (M) reference arrays need to be in sight of both cameras (C) to allow for stereotactic navigation of the microscope. The curved arrow on the top of the image shows limits of the range of motion of the camera. In prone positioning, the surgeon (S) points the microscope cranially, i.e. away from the camera, limiting the range even more. Only if the microscope reference array is pointing to the right, and the camera is put in the position shown above, the microscope can be tracked. The red line indicates the position to which the camera can be moved before losing stereotactic vision.*

## New insights

In the evaluations, the surgeons elaborated upon the aspects they learnt for every procedure. This free text field was used for a wide variety of experiences. Below, some of the experiences are summarized and elaborated upon, a learning effect can be observed during the evaluations. Aspects that were learnt in a previous procedure, are adopted to a new procedure. This had impact on how the surgeons assessed the technique over time. Most of the learning experiences were only observed incidentally, because the surgeons immediately addressed most experiences in the following procedure. Therefore, this paragraph is mainly a description of valuable experiences that were obtained.

### *Intraoperative MRI*

The modality with the biggest impact on the surgical workflow is the iMRI for which a number of new insights were experienced. Over time, more attention was paid to positioning the patient and the flex coils. Also more checks were built in for correct placement of the MRI table.

Another new aspect concerning iMRI was the new collaboration between radiologist and surgeon in the OR. The radiologist interpreted the MRI scans and the surgeon made the translation with the surgical situation. This close cooperation assured optimal clinical decision making. The specialists learnt how to interpret the different scan sequences and that the signal intensities in the intraoperative setting were much different from the preoperative setting and the postoperative setting. For example, surgical materials became apparent like gauzes and spongostan, each with their unique imaging characteristics. Besides, the OR team learnt how to remove air from the head by optimally filling the resection cavity with saline solution, to assure the best image quality.

The specialists observed that the hyperintensity on T2 sequences was not always congruent with T1 hypo-intensity. The specialists learnt how to interpret this discrepancy and diagnose the hyperintensity either as residual tumor or edema. Another observed peculiarity is the unfolding of the tumorous tissue by expansion over time, since the resection cavity is not manipulated during scanning. In several cases this led to bulging of the tumor tissue into the resection cavity, by expansion of the tissue underneath. The tissue was better identifiable on MRI and in the surgical setting after scanning.

*Intraoperative ultrasound*

After the introduction of the novel iUS device in February, the surgeons learnt to use and interpret iUS by acquiring multiple iUS images per procedure. The anatomy was visualized in an excellent way and the OR team learnt how to interpret the images. It was observed that the tumor was typically hyperintense on the iUS. After integration of iUS with the neuronavigation, the interpretation of the iUS has increased and led to a swifter scanning and interpretation process. The quality of the acquisitions increased over time after several interfering factors were identified. It was observed that gauzes and spongostan were interfering with the signal. Besides, the best probe positioning was determined and how the tissue-probe contact could remain stable, which increased image quality. Besides, acoustic enhancing artifacts and blood product artifacts were observed, resulting in a more difficult interpretation of the iUS image. The OR team learnt to be cautious in discriminating residual tumor from edema and artifacts based on iUS. However, the OR team also learnt that iUS can be a reliable tool in determining the location of potential residual tumor.

*Image guided surgery*

Regarding the registration and navigation techniques, four new insights have been identified. First, the preparation of the positioning of the patient is very important to make all navigable tools work properly in a later stage of the procedure. The surgeons have focused more on the patient positioning, which led to more successful image-to-patient registrations. Second, the position of the patient's face to the registration matrix was noted before scanning, since this facilitated quicker FOV selection. Since the patients are always scanned in surgical positions, the imaging protocol always needed to be adapted to the patient. FOV selection was different for every patient, and the position of the head to the isocenter varied between procedures. By preparation and planning the position, the FOV selection was quicker to execute. Besides the orientation of the FOV, the size of the FOV was also important to scan the registration fiducials in the array properly. Once the FOV was not correctly selected, the number of detectable fiducials was often insufficient. Third, another important factor in achieving a successful registration was by checking the position of the receiver coils, allowing enough signal to be measured from the registration fiducials. If the second and third remarks requirements are not met, the automatic registration software would not recognize the fiducials and an additional scan needed to be acquired. Last, regarding navigation, the surgeons experienced the advantages of acquiring a point cloud in the resection cavity, to get an additional source of information regarding the spatial dimensions of the residual tumor.

*Head-up display*

The new modality HUD resulted in new insights and applications during surgery. The dynamic contours and acquired navigation points could be projected in the microscopic view, providing the surgeon with additional information. For some procedures, this modality showed to be beneficial in identifying tumor residual. However, it was observed that the modality could also be distracting and confusing the surgeons, making the technique a burden on the process. The number of beneficial experiences with HUD is still limited, making the technique a nice addition to the armamentarium, but not a necessity. However, future research needs to be carried out to quantify the potential applications of this modality.

## Discussion:

During a period of seven months, the user experience of advanced technical OR modalities has been evaluated for 68 neurosurgical tumor debulking and biopsy procedures. An extensive analysis has been carried out, quantifying the surgeon's experiences regarding the individual technical modalities. Since the study is carried out shortly after the introduction of these technical modalities, a learning curve is inevitably incorporated into the analysis. For example, no problems involving the registration and navigation were reported after March. However, by evaluating every consecutive procedure, experiences and best practices have been identified and recommendations could be proposed.

To the best of our knowledge, no studies report on the usability of advanced surgical techniques in a highly complex neurosurgical environment. In other studies, surgical techniques are often compared to other modalities that share the same aim [48], [54], [55], [57], [59]. However, the relationship between different modalities, differentiating between dependency, redundancy and complementarity, is often not described.

The procedures that are described in this research are highly complex and multifactorial. The reason for a technique to work optimally is therefore not always easily showed. However, the relationship of every individual technique to other techniques has been defined. Based on this research, some recommendations are proposed to further optimize the surgical workflow. Optimizing the surgical workflow will remain an ongoing process of evaluation and implementation of new protocols.

An overall trend that was observed, is that the additional technical modalities, resulted in a large amount of additional information. Especially imaging techniques iUS and iMRI had an impact on the workflow by providing the surgeon with new information during the procedure. Other new techniques like the navigated microscope and HUD became decent addons for the procedure, but were not regarded as necessary in many procedures. Every new source of information needs to be interpreted immediately in the intraoperative setting, which was not always feasible or desirable. If the surgical situation was complex, additional information clouded the workflow of the surgeon.

Therefore, the more information is not always better and sometimes led to modalities being abandoned. Two main reasons for abandoning certain modalities, were 1) an increase in complexity of the procedure e.g. a hemorrhage to be controlled, or 2) when preparation of the technique took longer than 10 minutes. In these situations, the surgeons mentioned that the increase in complexity or disturbance of the workflow, resulted in the modalities to be a burden on the mental workload. Reduction of technique usage reduces the vastness of the procedure to a situation where the anatomical knowledge in expert hands plays the most import role, which is considered most time efficient in that moment. However, not using dedicated techniques could potentially lead to an increase of overall OR time, surgical risks and the number of suboptimal surgical results.

Surgery time is often limited and expensive, yet proper time investment is necessary for the most efficient, effective and safest implementation of technical OR modalities [56]. Identifying which modalities are necessary and which could pose a burden on the workflow is important for creating the optimal workflow per procedure. If innovative strategies are not explored, technical modalities are prone to qualify as a nice-to-have instead of a must-have. Therefore future research needs to be carried out in this high complex and high risk environment to assure optimal implementation in the surgical workflow.

## Limitations

Several limitations of this study need to be mentioned. First, the questionnaires were filled out by two surgeons in total, one surgeon per procedure. This inevitably led to an observer bias. Second, the questionnaires were not always filled out immediately after surgery. The time to fill out the questionnaire could be 2 weeks for some questionnaires. This inevitably led to recall bias, which was observed by the fact that the answers were less specific for these questionnaires. Third, a difference in questionnaire interpretation was observed, because of the choice of words in the question: 'Was the technique necessary to accomplish the surgical goal?'. In general, techniques were not strictly necessary to accomplish the surgical goal, but were helpful in the surgical process. These terms are quite vague and difficult to exactly specify the contribution of an individual technique. Every surgeon interprets the usability differently based on own associations, values and experience.

## Practical recommendations

During the evaluation period from December 2022 to March 2023, we have observed that there is a difference in usage of technical modalities before and during the procedure dependent on patient positioning. Therefore, a distinction is made between supine and prone patient positioning. Below, two guidelines are proposed considering the use of surgical techniques before, during and after debulking of the tumor. These guidelines should be regarded as a first step in defining protocols involving the technical OR modalities.

### *Surgical guideline: Procedures in prone position*

#### Before debulking

Before debulking can start, it is of great importance that the neuronavigation is properly setup and that optimal iMRI images are acquired. In prone positioning, the patient's neck needs to be flexed for the optimal surgical access in the suboccipital midline. The shoulders will be more elevated with respect to the DORO™ headframe. Therefore, the surgeon needs to install the MRI fiducial array and the table reference array before the patient is brought into final surgical position. While positioning, the surgeon needs to pay attention to the distance between the reference array and the shoulder of the patient. The reference array cannot press into the patients skin for the duration of the procedure. Even if the reference array fits and the skin is lightly touched, the array ought to be removed to avoid decubitus. However, removing the array will result in an extra step if navigation is desired during surgery, thereby increasing the chance of not using the navigation.

Moreover, the reference array should always be attached to the frame on the side of the patient's right ear. This will allow for better intraoperative detection of the reference arrays by the infrared camera. In prone position, the surgeons often operate on the left side of the patient, blocking the line of sight of the reference array. Besides, the array will physically obstruct the working field of the surgeon, which results in removal of the array.

iMRI scanning before surgery is only required in two scenarios. First, if preoperative imaging quality is poor, and the surgeon desires better quality images in surgical position. Second, if high accuracy of the neuronavigation is necessary, iMRI automatic registration is preferably performed. A high accuracy is necessary if the surgeon is planning on operating in close vicinity to vital structures. If the procedure is expected to be anatomically guided or if a bigger deviation in neuronavigation is acceptable, surface matching is recommended to initialize the neuronavigation. [60] Surface matching is more difficult and less accurate in prone positioning, but initialization will only take 10 minutes. This is much shorter than scanning and registering via iMRI, which can take up to 40 minutes including transfers. Besides, every patient transfer and iMRI scanning session can be a potential hazard for the patient. If iMRI scanning is indicated, the flex coils need to be positioned in such a way

that the signal of both the patient's head and the fiducials is detectable. The space between the head and fiducials and the flex coils should therefore be as close as possible.

After the registration is performed, the navigated microscope must be prepared. Before draping the microscope, the microscope's navigation array needs to be positioned pointing towards the right side of the microscope. If the array is not correctly positioned, the camera is not able to see the array intraoperatively because of the microscope's position during surgery, see figure 4.10. The reflective spheres should only be attached to the microscope if the surgeon desires the use of navigated microscope or HUD. Placing the spheres can also be done intraoperatively, as this will only take a minute to set up.

Lastly, iUS should always be used in a procedure and should be navigated, if possible. The reference array holder should be fixed to the transducer before draping the transducer and cable with a sterile cover. After draping the transducer, the sterile reference array with reflective spheres is attached onto the holder. The surgeon should always visualize the tumor after craniotomy, but before opening the dura. Scanning at this time point, creates the best image of the tumor before debulking. This facilitates interpretation of the images acquired during debulking. It is advised to acquire a navigated 3D iUS volume for comparison with iUS images made during debulking.

### During debulking

During debulking, the surgeon is advised to regularly inspect the resection cavity with the navigation pointer and iUS. To avoid regular manipulation of surrounding tissue to localize residual tumor, the navigation pointer and iUS can help in directing the surgeon to a certain area in the resection cavity. Head-up Display (HUD) can also be used for determining the location and extension of the pre-resection tumor volume. Both the contours and the projected MRI can help the surgeon in a more targeted approach of the tumor. It should be noted that this technique will become less accurate when debulking progresses and brain shift occurs. Moreover, our study showed that HUD is not always contributing to the surgical workflow for posterior fossa procedures.

Regarding using the iUS, a 3D volume acquisition is not always necessary for debulking, but 2D live imaging is recommended. However, images that show residual tumor, should be acquired in a 3D volume. Again, this allows for a comparison with additional acquisitions later in the procedure.

### After debulking

Before closure of the incision, an iUS swipe should always be made. An acquisition can be made in a couple of minutes and it gives the surgeon an indication of potential residual tumor tissue. Although the residual seen on navigated iUS visualizes the most recent anatomical situation, accurate volume estimation of the possible residual in the resection cavity is more difficult. Therefore, iUS should be used to guide the surgeon to a approximate location of possible remnant.

If iMRI is available and the patient is eligible, a post debulking scan always needs to be made. Potential residual could be recognized before closure. If no residual is showing, the iMR images could directly serve as postoperative MRI. This saves the patient from another scanning session with anesthesia the day after surgery.

### *Surgical guideline: Procedures in supine position*

The procedures in supine position are divided into three different surgical approaches: interhemispheric transcallosal, pterional and convexity approaches. Preparation and application of the modalities is comparable between the approaches, but also shows differences. Below, the general guideline for procedures in supine position is provided. Differences between approaches are described separately.

#### Before debulking

First, the navigation should be set up which is important in determining the size and location of the incision for procedures in supine position. In supine position, the registration method surface matching suffices the accuracy required for the neuronavigation. In supine position, surface matching is much quicker since the patient's face is facing towards the camera. The face has more unique structures describing a surface that is more accurate for registration, as compared to the back of the patient's head in prone positioning.

Second, before draping the microscope, the microscope reference array should be placed facing to the front. In supine positioning, the surgeon points the microscope in caudal direction during surgery, pointing the array directly at the camera. Mounting the reflective spheres of the microscope reference array is recommended, but not necessary. The surgeon needs to determine whether the navigated microscope will be used. Mounting the spheres will only take one minute and will therefore not disturb the surgical workflow.

Third, iUS should always be prepared and navigated if possible. Navigation of iUS is highly recommended in supine positioning, because the image quality tends to be poorer when scanning in supine positioning. Navigation of iUS will assure better image interpretation. However, if navigation is not possible, iUS still is regarded valuable in providing a quick update of the surgical situation.

The first 3D navigated iUS swipe needs to be made before dura opening for the best initial image of the anatomy. Tumors are often deeply seated if a pterional or interhemispheric transcallosal approach is planned. Obtaining an image of these deeply seated tumors with iUS is difficult, because the spatial resolution decreases with increasing depth. On the other hand, convexity tumors are located closer to the dura, allowing for imaging with higher resolution. The initial scan needs to be made to find the optimal parameters for visualization. The depth and frequency need to be changed depending on the tumor location and size.

#### During debulking

The trajectory towards the tumor is often anatomically guided for pterional, interhemisperical transcallosal and convexity approaches. However, the navigation pointer could be used to quickly determine a point of entry or to identify the extension of the tumor. The pointer can also be used as a confirmation for the surgeon to be more certain in proceeding working towards a specific direction. During debulking, HUD can help the surgeon in showing the tumor extent, which is particularly helpful for deeply seated tumors. Because of the key-hole principle in neurosurgery, deeply seated structures can only be viewed through a small surgical corridor. HUD can extent the microscopic vision by projecting the extent of the tumor. Moreover, HUD helps students in the OR to learn how to interpret the microscopic images.

It should be noted that the navigation and HUD will remain rather accurate while debulking suprasellar tumors, whereas the accuracy is decreasing while debulking intraventricular and convexity tumors due to brain shift. Navigated iUS should be used in these procedures to obtain the most recent anatomical overview. The iUS images will show the surgical cavity with potential remnants, but could also visualize the brain shift that occurred. The resolution of iUS images in a convexity approach will remain of good quality, since the

resection cavity is situated closer to the transducer (<5 cm) which allows for high resolution imaging. However, iUS images are hard to acquire in the pterional and interhemispheric transcallosal approaches. The resection cavity is often situated deeper (>7 cm) and filling the resection cavity is often difficult. The supine patient positioning allows fluid to easily drain from the cavity. Besides, the small surgical corridor complicates good contact between the tissue and transducer. Moving the table and using gauzes are recommended to fill the cavity sufficiently and allow for optimal image quality.

### After debulking

After debulking, the cavity should always be checked for residual tumor. Since the depth of the tumor and the small surgical corridor complicate visualization of the cavity under the microscope, it is recommended to use iUS and iMRI. Additional imaging is often considered important in confirming a GTR or for detection of residual tumor. First, iUS images should be made with a sufficiently filled cavity and good tissue transducer contact. If residue is visible on iUS, the surgeon can try to localize and decide to additionally resect the tumor. If the iUS images are inconclusive or negative for residual tumor, iMRI should be performed. Also in iMRI acquisition, it is important to minimize air in the surgical cavity. In this scanning session, a scan should be made for registration purposes. Since the patient already needs to be scanned for diagnostic purposes, an additional scan should be indicated for automatic registration. If residual tumor is visible on iMRI and the surgeon decides to proceed tumor resection, the navigation pointer could be used to localize the remnant based on the new imaging information.

### Future perspectives

In this study, the evaluation of the different technical modalities in the novel Neuro OR Suite led to new research directions. The effectiveness, efficiency and safety of the OR modalities should be explored and identified for optimal implementation in the surgical workflow. New research directions regarding intraoperative imaging are posed below.

Regarding iMRI, three research directions have been defined. First, we found that the image quality of iMRI was varying between patients and procedures. The signal-to-noise ratio was affected by pneumocephalus, surgical materials, placement of flex coils and MRI scanner parameters. Therefore, different ways for optimization of iMRI signal-to-noise ratio should be explored.

Second, we found that the T1 weighted and T2 weighted imaging did not always show the same potential tumor remnant. T1 images often show low contrast of potential tumor remnants, whereas T2 images often shows better contrast. However, T2 images tend to visualize tumors larger than T1 images, complicating surgical decision making. Future research should focus on the differences that are observed between the sequences compared to pathological outcomes of potential tumor remnants.

Last, the use of diffusion tensor imaging (DTI) in pediatric oncological surgery is not extensively used yet. However, DTI may provide additional information regarding the location of eloquent fiber tracks [61], [62]. These fiber tracks can also be projected in the surgical microscope or in the navigation module creating new possibilities. Future research should explore the value of DTI in pediatric neurosurgery.

Regarding iUS, four research directions have been defined. First, it was observed that B-mode imaging showed congruency with MR imaging. It was observed that iUS imaging in supine position was harder because of deeper seated structures and fluid that is not easily retained in the cavity. Additional research needs to be carried out to optimize the image acquisition for B-mode imaging. Second, it was observed that iUS might be more congruent

with T2 imaging instead of T1 imaging. Future research has to show whether this observation holds true and in combination with the iMRI research, this affects the way iUS will be used. If it appears that T2 is overestimating the volume, and iUS is congruent with T2; this means that iUS is also overestimating the volume and not a reliable tool to base the tumor volume upon.

Third, iUS shows other potential applications as other research has already pointed out. Contrast enhanced ultrasound, Doppler imaging and elastosonography are new applications of iUS, which show to have potential in pediatric neurosurgery. [35], [63]–[66] These new ways of imaging should be further explored.

Last, navigated iUS shows the most recent update of the anatomical situation. When overlaid on the preoperative MRI, the iUS images show brain shift and the amount of residual left. The observed brain shift could be used to update the navigation. The imaging information could be used to generate a virtual MRI, which is a software generated MRI based on newly acquired image information. These two research directions could be explored further to explore the additional value of navigated iUS.

## Conclusion

In this study, a comprehensive analysis of eleven intraoperative technical modalities within our center's Neuro Operating Room Suite has been conducted. Five of these techniques were newly introduced to the neurosurgical armamentarium: intraoperative MRI, intraoperative ultrasound, automatic iMRI based image registration, navigated microscope and head-up display. The different roles of the eleven modalities in the surgical workflow have been defined and described based on questionnaires filled out in 68 procedures. A Likert score was assigned to indicate the necessity of each technique. It was observed that the intraoperative imaging, registration and navigation modalities were in general regarded as helpful for the procedure. Differences in preparation and intraoperative usage of modalities between supine and prone patient positioning have been identified. It was observed that planning of the patient positioning is important for iMRI and iUS acquisition and for optimal neuronavigation usage. Furthermore, finding the optimal configuration of using OR modalities per procedure is difficult, because of the variety of procedures, surgical approaches and technical modalities. Based on the observations in this study, first guidelines for supine and prone position have been proposed to work towards optimal deployment of intraoperative technical modalities.

# V

# Illustrative intraoperative ultrasound cases in pediatric oncological neurosurgery

This chapter highlights three illustrative cases in which intraoperative ultrasound showed to be a valuable addition to the neurosurgical armamentarium. Intraoperative ultrasound could be deployed for different reasons during the procedure, in the planning stage: but also during the resection phase. This chapter is a prelude to the next chapter in which iUS is integrated with the neuronavigation and quantitatively analyzed.

## Introduction

As mentioned in chapter III.II, iUS has played an increasingly important role in neurosurgery. The creation of smaller transducers ensured better transducer-tissue contact. Moreover, the smaller piezoelectric crystals allowed for higher spatial resolution images which are necessary for imaging the complex anatomy of the brain. One of the benefits of iUS is its independency of neuronavigation, although still providing an impression of the location of anatomical structures. The non-invasive and real-time characteristics make iUS a valuable addition, allowing instant and quick updates during surgery without posing a burden on the patient.

In our series, we always made an iUS image before dura opening to obtain the most recent image of the anatomy, which could have changed over time or due to different patient positioning. In case of a low grade or recurrent tumor, preoperative imaging may be performed a couple of months earlier. At the time of surgery, the tumor may have increased in size, which can be quickly verified before starting debulking the tumor. The involvement of relevant anatomical structures can be visualized this way. This chapter describes our experiences regarding three cases where iUS played an important role in the surgical process.

## Illustrative Cases

### Case 1

A 7 year old girl presented with papilledema and mild gait and arm ataxia after period of head aches and nausea suggestive for hydrocephalus. Brain MRI showed a gadolinium enhancing lesion (4.2 ml) with a large cystic component (62.7 ml) in the posterior fossa region. The tumor showed adherence to the left cerebellar hemisphere. A suboccipital craniotomy with a midline incision from inion to C1 was planned. The patient was positioned in prone position with the neck flexed. After the craniotomy was performed, the ultrasound transducer (N13C5, BK Medical) was placed on the dura. The B-mode parameters were set to a depth of 9 cm, a frequency of 10 MHz, a sector width of 140% and an auto-gain of 12 dB.

Directly after placing the transducer on the dura, the large cyst was identified and shortly after, the solid part of the tumor was also identified; as visualized in figure 5.1. An ultrasound distance measurement was performed, where the maximal depth of the solid part of the tumor was defined at 30.4 mm. Interesting to note, is the effect of the cyst on the ultrasound signal. Because the cyst is a large structure with a low acoustic impedance, the acoustic enhancing artifact (AEA) can be clearly observed in figure 5.1 (see also Chapter III.II on AEA). The structures distant from the cyst and between the green lines show to be more hyperintense than the structures outside these lines. The steep intensity transition is best observed for the tentorium and cerebellar cortex, demarcated by the green lines.

After dura opening, protrusion of the cerebellum was observed. Since no neuronavigation was available, the surgeon used the ultrasound to identify the best location of entry into the lesion. First, it was necessary to release fluid from the cyst in a controlled way to reduce the tension. The surgeon used ultrasound guidance to determine the location for incision in the cerebellar cortex, assuring that the Dandy needle would not puncture the tumor. This trajectory is annotated with an orange arrow in figure 5.1. After the tension of the cyst was reduced, the solid part of the tumor became visible after some exploration under the surgical microscope. The tumor and cyst wall were dissected from surrounding tissue and resected piece-wise with the use of microsurgical instruments. After removal of the tumor based on the vision under the surgical microscope, a final ultrasound swipe was performed to confirm a gross total resection (GTR).

Regarding this case, iUS contributed to the surgical procedure for several reasons. First, iUS was used for acquiring more information regarding the tumor size and location, which helped the surgeon to plan the surgical approach. Second, iUS was deployed to guide the surgeon to place the needle in the cystic part of the lesion, avoiding puncturing the solid component and minimizing the damage to the cerebellar cortex  Last, iUS was

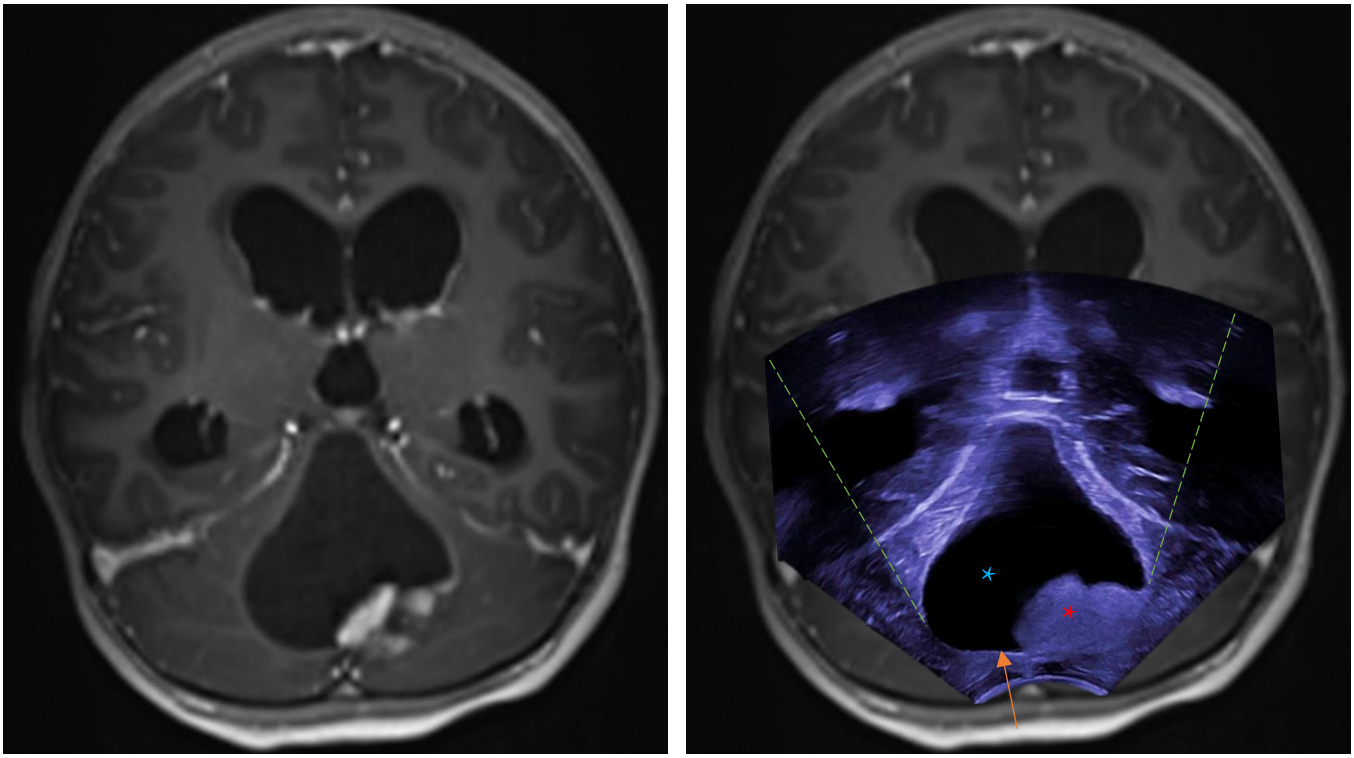

*Figure 5.1: The image on the left shows the preoperative T1 weighted Gadolinium enhanced MR image of the lesion in the posterior fossa. The image on the right shows the ultrasound image overlaid on the MRI. The solid (red) and cystic (blue) components of the tumor are clearly visible. The orange arrow shows the entry point of the iUS guided Dandy needle. The green lines demarcate the area that shows AEA caused by the large cysticcomponent.*

used to confirm a GTR, assuring no additional resection was necessary. Overall, iUS did not pose a burden on the surgical workflow. Preparation of the US machine is done during craniotomy, which led to no increase in total OR time. The swipes that were made were all made within 3 minutes, again not leading to a big increase in OR time. Using the iUS may even have led to a quicker and safer approach to the tumor, since the surgeon was assured with the real-time imaging information.

### Case 2

A 3.5 months old girl presented with nausea, vomiting and discomfort suggestive for hydrocephalus. Brain MRI revealed a large contrast enhancing lobular tumor (72.5 ml), suspect for a plexus choroid papilloma, floating in the posterior horn of the right lateral ventricle. The tumor showed adherence via a stalk to the lateral wall of the ventricle. This tumor caused an overproduction of cerebral spinal fluid (CSF) resulting in a hypersecretory hydrocephalus.

Optically tracked neuronavigation was not available, since the baby's skull was too immature to be fixated in a head frame. The presence of fontanelles allowed for ultrasound acquisition without opening the skull, which already provided information about the position and appearance of the tumor. This information confirmed the planned parieto-occipital incision. The B-mode acquisition parameters were set to a depth of 10 cm, a frequency of 10 MHz, a sector width of 140% and an auto-gain of 12 dB. The in-plane resolution was 0.24 mm.

After the craniotomy was performed, the ultrasound transducer was placed on the dura and a peculiar image of the tumor was seen. The intratumoral structure as seen on the preoperative MRI, was more prominently imaged with a higher resolution on iUS. The lobular structure was clearly visible, as shown in figure 5.2. Moreover, it

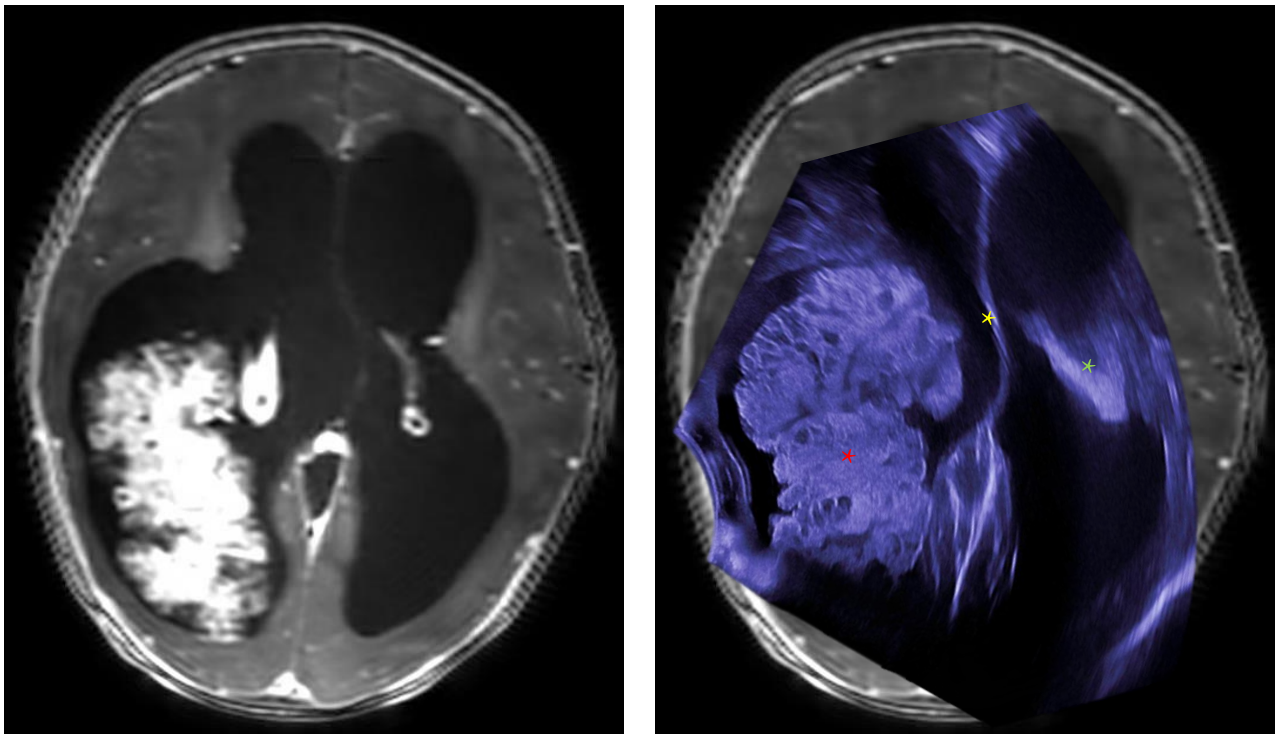

*Figure 5.2: The left image shows the intraventricular lobular tumor on contrast enhanced T1 weighted MRI. The right image shows the ultrasound overlay of the same location. It can be noted that the position of the tumor (red) and normal choroid plexus (green) is different, because of a different head position. The convexity of the septum pellucidum (yellow) caused by the high pressure can be more prominently observed in the ultrasound image.*

can be seen that the tumor has a different location and appearance between the two imaging modalities, because of patient positioning. The patient's head was tilted to the left for surgery, which resulted in the movement of the tumor due to gravity. The same effect can be observed in the contralateral ventricle for the normal functioning choroid plexus, which is hyperintense on ultrasound imaging. It can also be observed that the septum pellucidum is convex towards the left ventricle, because of the CSF accumulation in the right ventricle.

After opening of the dura, iUS was used to guide the placement of a Dandy needle through the cortex into the posterior horn of the right lateral ventricle. This resulted in drainage of the CSF out of the lateral ventricle, immediately releasing pressure. Then the tumor was shrunken by coagulation to work towards the stalk, which was coagulated and dissected, which allowed tumor removal. A final iUS swipe was made to confirm total extirpation of the tumor.

This case highlights the potential iUS has for high resolution real-time imaging. The intratumoral structures were considerably better defined compared to the preoperative MRI. Besides, the movement of the head of the patient resulted in the movement of the tumor, changing the anatomy compared to the preoperative MR imaging. iUS showed the most recent representation of the anatomy, allowing the surgeon to optimize the surgical strategy.

## Case 3

A 14 year old boy presented with episodes of local temporal lobe epilepsy with bilateral spreading. T1 weighted contrast enhanced MRI revealed a non-enhancing lesion (26.2 ml) in the right temporo-insular region, suspect for a dysembryoplastic neuroepithelial tumor (DNET), see figure 5.3.

The patient was positioned supine with the head tilted to the left, a temporal incision is made and craniotomy is performed. Before opening of the dura, ultrasound images were made with parameters set to a depth of 7.5 cm,

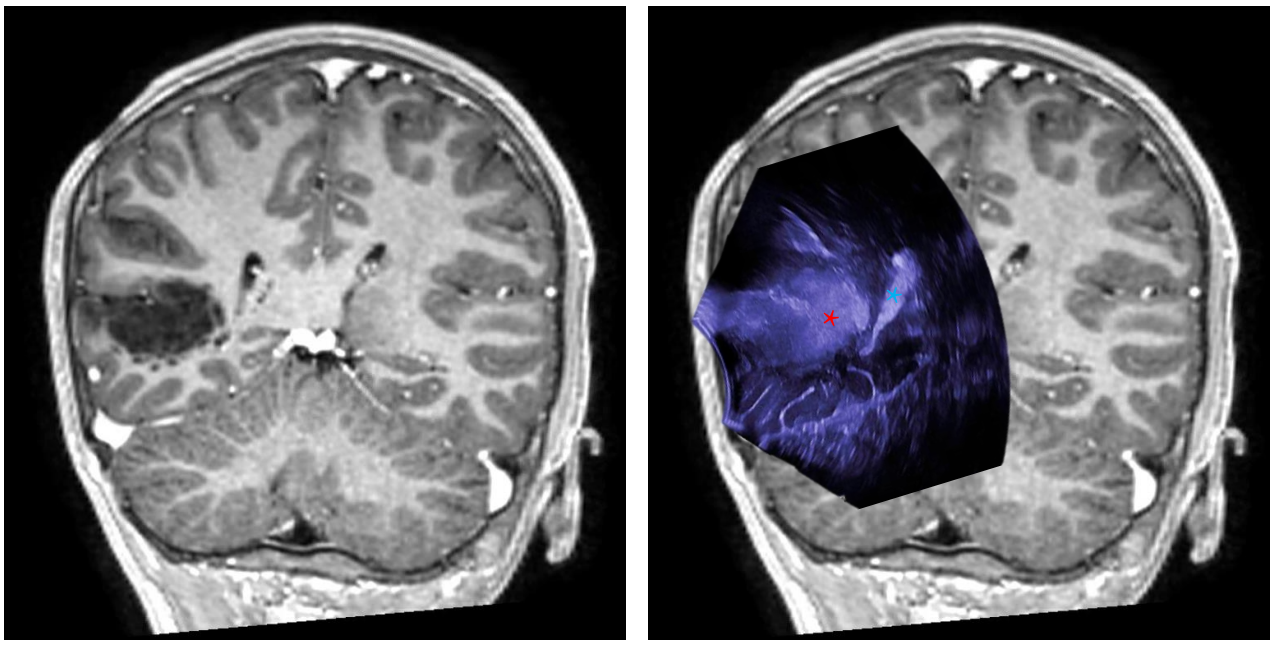

*Figure 5.3: The left image shows the hypointense nodular lesion in the right temporal lobe on T1 weighted contrast enhanced imaging. The right image shows the concordant iUS image overlay, where the lesion is hyperechogenic (red). The choroid plexus in the lateral ventricle is shown as a sharply defined hyperechogenic structure (blue).*

a frequency of 8 MHz, a sector width of 100% and an auto-gain of 12 dB. The frequency was decreased from 10 to 8 MHz to improve depth resolution. The tumor was quickly recognized as a clear hyperechogenic structure, as shown in figure 5.3. Besides the tumor, the tentorium became apparent and served as a landmark. Similarly, the choroid plexus in the right lateral ventricle was identified by the characteristic morphology and ultrasound hyperintensity. It can be observed that the tumor lies in very close vicinity from the lateral ventricle, which provides the surgeon with valuable information regarding the maximal extent of resection.

After dura opening, the tumor was quickly identified and appeared slightly grayish compared to the surrounding tissue. After some debulking, more white tissue began to show, which created the impression of being close to the boundaries of the tumor. Before a iMRI scan would be made, iUS was used to identify residual tumor. It seemed that only a third was removed yet and that the impression solely based on microscopic vision was incorrect. With the additional iUS information, the surgeon decided to continue tumor debulking. This time, knowing that some parts of the tumor are intrinsically grown between white matter tissue. After removing a small part of the white matter, a larger part of the grayish tumor tissue appeared. Eventually, iUS was used several times to update the debulking process. This led to efficient and safe tumor removal, steering the surgeon more directly to areas that still contained tumor tissue. Figure 5.4 demonstrates the debulking procedure, where the choroid plexus is delineated in blue. This structure was of importance in determining the maximal safe extent of resection.

When the maximal safe extent of resection was reached based on iUS, an iMRI scan was made. This revealed some satellite lesions still being in situ, in concordance with iUS imaging. However, the lesions were small and deeply seated and because of the low grade character of the tumor, it was deemed unnecessary taking the risk to remove these. The patient did not experience any epileptic episodes after surgery.

This case highlights the flexibility and versatility of iUS. Without iUS, at least one additional iMRI scanning session would have been needed, prolonging the procedure with an hour. Besides, the quick and flexible application of iUS imaging during surgery, allows the surgeon to obtain new information instantly. This reduces the uncertainty during surgery and led to a more efficient and safer way of tumor debulking. Moreover, this

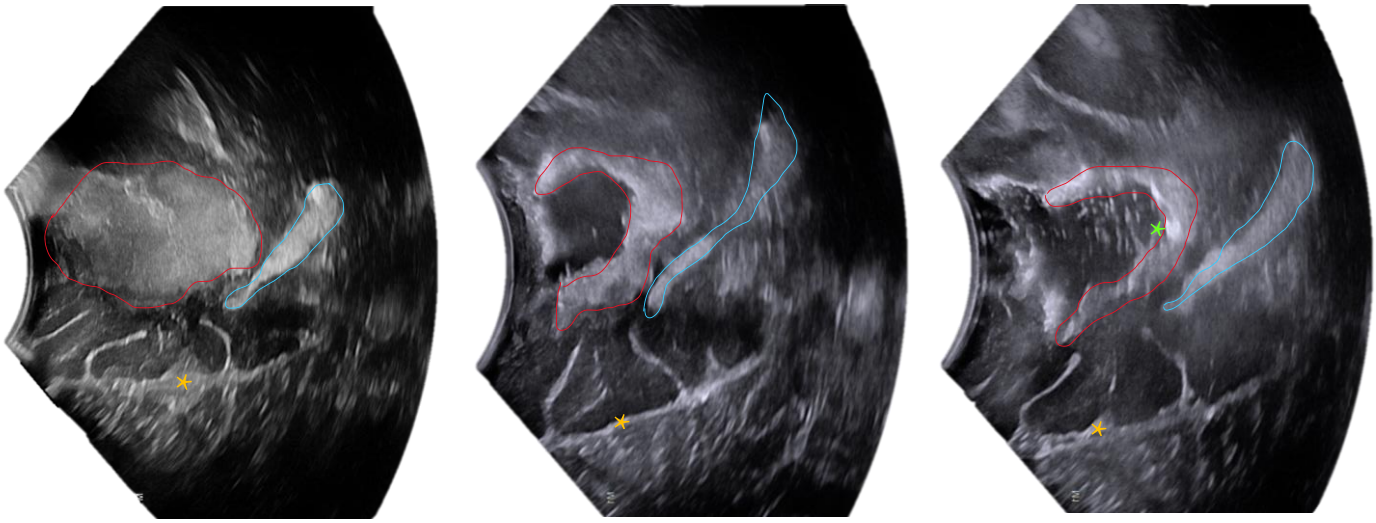

*Figure 5.4: Serial iUS swipes were made to monitor the resection progress of the tumor (red). The right lateral ventricle (blue) lies in close vicinity to the tumor and serves together with the tentorium (orange asterisk) as landmarks in localization. While keeping track of the landmarks, the surgeon can monitor the amount of residual tumor. In the right image, white specks can be observed in the resection cavity, which are small air bubbles dissolved in the saline solution. At the bottom of the cavity (green) a hyperechoic structure can be observed, this is probably a blood product. Both effects affect the image quality and interpretation.*

shows again the importance of iUS imaging before dura opening. Without this initial baseline, discrimination between tumor and choroid plexus would have been difficult. Also, while surgery progresses, the surgical field is more disturbed. More blood products are present and air is present in the cavity. Both effects affect the interpretability of the image, see description of figure 5.4.

## Discussion:

In this chapter, three patient cases were highlighted in which iUS has shown to be of additional value to the surgical procedure. We demonstrated that without neuronavigation, iUS can be easily deployed and it provides detailed anatomical information about the tumor and neighboring structures. In the first case, iUS showed with high detail where the tumor was attached to the cerebellar cortex, upon which the surgical strategy was adapted. Moreover, iUS was used as a reliable method for very precise needle placement, avoiding puncturing the tumor while decompressing the cyst. The similar approach was demonstrated in the second case to release excessive CSF from the lateral ventricle. This method may be more reliable than the navigation pointer. With iUS, the surgeon can 'see inside' and follow the tip of the needle, whereas the navigation pointer only shows the entry point. In the second case, preoperative imaging would not have sufficed, since the tumor freely moved within the ventricle, depending on patient positioning.

There are some challenges we observed regarding iUS acquisition. The iUS image with the best image quality will always be the image made right before dura opening. At this stage, the surgical field is still undisturbed and free of blood products and air. Once the dura is opened, CSF will drain from the brain and air can enter the brain. For every iUS acquisition, it is important to fill the cavity with saline solution to remove as much air as possible. However, for some surgical approaches like the pterional approach, it is more difficult to keep the cavity filled with saline solution while acquiring images. Another challenge is the brain shift occurring during surgery, to assure a good surface contact with the transducer, the transducer needs to be placed deeper in the brain. This causes the image to be less comparable to previous iUS images. This effect can be observed in figure 5.4, the tentorium (orange asterisk) appears to be at another position, because the transducer has been inserted deeper into the cavity. These challenges complicate interpretation of the image at a later stage in surgery. The image quality decreases due to presence of artifacts and images are less comparable, complicating landmark and tumor identification. Therefore, navigated ultrasound is desirable to maintain image interpretability, when anatomy is hard to recognize or when image quality decreases.

# VI

# Diagnostic value of navigated intraoperative ultrasound in pediatric oncological neurosurgery

## Introduction

Pediatric central nervous system tumors are known for having a poor prognosis and are the most common cause of death among all types of childhood cancers [1]. Gross surgical resection of tumor tissue without inducing major neurological deficits, remains the main treatment option in most cancer types [2]–[4]. Enlarging the extent of resection (EoR) is associated with prolonged survival, described for both the adult and pediatric patient population [5]–[8]. Therefore, surgeons are striving to achieve a near-complete resection.

Reaching near-complete resection by increasing the extent of resection becomes increasingly complex when debulking of the tumor proceeds for several reasons. First, tumor tissue may visually appear rather similar to healthy brain tissue, leaving the surgeon with the dilemma of further reducing tumor volume and increasing the risk of inducing neurological deficit when approaching the tumor borders. Second, since neurosurgery is often operating through a keyhole, looking around corners is rather difficult. This makes the surgeon blind to areas potentially containing tumor tissue. Third, the registration of the neuronavigation becomes increasingly less accurate due to brain shift. When opening the dura, loss of cerebrospinal fluid and pressure differences will result in gravity-induced brain shift. Another reason for brain shift is debulking of tumor which causes re-expansion of previously compressed tissue. Inaccurate navigation results in abandoning the technique in obtaining reliable information during the procedure. [33], [43] These reasons show the importance of obtaining additional information regarding the localization of the tumor during surgery. Additional information might direct the surgeon towards a new strategy in attempting to achieve the previously set surgical goal.

Several techniques have been used to identify tumor tissue intraoperatively, of which intraoperative MRI (iMRI) and intraoperative ultrasound (iUS) play an increasingly important role. These techniques enable visualization of the tumor intraoperatively to be able to 1) assess whether the surgical goal is reached, 2) identify potential tumor remnants or 3) update the neuronavigation with newly acquired data. iMRI and iUS both have their advantages and disadvantages, iMRI is known to be a burden on the surgical workflow and a time and resource-

intensive modality. On the other hand, iUS is unable to create a synoptic view of the brain and the image quality is often inferior to MRI, hampering interpretation.

### Navigated iUS related to iMRI

As discussed in chapter III.II, the integration of iUS with IGS led to an increase in interpretability of iUS images during surgery. The iUS images provide an update overlaid on top of the preoperative MRI. However, iUS shows to be more prone to artifacts and iMRI is therefore still regarded as gold standard in detecting residual tumor during surgery.[48] In literature, most studies focused on the value of either one of the two modalities. Only two recent studies report on the integration of neuronavigation, iUS and iMRI [34], [54]. Both studies focused on the adult population, where tumors are often more peripherally located. Only one study by Carai et al. [67] describes the role of iUS in the pediatric population, however without the usage of neuronavigation and iMRI. A difference between the adult and pediatric population may be observed. As described in chapter II, pediatric tumors are often more centrally located which means that tumors need to be imaged at a greater depth. As described in chapter III, the spatial resolution of iUS decreases with increasing depth due to attenuation of high frequency acoustic waves. This could complicate visualization of deeply seated tumors with iUS.

The abovementioned studies report on the specificity and sensitivity of iUS in detecting residual volume, and demonstrate qualitative assessment of the images. Only Hou et al. [54] reported quantitatively on the volume of the segmentations created on iUS and iMRI. However, no metrics regarding position or voxel intensity for comparison between the two modalities were mentioned.

In this study we investigate the diagnostic value of iUS in pediatric surgery. The diagnostic value is defined two-fold. First, the diagnostic value of iUS in pre-resection tumor visualization: determining size, location and appearance, is compared to preoperative MRI. Second, the diagnostic accuracy of iUS in detecting residual tumor volume is clinically assessed. Moreover, the diagnostic value of iUS in visualizing tumor volume and position is quantitatively compared to intraoperative MRI.

Based on previous studies [31], [34], [35], [41], [52]–[54], [67], [68], we hypothesized that iUS has a good diagnostic value. First, in visualizing tumor size and location compared to preoperative MRI before resection. Second, we hypothesize that iUS has a good diagnostic accuracy (>80%) in detecting residual tumor.

## Materials and methods

### Patient population and inclusion criteria

All patients undergoing an image guided neurosurgical tumor resection procedure with the use of iUS and iMRI were included in this prospective study between March and June 2023 at the Princess Máxima Center in Utrecht. Exclusion criteria were: 1) if no neuronavigation, iUS or iMRI was available or 2) if the severeness of artifacts on iUS imaging did not allow any image interpretation.

### Data acquisition

In this study, iUS images are acquired at two time points during the surgical procedure. The first acquisition is done right before opening of the dura, this acquisition is called iUS1. The second acquisition is done right before iMRI scanning, this acquisition is called iUS3. No additional resection can be done after iUS3, because this would change the anatomical situation before iMRI acquisition. Nevertheless, an optional acquisition can be made

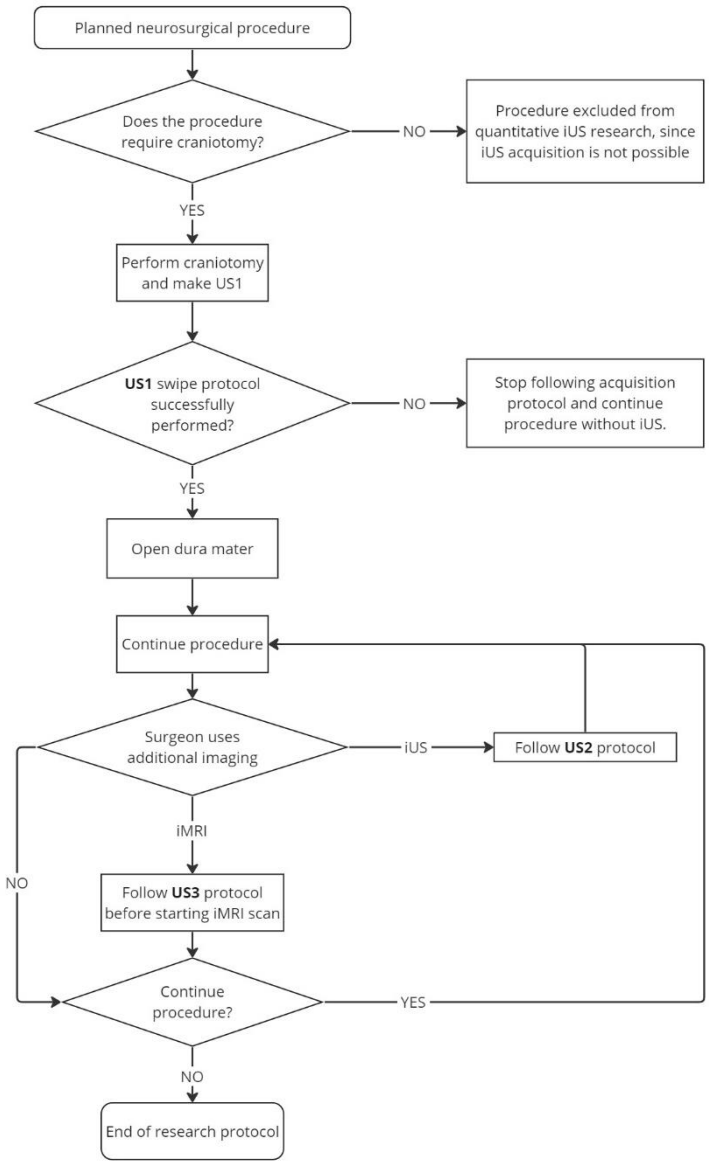


*Figure 6.1: Acquisition protocol of iUS. iUS1 is the acquisition right before dura opening. iUS2 is an optional acquisition, which is made on surgeon's desire. The final acquisition moment is just before iMRI scanning, called iUS3.*

upon desire of the surgeon to check the resection progress, this acquisition is called iUS2. This chronological acquisition protocol is visualized in figure 6.1.

### *Intraoperative Ultrasound*

The intraoperative ultrasound acquisitions were performed with a 2D neuro-cranial curvilinear transducer (N13C5, BK5000, BK Medical, Denmark), which has a frequency range of 13-5 MHz and a surface area of 29x10 mm. The initial parameters for iUS acquisition were a frequency of 10 MHz, a sector width of 140%, and auto-gain was enabled. An initial estimation of the acquisition depth was based on a depth measurement in the pre-surgical planning software (Brainlab, Munich, Germany), which often resulted in an acquisition depth between 7 and 11 cm. Before acquisition, the reference array base was clamped to the transducer, then the transducer and cable were placed in a sterile sheath, assuring that ultrasonic gel covered the entire probe surface. Finally, the sterilized reference array could be screwed tightly on the base, which is now covered by the sterile sheath, as

depicted in the left image of figure 6.2. Now, the ultrasound transducer can be tracked by the Brainlab Buzz Navigation system (Brainlab, Munich, Germany), see figure 3.11.

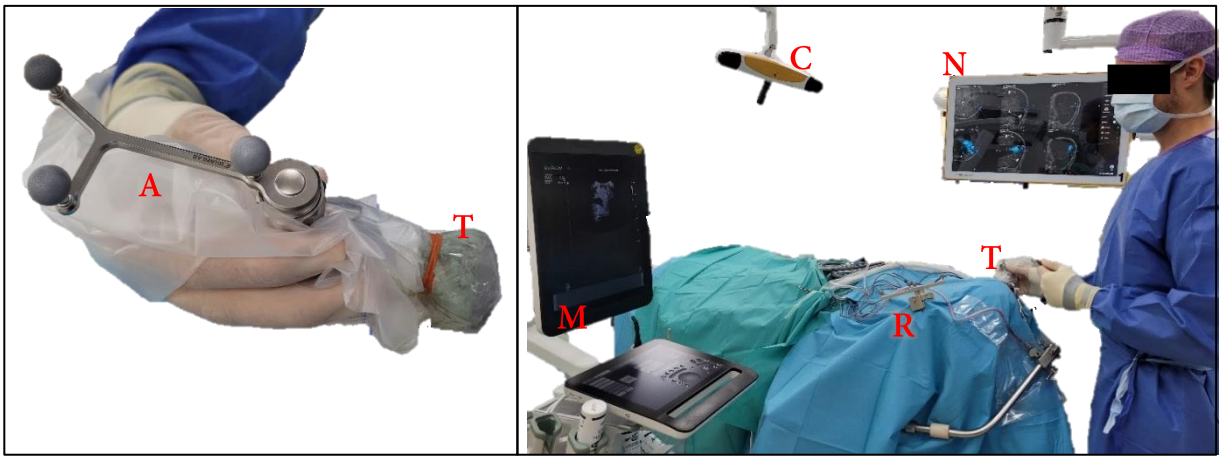


*Figure 6.2: The left image shows the transducer draped in a sterile cover, with ultrasonic gel at the transducer tip (T). The sterile array with fiducials (A) is mounted on top. In the right image, camera (C) will track the transducer's (T) position relative to the reference array (R). The live ultrasound image can be viewed on the iUS machine (M), whereas the navigated image can be seen on screen (N). Here the integration with preoperative MRI is visualized. Volumes that are acquired are also shown here.*

The right image of figure 6.2 shows the setup of the integration of the ultrasound machine (M) with the neuronavigation (N), where transducer (T) is tracked by the camera (C), which determines the location relative to reference array (R). Before using the transducer to create a 3D volume, an initial exploration of the tumor in 'live mode' was done. This allowed for fine-tuning of the initial parameters. If necessary, depth was adjusted and if the contrast of deeper structures was low, the frequency was decreased to 8 MHz.

The integration with the neuronavigation allows for 3D volume reconstruction of consecutive 2D B-mode iUS images in the navigated iUS module (Brainlab, Munich, Germany). The position of the 2D image is stored and used by the software in reconstructing the 3D volume, an example is provided in appendix 6A. The resolution of the 3D images was 0.24x0.24 mm in-plane resolution and 1mm slice thickness. Depending on the number of acquired 2D images, volume reconstruction took up to one minute. After 3D volume reconstruction, the initial scanning parameters were kept the same for additional scans, only the frequency was decreased to 8 MHz, if necessary.

For every acquisition moment, at least two volumes were acquired, each in a different orthogonal imaging plane, e.g. for a suboccipital approach, images were acquired in axial and sagittal planes. The first image of the volume should be further than the outer boundary of the tumor on one side. Then the transducer is moved to scan the entire tumor. Once the other outer boundary is scanned, the acquisition is stopped, this acquisition workflow is depicted in figure 6.3. An elaborate acquisition protocol is included in the appendix 6B.

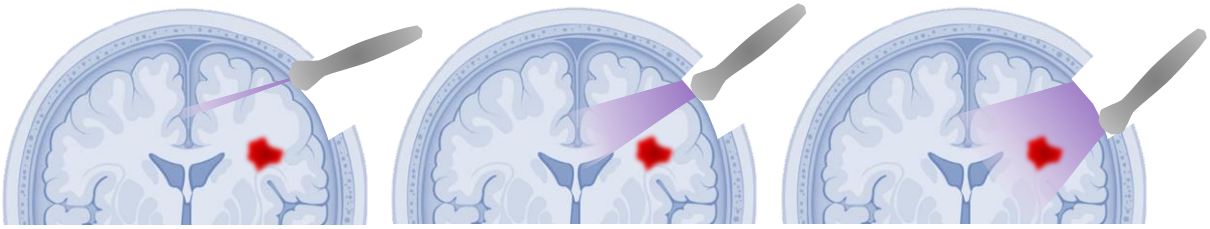

*Figure 6.3: Schematic overview of iUS acquisition of volume. The acquisition is started at one side of the tumor, with the first frames outside the tumor. Then the transducer is moved to scan the entire tumor volume. The acquisition is stopped once the tumor is no longer visible in the iUS images.*

### *Intraoperative MRI*

Two different MRI acquisitions are defined for comparison with iUS volumes, one before and one during tumor resection. Every patient was scanned at least one day before surgery, either for diagnostics or surgery. These images were used to plan the procedure upon, e.g. the surgical trajectory and the tumor segmentation. Although interhospital differences were present in imaging protocols, the protocols always contained T1 weighted imaging with and without gadolinium and T2 weighted imaging. The resolution was varying between 0.45 and 1 mm in-plane resolution and 0.6 and 1 mm slice thickness.

In the intraoperative setting, patients were scanned with a 3T 70 cm bore MRI scanner (Ingenia Elition X , Philips Medical System Nederland B.V., Best, Netherlands). If the patient was eligible for automatic registration based on iMRI, the patient was scanned under general anesthesia in the surgical position before incision. This imaging protocol consisted of three 3D scans; two T1-weighted Magnetization Prepared Rapid Gradient Echo (MPRAGE) images and a T2-weighted image without contrast. In the intraoperative setting, the same protocol was run, with an additional T1-MPRAGE image with gadolinium. The specifications of the scanning protocols are provided in the appendix 6C.

## Clinical assessment of residual tumor

After acquisition of the iUS3 volume, the surgeon assessed the iUS image for the presence of residual tumor, which was done before iMRI acquisition. If the images were inconclusive, the neuroradiologist was consulted for assessment. The presence of residual tumor on iMRI was evaluated by the surgeon in consultation with the neuroradiologist. Based on this interpretation, the surgeon decided whether continuation of tumor resection was necessary and safe. If residual tumor was detected in both iUS3 and iMRI, iUS3 was included for further quantitative analysis. The data form that was used during the OR for qualitative assessment of the iUS images is included in appendix 6D.

## Creating segmentations

After data acquisition of iUS1 and iUS3 scans, further analysis was similar for both volumes. First, the tumor segmentations were created using a semi automatic segmentation tool (Smart Brush in Object Manipulation module, Brainlab, Munich, Germany). The image quality of the volume reconstruction was assessed for all acquisitions in iUS1 and iUS3. For both iUS1 and iUS3, the least artifactual acquisitions were used for further analysis. The quality of the segmentations is dependent on the contrast differences between tumor and surrounding tissue as interpreted during segmentation. If structures on iUS imaging were unidentifiable due to artifacts or incomplete acquisitions, no segmentation was created and the volume was excluded from further analysis. All solid tumor components were segmented in all images, large solitary cystic components (> 2 $cm^3$) were excluded from the segmentation, avoiding bias in the intensity based metrics as described below.

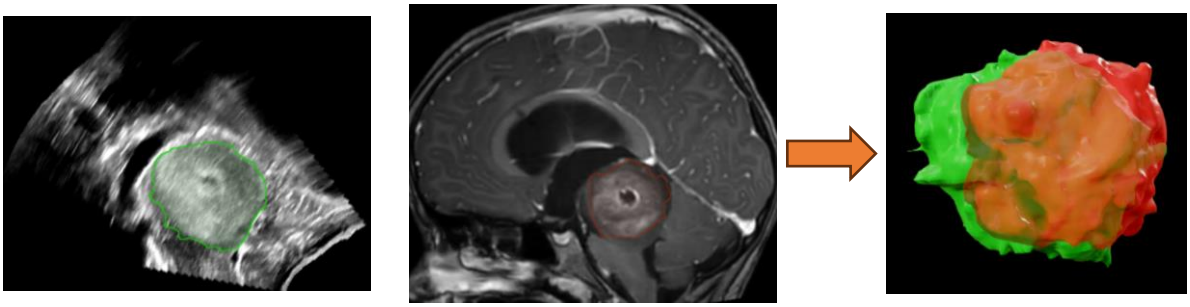

*Figure 6.4: Examples of iUS1 and preoperative MRI segmentations are shown in respectively green and red. A 3D volume rendering is shown in the right image.*

The iUS tumor volumes are first segmented in both iUS1 and iUS3, an example is shown in the left image of figure 6.4. Second, the tumor was segmented in the T1-weighted gadolinium enhanced images, in both preoperative and intraoperative scans. Clinically, T1-weighted gadolinium enhanced images are typically used to plan (additional) tumor resection. Therefore, the segmentations were based on the gadolinium enhanced images. To verify that non-enhancing parts of the tumor are included in the segmentations, T2-weighted imaging was used as guidance. However, the segmentation boundaries were based on gadolinium enhanced images. Discrimination between lesion and ischemia was based upon the radiological report. Images and segmentations were exported to DICOM (Digital Imaging and Communications in Medicine ) image format for further analysis in Python.

## Data analysis

The data analysis pipeline is divided in three parts. In the first part, image fusion pairs were retrieved and transformation matrices were constructed to transform the source image to the destination image. In the second part, the transformation matrices were applied to the source image and the corresponding segmentation. In the last part, different quantitative metrics were derived from the transformed segmentations. The data analysis were executed in Python (version 3.7) for quantitative analysis of the segmentations, a schematic overview is provided in figure 6.5. Python scripts are provided in supplementary materials.

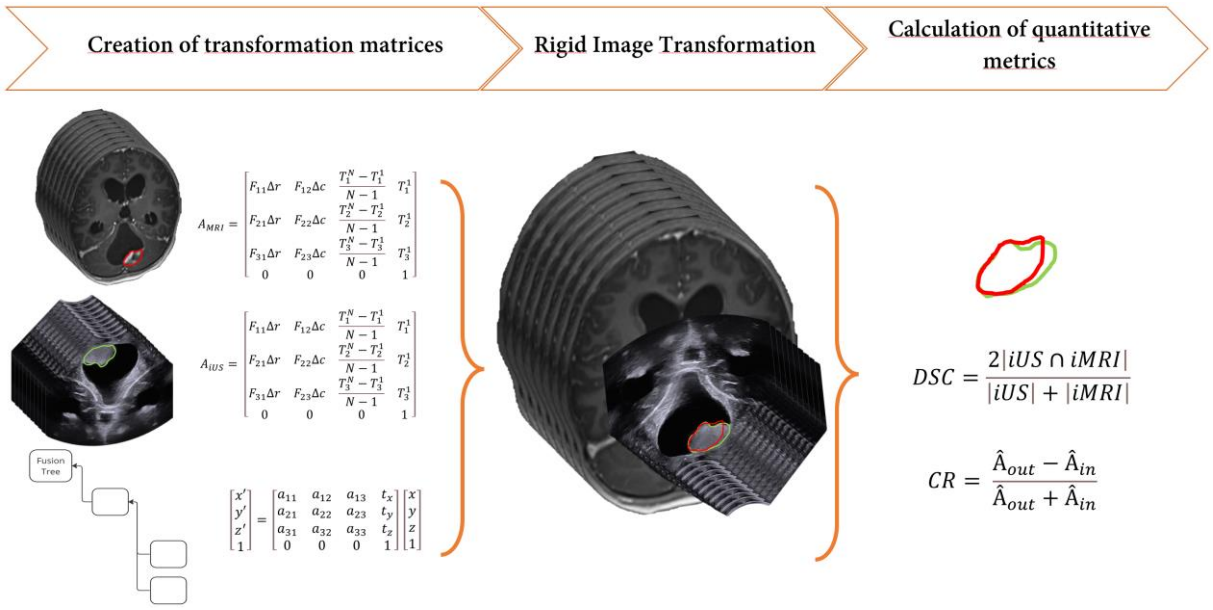


*Figure 6.5: Overview of data analysis pipeline. The first part involves creation of transformation matrices, combining matrices that are retrieved from the software an DICOM information. The second part involves rigid image transformation, where the combined 4x4 transformation matrices are applied to bring the iUS volume and segmentations in the MRI destination volume reference space. In the last part, the quantitative metrics are derived from the two transformed segmentations.*

### *Creating transformation matrices*

During data export, information of the fusion between iUS and iMR images is saved in 4x4 fusion matrices, while the original images are preserved. The fusion matrices need to be applied to the images, to enable comparison between the volumes in a coordinate space with the same frame of reference (FoR).

The images are stored in pixel coordinate space, yet the fusion matrix is applied to the images in millimeter coordinate space. Therefore, to transform an image from the source to the destination coordinate space, the

source image first needs to be transformed to millimeter coordinates, the transformation matrix for a multi slice volume derived from the DICOM information is provided in equation 6.1. F is derived from the Image Orientation Attribute with tag (0020, 0037), Δr and Δc are derived from the Pixel Spacing Attribute (0028, 0030). T is the Image Position Attribute (0020, 0032), which is a vector for multi slice volumes. $T_1^1$ refers to the position of the first image, N refers to the number of slices.

$$A_{multi} = \begin{bmatrix} F_{11}\Delta r & F_{12}\Delta c & \frac{T_1^N - T_1^1}{N-1} & T_1^1 \\ F_{21}\Delta r & F_{22}\Delta c & \frac{T_2^N - T_2^1}{N-1} & T_2^1 \\ F_{31}\Delta r & F_{23}\Delta c & \frac{T_3^N - T_3^1}{N-1} & T_3^1 \\ 0 & 0 & 0 & 1 \end{bmatrix} \quad (6.1)$$

*Rigid image transformation*

As discussed in Chapter III, a benefit of using 4x4 transformation matrices is the possibility to easily combine transformations by multiplying the matrices. By multiplication, a source image ($I_{source}$) can directly be transformed to the FoR of the destination image. Depending on the data plans in the Brainlab software, multiple fusion matrices may be applied to transform to the desired FoR, the order of fusions depends on the fusion tree created by Brainlab (see appendix 6E). Another benefit of using transformation matrices is the ability to invert the transformation by inverting the matrix. This is done in the last step to transform from millimeters to pixel coordinates. An example of a transformation matrix multiplication from source to destination image coordinates is shown in equation 6.2; I indicates the image volume, A indicates the matrix relating pixel to millimeter coordinates. Fusion matrices are indicated by F. The order of this matrix multiplication is important to obtain the desired transformation. After transformation of the source image to the destination reference spacing, a transformed image needs to be reconstructed. Because and image is a collection of discrete points, changing the size and orientation of an image, requires resampling of voxels to fill missing information or merge information. Cubic spline interpolation was applied to resample the intensities of the transformed image.

$$I_{dest} = A_{dest}^{-1} F_2 F_1 A_{source} I_{source} \quad (6.2)$$

*Quantitative metrics*

To quantify the diagnostic value of iUS in detecting and characterizing tumor tissue, three metric categories are posed. These categories are metrics based on pixel intensity, volume and overlap of the created segmentations. For iUS1 segmentations, all three metric categories are determined. For iUS3 segmentations, only volume and overlap based metrics are calculated. Since in this stage the detectability and amount of residual tumor mass is more important than tumor characterization based on pixel intensity.

First, the pixel intensity based metrics are derived from the segmentations. The first metric in this category is the degree of heterogeneity of pixel intensity within the tumor. This metric is described as the normalized standard deviation of the pixel intensities within the segmentation. For instance, a tumor with homogeneous pixel intensity, will show a low normalized standard deviation. We hypothesized that a tumor with high heterogeneity, i.e. with enhancing and non-enhancing parts, also shows higher heterogeneity in the iUS, since the tumor structure is more heterogeneous. The second metric to quantify pixel intensity is the contrast ratio, which is defined as the difference in intensity between tumor and surrounding tissue. The larger the contrast ratio, the better the tumor is detectable in the image, whereas a contrast ratio of zero means poor contrast. A

negative contrast ratio indicates a hyperintense tumor. The contrast ratio is defined in equation 6.3, where Â indicates the mean voxel intensity, regarding the in- and outside of the tumor segmentation.

$$CR = \frac{\hat{A}_{out} - \hat{A}_{in}}{\hat{A}_{out} + \hat{A}_{in}} \qquad (6.3)$$

Since the contrast difference is only important in identifying the tumor at the tumor boundaries, the region outside the segmentation was defined as the area after a morphological dilating operation with a structural element of 2x2x2 px was performed. Likewise, the region inside the segmentation was defined as the volume of the segmentation after a morphological eroding operation, to avoid including segmentation errors at the boundaries of the tumor.

Second, the overlap based metrics were calculated, which are divided into the Dice Similarity Coefficient (DSC) and the Hausdorff distance [69]. The DSC provides an indication of the degree of overlap, combining volumetric and positional information. The expression for DSC is provided in equation 6.4, where twice the set of voxels in the iUS and iMRI segmentations is divided by the sum of both volumes. The degree of overlap is inherent to the quality of the segmentation, since this affects the volume and morphology. Besides, the quality of the registration for neuronavigation is important for optimal positioning of the navigated iUS on the MRI, therefore also affecting the DSC. A DSC ranging between 0.7 and 0.9 is considered as a good similarity of the volumes between the both modalities.

$$DSC = \frac{2|iUS \cap iMRI|}{|iUS| + |iMRI|} \qquad (6.4)$$

Since the DSC is sensitive for small volumes, Hausdorff distances and volume errors are also calculated. The Hausdorff distance describes the Euclidean distance between every individual point in one volume to the closest point in the other volume. The maximum Hausdorff distance is prone to outliers, therefore the 95$^{th}$ percentile is calculated. Likewise, separate HD 95$^{th}$ percentile for the decomposed distances are calculated, so for the x-, y-, and z-direction in the destination image. These decomposed HD values can indicate if a systemic shift towards one direction is existent, whereas the HD 95th percentile is non-directional. A HD 95th percentile smaller than 1 cm was regarded as clinically relevant, since this approaches the surgical margins according to literature. [70], [71]

In the last category, the volumetric based metrics are defined as the absolute volume errors. The absolute volume error is defined as the absolute difference between the iUS and iMRI volume. To show the effect of total volume of the tumor on the absolute volume difference, Bland-Altman plots are created.

## Results

A total of nineteen patients that underwent a tumor debulking procedure with navigated iUS were included between March and June 2023. The patient population consisted of 12 males and 7 females, the mean age was 8.1 years (±4.1). The iMRI-based registration method was the most used method (11). The median tumor volume was 21.1 ml (IQR: 34.5 ml), as measured on T1 weighted contrast enhanced MRI. Further patient characteristics are provided in table 6.1.

A total of 18 patients was included for further analysis of iUS1, one patient was excluded due to poor image quality. After tumor debulking, two patients were excluded from further analysis because of artifactual images and unavailability of iUS. Ten patients showed no residual tumor on iMRI and were therefore not included for further qualitative analysis. A total of 7 patients that were included for further quantitative analysis. The patient inclusion for the different analyses is visualized in a flowchart in figure 6.6.

*Table 6.1: Patient population characteristics*

| # | Sex | Age (years) | Tumor type | Surgical position | Registration method | Tumor volume (preop-MRI) [ml] |
|---|---|---|---|---|---|---|
| 1 | Male | 9 | Pilocytic Astrocytoma | Supine | Surface Matching | 20.3 |
| 2 | Female | 3 | Ganglioglioma | Prone | MRI-based | 38.6 |
| 3 | Male | 12 | Pilocytic Astrocytoma | Supine | Surface Matching | 59.4 |
| 4 | Female | 3 | Pilocytic Astrocytoma | Supine | iMRI-based | 42.9 |
| 5 | Female | 9 | Medulloblastoma | Prone | Surface Matching | 21.3 |
| 6 | Male | 10 | Pilocytic Astrocytoma | Prone | iMRI-based | 6.2 |
| 7 | Female | 7 | Craniopharyngioma | Supine | iMRI-based | 37.4 |
| 8 | Female | 3 | Medulloblastoma | Prone | Surface Matching | 21.1 |
| 9 | Male | 9 | Pilocytic Astrocytoma | Supine | iMRI-based | 3.3 |
| 10 | Male | 9 | Pilocytic Astrocytoma | Prone | iMRI-based | 3.7 |
| 11 | Female | 4 | Ependymoma | Supine | Surface Matching | 63.3 |
| 12 | Male | 2 | Ependymoma | Prone | iMRI-based | 107 |
| 13 | Male | 9 | Craniopharyngioma | Supine | iMRI-based | 0.53 |
| 14 | Male | 13 | Giant cell astrocytoma | Supine | iMRI-based | 1.1 |
| 15 | Male | 8 | Low grade glioma | Supine | Surface Matching | 24.4 |
| 16 | Male | 13 | Medulloblastoma | Prone | Surface Matching | 0.35 |
| 17 | Male | 7 | Craniopharyngioma | Supine | iMRI-based | 16.7 |
| 18 | Female | 6 | Medulloblastoma | Supine | iMRI-based | 32.4 |
| 19 | Male | 18 | Low grade glioma | Supine | Surface Matching | 0.88 |

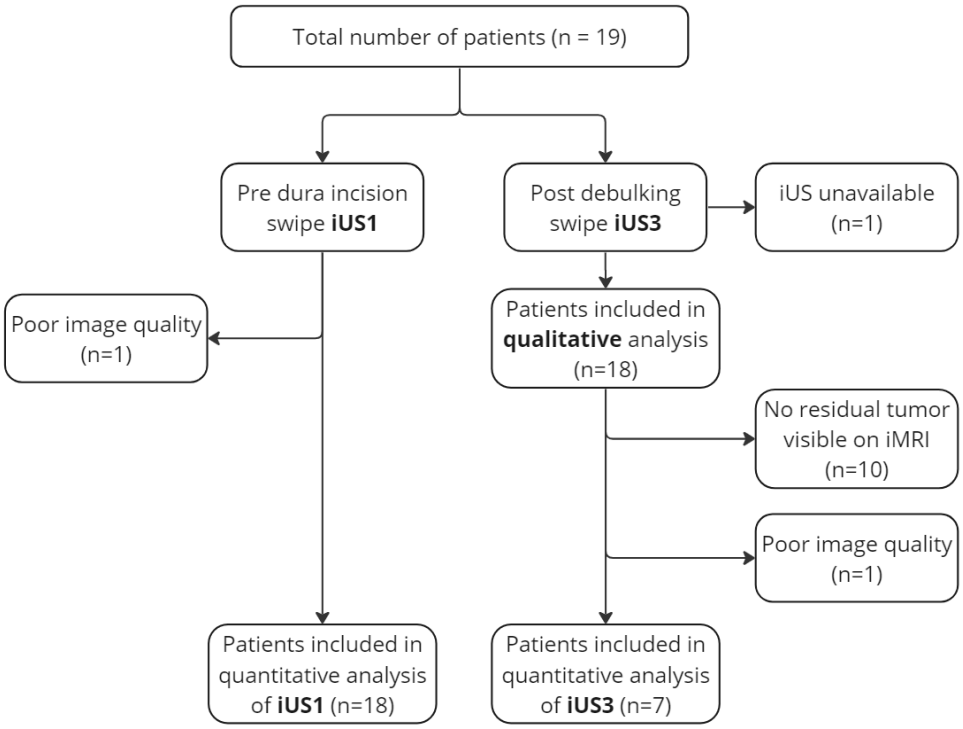


*Figure 6.6: Flowchart of patient inclusion, divided in iUS1 and iUS3 acquisitions.*

## Tumor characterization: iUS1

The tumor was clearly visualized with iUS in 18 patients. One patient has been excluded from iUS1 analysis, because a highly calcified tumor caused acoustic shadowing resulting in poor image quality. Segmentations were created in both iUS1 and preoperative T1w-contrast enhanced MRI in 18 patients. An example of the segmentations is shown in figure 6.7.

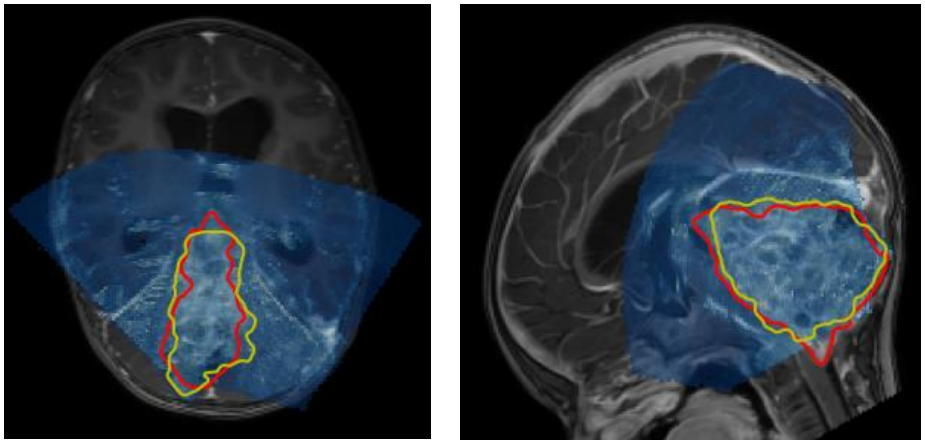

*Figure 6.7: Example of iUS1 (yellow) and preoperative MRI (red) segmentations of a large posterior fossa tumor. In blue the iUS image is overlaid on the T1w-contrast enhanced MRI, based on neuronavigation.*

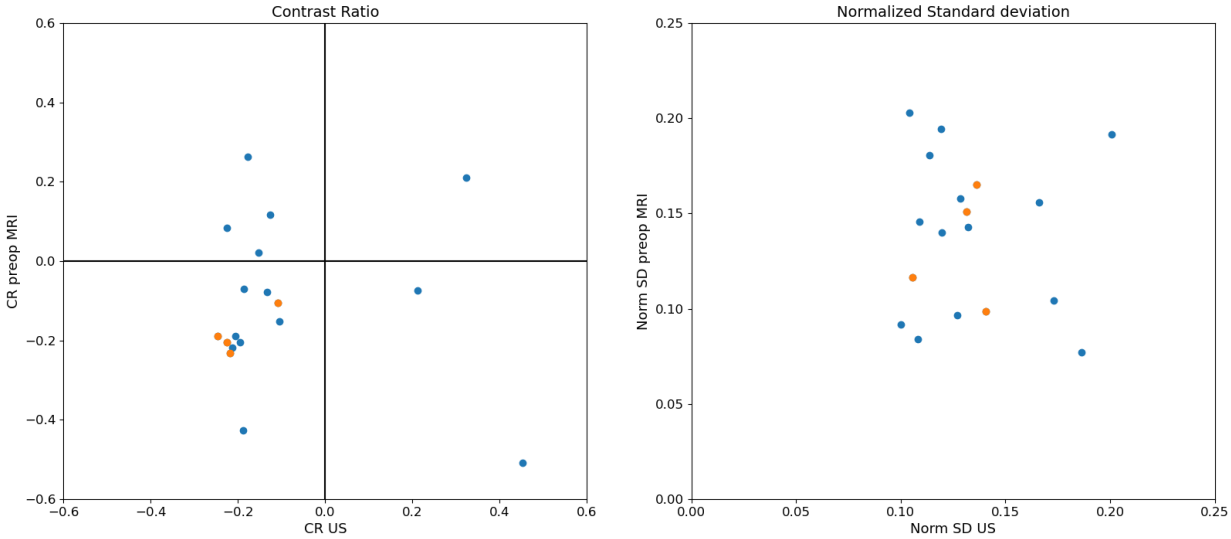


*Figure 6.8: Pixel based metrics for iUS1 acquisition. The image on the left shows the contrast ratio. The image on the right shows the normalized standard deviation. Orange represents high grade tumors, low grade tumors are shown in blue.*

### *Voxel based metrics*

The voxel based metrics are divided in contrast ratio (CR) and the normalized standard deviation. We found a median CR of -0.13 (IQR: 0.20) for MRI and -0.19 (IQR: 0.08) for iUS1. Figure 6.8 shows two scatter plots, where the orange data points show the high-grade tumors, the blue data points show low-grade tumors. This separation is made to show a possible difference in tumor characterization. On the left image, 5 tumors showed positive CR on MRI, indicating a hypointense tumor (CR>0). It can also be observed that all tumors were hyperintense on iUS (CR<0), except for one tumor. Regarding the normalized standard deviation, a median of 0.13 (IQR: 0.03) was found for MRI, and 0.14 (IQR: 0.06) for iUS. Although the ranges of the normalized standard deviation were comparable, it can be observed in the right image of figure 6.8 that there is no correlation between the two modalities, confirmed by a Pearson correlation coefficient of 0.03.

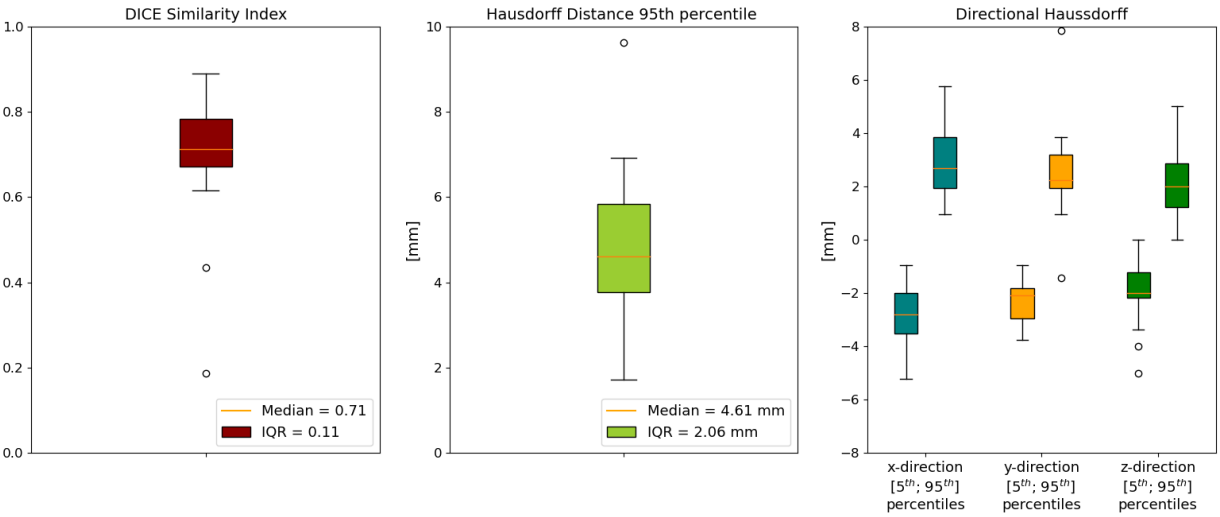


*Figure 6.9: Overlap based metrics for iUS1 acquisition. The left image shows the DSC with a median of 0.61. The middle image shows the Hausdorff distance 95$^{th}$ percentile with a median of 5.84 mm. The directional HD is shown in the right image, the x-, y-, and z-directions are represented by blue, orange and green, respectively. The left boxplot of the pair represents the 5$^{th}$ percentile of HD that describes the negative attribute. The right boxplot represents the 95$^{th}$ percentile of HD, describing the positive attribute. It can be observed that the plots are distributed around zero, showing no bias towards a positive or negative direction.*

### *Overlap based metrics*

The overlap based metrics are described by the Dice similarity coefficient (DSC) and the 95$^{th}$ percentile of Hausdorff distance (HD). For the 18 segmentations, a median DSC of 0.71 (IQR: 0.11) was found. Which is within the range of a good similarity, although on the lower side. The median HD 95$^{th}$ percentile was 4.61 mm (IQR 2.06 mm). The x-, y- and z-components of the HD have been calculated, where the 5$^{th}$ percentile expressed negative distances and the 95$^{th}$ percentile positive distances. The found medians were: -2.80 (IQR: 1.52) and 2.69 (1.90) for the x-direction, -2.08 (IQR 1.14) and 2.22 (IQR 1.25) for the y-direction, and -2 (IQR 0.96) and 2 (IQR 1.66) for the z-direction. The HD 95$^{th}$ percentile that were found are considered clinically relevant, being smaller than 10 mm.

### *Volume based metrics*

The volumetric based metrics are shown in figure 6.9, showing a Bland-Altman plot in the left image. This plot type shows the average of the two volume measurements on the x-axis and the difference between both measurements on the y-axis. Which visualizes the difference between two measurements related to the size of

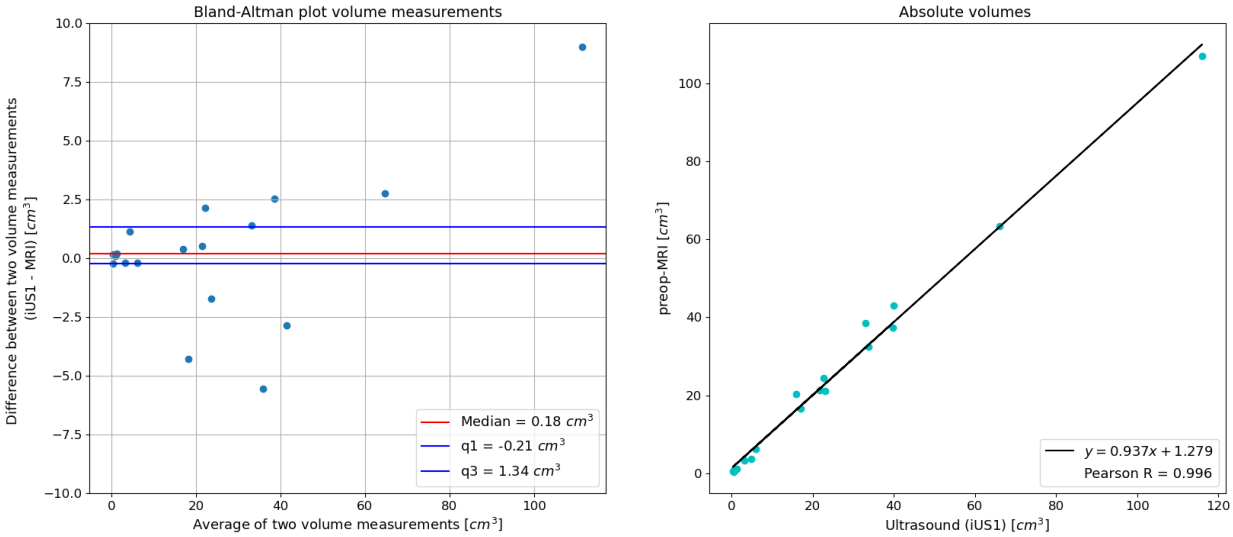


*Figure 6.10: Volume based metrics of iUS1 acquisition compared to preoperative MRI. The Bland-Altman plot in the left figure shows the relation between the average tumor volume and difference between the iUS and MRI measurements. The right figure shows the absolute volumes plotted per patient for iUS and MRI. A regression line is plotted and shows a coefficient of 0.937. The Pearson correlation coefficient is 0.996.*

the tumor volume, with volumes ranging from 0.35 to 107.0 cm³. It can be observed that the difference increases with increasing tumor volumes. Regarding the volume difference, a median of 0.18 cm³ (IQR: 1.55 cm³) was found, which shows that there is no obvious skew to either an over- or underestimation of the volume on iUS1. The median of the absolute value of all volume differences, was 1.28 cm³ (IQR: 2.50 cm³). The right image in figure 6.9 shows a scatter plot with a regression line which shows high correlation between the volume measurements of iUS1 segmentations and preoperative MRI. A high Pearson correlation coefficient of 0.996 was found.

## Residual tumor detection: iUS3

The iUS3 images of 18 patients were assessed for residual tumor by the surgeon. For 8 patients, no residual tumor was seen on iUS. Ten patients showed to have residual tumor based on iUS, in 2 cases interpretation was

*Table 6.2: Contingency table for diagnostic performance of iUS in detecting residual tumor*

| *Residual tumor* | *iUS Pos* | *iUS Neg* | |
|---|---|---|---|
| iMRI Pos | 8 | 0 | 8 |
| iMRI Neg | 2 | 8 | 10 |
| | 10 | 8 | 18 |

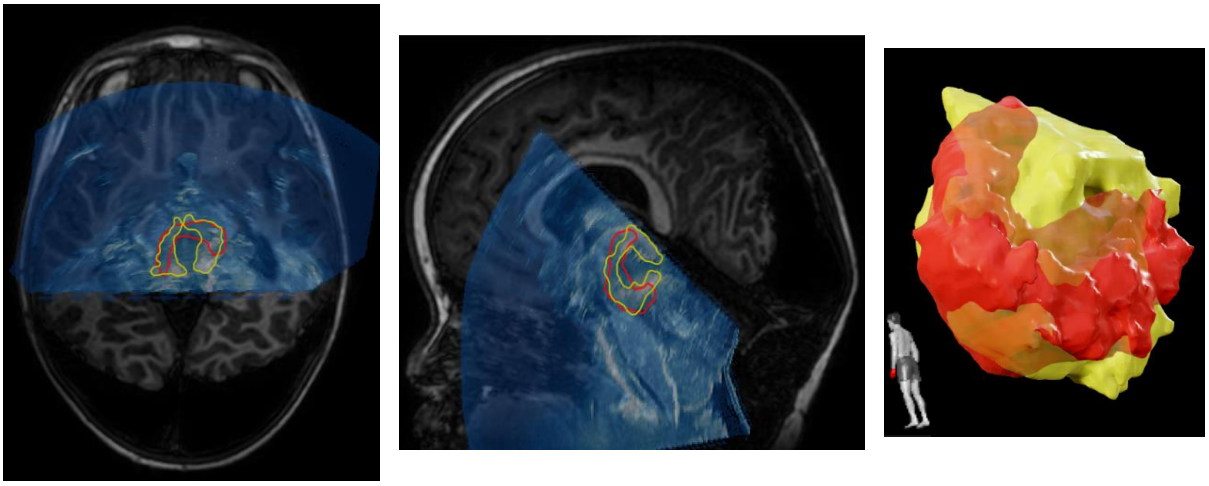

*Figure 6.11: Example of iUS3 (yellow) and iMRI (red) segmentations of residual tumor volume. iUS image is overlaid in blue on T1w MRI. The right image shows the three dimensional rendering of the residual tumor segmentations, iUS (yellow) and iMRI (red). The orientation is shown in the left lower corner.*

impeded due to artifacts. These cases were regarded as positive for residual tumor. Based on the iMRI sequences, 10 cases were assessed negative for residual tumor. In 8 cases, residual tumor was seen on iMRI, as shown in table 6.2. This yielded a sensitivity of 100% and a specificity of 80%. Seven out of eight cases showed no artifacts in the imaging of residual tumor on both iUS3 and iMR images. One case was excluded from further quantitative analysis, since creation of a segmentation was not possible due to poor image quality . A mean extent of resection (EoR) of 74.2% was found for the other seven cases, which were included for further quantitative analysis. An example of a segmentation is shown in figure 6.11.

### *Overlap based metrics*

The DSC and HD 95$^{th}$ percentile were determined for the segmented residual tumor volumes. A median DSC of 0.61 (IQR: 0.17) was found, which was considered a moderate score. A median HD 95$^{th}$ percentile of 5.84 mm (IQR 2.56 mm) was found, which was considered clinically relevant (< 1 cm). The found medians for the directional HD were: -2.61 (IQR: 0.59) and 4.79 (3.01) for the x-direction, -2.61 (IQR 2.00) and 1.92 (IQR 1.35) for the y-direction, and -2 (IQR 1.88) and 2 (IQR 0.56) for the z-direction. Which does not show a clear bias towards one direction, as shown in the right image of figure 6.12.

### *Volume based metrics*

The left image of figure 6.13 shows the Bland-Altman plot of the volumes calculated from the iUS3 and the iMRI segmentations, with volumes ranging from 0.90 to 7.95 cm$^3$. Regarding the volume difference, a median of 0.14 cm$^3$ (IQR: 1.89 cm$^3$) was found. The median of the absolute value of all volume differences, was 0.82 cm$^3$ (IQR: 1.87 cm$^3$). The right image of figure 6.11 shows a scatterplot with a regression line with coefficient 0.633. This coefficient indicates an overestimation of the residual tumor volume on iUS as compared to iMRI. Besides, a

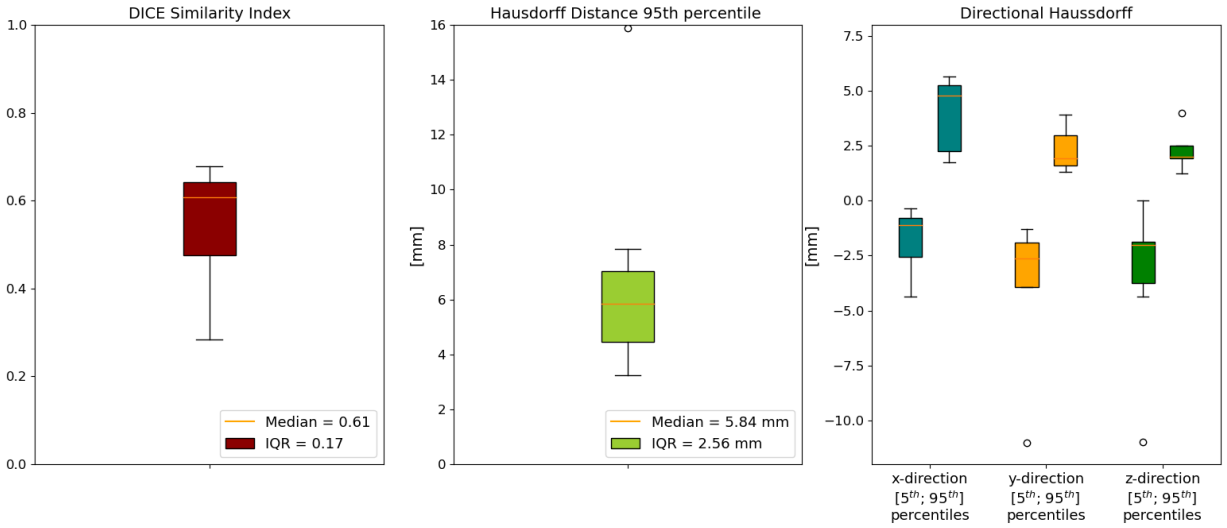


*Figure 6.12 : Overlap based metrics for iUS3 acquisition. The left image shows the DSC with a median of 0.61. The middle image shows the Hausdorff distance 95th percentile with a median of 5.84 mm. The directional HD is shown in the right image, the x-, y-, and z-directions are represented by blue, orange and green, respectively. This plot also shows no bias towards neither the positive nor negative direction.*

lower Pearson correlation coefficient of 0.853 was found, compared to the iUS1 findings. A lower DSC in this analysis can be explained by a slight overestimation of the volume on iUS3 images, whereas the HD 95$^{th}$ percentile shows only a slight increase compared to the US1 acquisitions. Smaller post-debulking volumes have a more pronounced impact on the DSC, as DSC is more sensitive to changes in smaller volumes.

## Discussion

In this study, navigated iUS was used during 19 tumor debulking procedures. Regarding the first iUS acquisition (iUS1), the calculated volumes of the 18 segmentations highly correlated (R=0.996) with the volumes of the MRI segmentations. A good DSC and HD 95$^{th}$ percentile were found and are considered clinically relevant. Besides, all tumors, except for one outlier, showed hyperechogenicity. The metrics contrast ratio and voxel heterogeneity

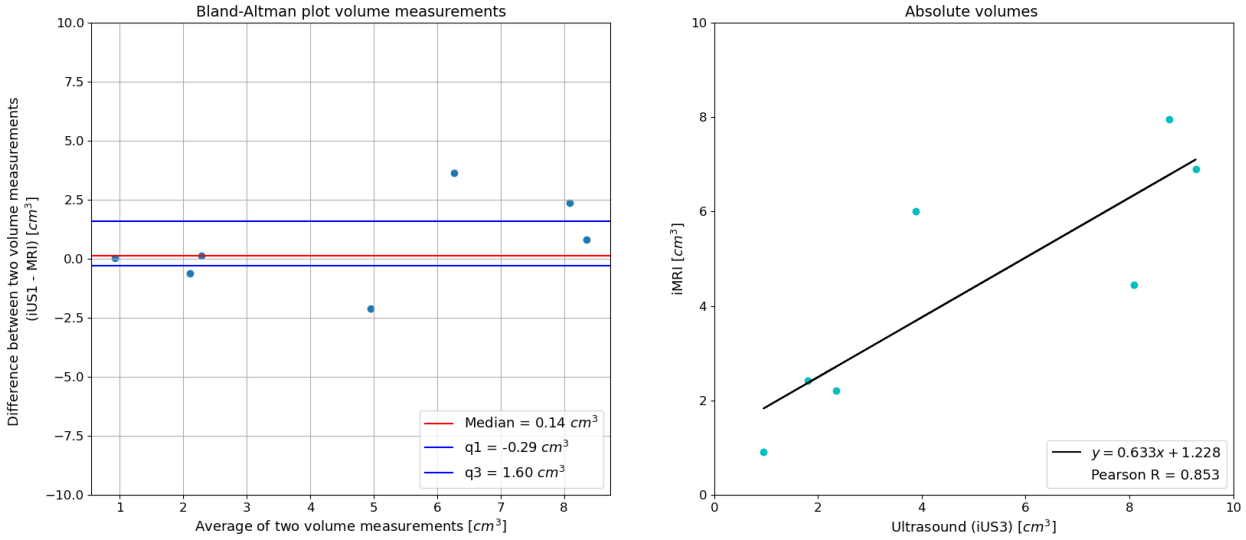


*Figure 6.13: Volume based metrics of iUS3 acquisition compared to iMRI volumes. Absolute and relative volume errors are shown in the left and middle figure respectively. The right figure shows the absolute volumes plotted per patient for iUS and MRI. A regression line is plotted and shows a coefficient of 0.633. The Pearson correlation coefficient is 0.853.*

showed no correlation between iUS1 and MRI. This rejected both hypotheses that stated that both voxel heterogeneity and contrast were correlated between iUS and MRI.

Regarding our findings of the post debulking acquisition (iUS3), our study demonstrated that iUS has good diagnostic accuracy (89%) in detecting residual tumor. Ultimately, seven cases were included for further quantitative analysis. The median absolute volume difference of iUS3 (0.82 ml) was slightly lower than iUS1 (1.28 ml) findings. However, the smaller residual volumes yielded higher relative volume differences for iUS3 (25.7 %) as compared to iUS1 (7.71%). Moreover, the median DSC (0.61) is lower and the median HD 95th percentile (5.84 mm) is higher compared to iUS1. It was as expected that the metrics would be poorer for iUS3 compared to iUS1 acquisition, due to multiple factors affecting image quality and navigational accuracy.

Recently, multiple studies have reported that navigated iUS shows to be a good addition to the neurosurgical armamentarium [31], [34], [35], [41], [52]–[54], [67], [68]. However, few studies report on a quantitative analysis of iUS. To the best of our knowledge, only Hou et al. [54] created segmentations in both iMRI and iUS images to report on the created volumes. However, no other quantitative metrics to evaluate diagnostic value of navigated iUS were reported. Therefore, the quantitative metrics in this study are not directly comparable to other studies. Nevertheless, other studies reported on visual assessment considering the congruency between images and the diagnostic value of iUS in detecting residual tumor. Bastos et al. [34] report on high visual congruency of navigated iUS with iMR images. These findings were confirmed by the high correlation between tumor volumes on iUS and iMRI in our research and the good DSC and HD 95$^{th}$ percentile. We found that the segmented volume in iUS1 shows to be a good predictor of the volume on the preoperative MRI. This means that iUS can be reliably used in determining tumor volume when preoperative MR imaging was performed several weeks in advance. In one case we observed good visual congruency, but the tumor on the iUS was showing a larger volume than the preoperative MRI. This volume increase was ascribed to tumor progression between the iUS acquisition and the preoperative MRI being made two months before, as shown in figure 6.14.

Regarding the detection of residual tumor on iUS imaging, the sensitivity and specificity found in this study were congruent with only some studies. In general, there is no consensus in literature regarding the sensitivity and specificity of iUS in detecting residual tumor. Quintana-Schmidt et al. [72] reported a sensitivity of 94.4% and a specificity of 100%. Shetty et al. [73] found a sensitivity of 78% and specificity of 83%. However, Hou et al. [54] reported a lower sensitivity of 46% and a similar specificity of 96%. Only one study by Carai et al.[67] describes the diagnostic value of unnavigated iUS in a large pediatric population (n=154) with a sensitivity and specificity of 86% and 99%. Our study population is significantly smaller, so a small number of inconclusive results has affected the diagnostic metrics. The two inconclusive cases in our study were considered positive for residual tumor, leading to a lower specificity than reported by other studies. However, false positives for residual tumor will not directly lead to resection, but rather directs the surgeon's attention to the suspected area. Which makes iUS a clinically relevant source of intraoperative information.

The contrast ratios described in our research show that all tumors are hyperintense on iUS, which is also described in a study by Dixon et al. [52]. In this study, the echogenicity of tumors is expressed qualitatively, describing a slight difference between high-grade gliomas and low-grade gliomas. High-grade gliomas are generally slightly more echogenic and more heterogenous in echotexture. This difference is not observed in our study, taking the low amount of patient numbers into consideration. In our data, one patient showed to have a sharply delineated and highly hyperintense tumor on T1 weighted MRI, whereas the lesion showed to be

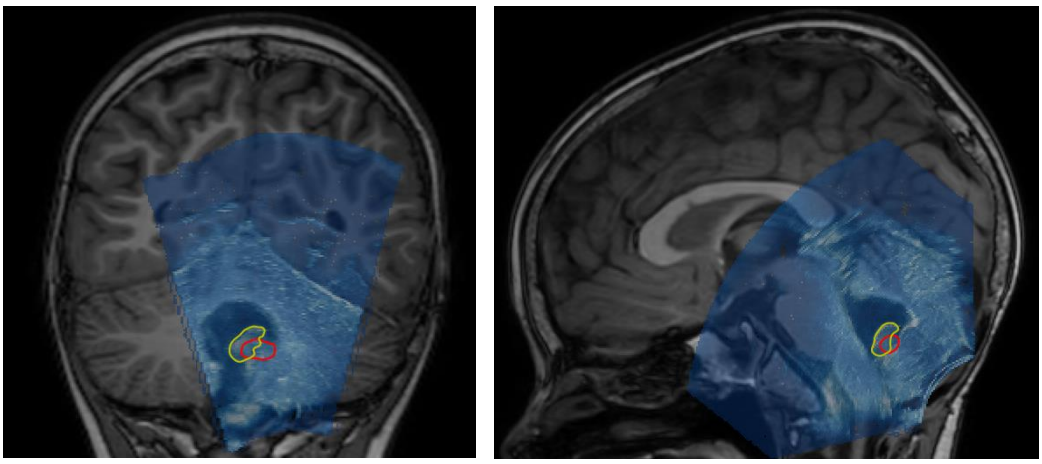

*Figure 6.14: Patient with preoperative MRI of >2 months before surgery. The MRI segmentation (red) was smaller than the iUS1 segmentation (yellow), showing growth of the tumor after 2 months.*

hypointense on iUS, see Appendix 6F. This indicated that the tumor was not dense and solid, but rather consisted of an oily substance, given the high T1 signal.

A moderate median Dice similarity coefficient has been found in this study in describing the degree of overlap between the two volumes. In two cases, the DSC was considered poor with 0.44 and 0.19 respectively, see the outliers in the left image of figure 6.9. These poor scores can be explained by the small tumor volumes of 0.53 $cm^3$ and 0.35 $cm^3$ , with a HD $95^{th}$ percentile of 3.94 mm and 4.78 mm. These distances are relatively large compared to the small volumes, greatly impacting the degree of overlap, which results in a poor DSC. As can be observed in figure 6.14, the small tumor volumes, spatial displacement of the tumor, and the high relative volume difference result in a low DSC.

These same effects can explain the lower DSC observed for the iUS3 segmentations, where the volumes are logically smaller than the iUS1 segmentations. Besides, the image quality was affected by surgery resulting in generally poorer images than those acquired before tumor debulking. The poorer image quality made segmenting the tumor more complex. As described by multiple studies [48], [49], [52], [74], acoustic enhancing artifacts (AEA), contusion, and edema are hyperechoic and could be mistaken for residual tumor. This could have led to suboptimal tumor segmentations in the iUS3 image. Therefore, we would like to stress that acquiring an iUS1 image is important for better interpretation of an iUS3 image.

### Limitations

Six limitations concerning our study need to be mentioned. First, patients that were included underwent surgery in the only pediatric neurooncological center of the Netherlands, therefore selection bias was inevitable. Second, only two surgeons were involved in acquisition and assessment of the iUS images, inevitably inducing information bias. Third, the number of patients was rather low, which did not allow for extensive statistical analysis.

Fourth, the recent implementation of the intraoperative ultrasound integrated with the neuronavigation resulted in inevitably including a learning effect. The ultrasound machine was introduced in February 2023 and integrated with the neuronavigation in March 2023. Therefore, the OR team encountered challenges while initializing and utilizing navigated iUS during the first acquisitions. First, we found that the positional information of the neuronavigation was not correct in four cases. In one case, the reference array of the

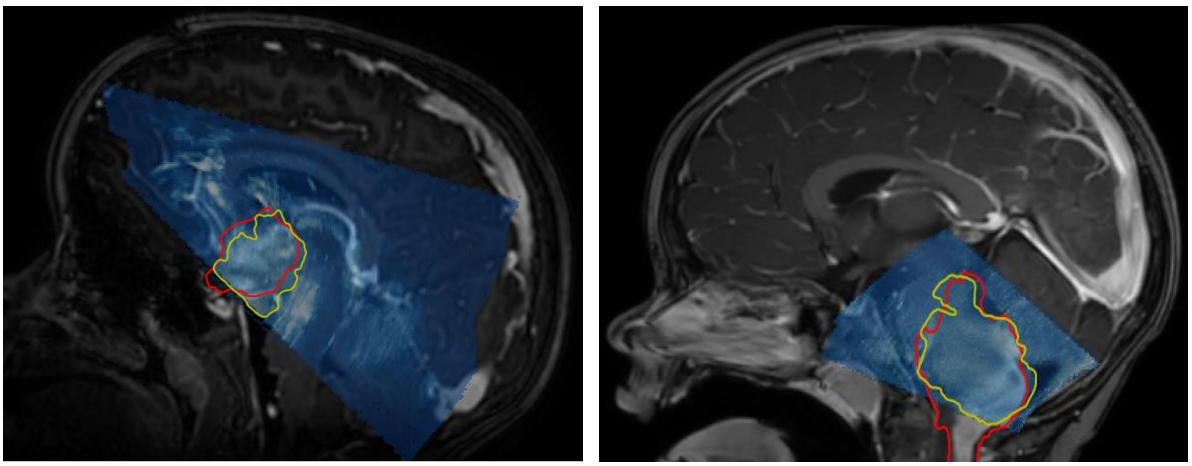

*Figure 6.15: Two examples of incomplete tumor volume acquisition for iUS3 (left) and iUS1 (right). In both examples the iUS segmentation (yellow) is limited to the image boundary of the iUS volume, resulting in an underestimation of the tumor volume.*

neuronavigation was not correctly mounted to the table, causing a systemic shift of the ultrasound images and other navigation tools in the preoperative MRI. This could be directly addressed, since the iUS visualized this deviation clearly. During another procedure, the optical array was not correctly mounted to the iUS, again resulting in a deviation in the neuronavigation. Lastly, in two cases, the positional information of the iUS was lost due to reregistration based on iMRI. Since the positional information was clearly inaccurate in the four described cases, manual image fusion was performed to correct for this deviation. The Dice scores were separately analyzed, but the corrected group was not higher than the uncorrected group (see also boxplots in appendix 6G).

Fifth, the image acquisition was affected by patient positioning and the size of the craniotomy. We observed that both iUS1 and iUS3 acquisitions are more difficult for patients in supine position. Before dura opening, the convex surface of the brain complicated proper transducer-tissue contact. Therefore, acquisition in two planar directions is important to obtain an image with the optimal transducer-tissue contact. After dura opening and tumor debulking, the cavity needs to be filled with saline solution to obtain an iUS image. However, the supine position causes fluid to drain from the cavity, impeding visualization of the entire tumor volume, see left image of figure 6.15. In one case, we observed that the craniotomy was not large enough in order to visualize the entire volume of the tumor. There was a large extension of the tumor in the spinal canal. The angle to visualize this extension could not be realized with the size of the craniotomy, see right image of figure 6.15. Both transducer-tissue contact and craniotomy size caused incomplete tumor acquisition in three patients. This affected the outcome of the volume and DSC metrics.

Sixth, only one interpreter created all segmentations, which could have induced a bias in the data based on one interpretation. Moreover, creation of segmentations was rather difficult in images with artifacts. Both the image quality on iMRI and iUS could hamper accurate segmentation creation. On iMRI, this was due to low signal or pneumocephalus. On iUS, this was due to presence of blood products, edema, ischemia, or surgical materials like spongostan. Therefore, comparison with iUS1 is important to discriminate between the different types of hyperechogenicity.

## Recommendations

Based on our findings and previous studies, we recommend to add navigated intraoperative ultrasound to the neurosurgical armamentarium for several reasons. First, we found a high volumetric similarity before dura opening, allowing the surgeon to obtain additional reliable information regarding the tumor. Second, we showed a high sensitivity for detection of residual tumor in concordance with previous study [54], [67], [72]. The specificity value of iUS was lower in our work than in previous studies, however it was still considered good.

Third, our work showed that in clinical practice, iUS is a valuable tool in detecting residual tumor. If no residual tumor is seen on iUS, one may assume that there is also no residue visible on iMRI. However, if there is residue visible on iUS, the surgeon is advised to reinspect the resection cavity microscopically. Navigated iUS provides the surgeon with an overview of the anatomy without disturbing the surgical workflow. This overview can be created both before, during and after surgery which can minimize excessive manipulation of healthy brain tissue to search for tumor remnants or for orientation. It is advised to acquire a three dimensional volume for every scanning session, so a comparison can be made with a later swipe.

We showed that the iUS3 images were less comparable to iMRI. Even though our findings showed moderate metrics, iUS can direct the surgeon's attention to the suspected areas. However, accurate residual tumor volume estimation is difficult, as shown by our results. This is in accordance with previous studies [34], [49], [74] that recommend to remain cautious in removing residual tumor solely based on iUS information, as image artifacts complicate interpretation of the exact tumor volume.

## Practical considerations

Besides diagnostic value, iUS also has several practical advantages compared to iMRI. First, iUS has a minor burden on the patient and the surgical workflow since the patient does not need to be covered with sterile packing and transferred to another room to be scanned. Moreover, scanning with iUS is instant while iMRI protocols often require approximately 20 minutes, resulting in a total increase of OR time of 60-90 minutes per session. Second, since iUS is a real-time flexible and portable tool, it can be easily used during surgery, and limits the need for potentially hazardous exploration of the resection cavity. Besides, iUS enables visualizing intraoperative neuronavigational accuracy loss, prolonging the usability of neuronavigation despite potential brain shift. The third benefit is the fact that iUS operates independent of any image-to-patient registration. In order to achieve accurate navigation, the patient's head needs to be fixated in a head clamp. However, not all children are eligible to have this clamp fixed due to an unmatured cranium. In this case, iMRI cannot be used to navigate on, whereas iUS can be deployed without the need of registration. Lastly, iMRI with all its procedural adjunctions is notoriously resource expensive, which means that not every institute can afford such an advanced modality in the intraoperative setting. iUS on the contrary, shows to be more than ten times less expensive and is therefore more widely accessible for a broader audience. [34], [75] Our findings and these practical advantages qualify iUS as a good alternative if iMRI is not available.

## Future perspectives

In this study, T1 weighted gadolinium enhanced iMR images were used as comparison, since this is still considered as the gold standard in detection of tumor and residual tumor in our center. However, in several cases it has been observed that T2 weighted imaging provided a different residual tumor volume as compared to T1 weighted imaging. In our study we saw two cases in which residual tumor volume on iUS showed better congruency with T2-w images than T1-w contrast enhanced images. Therefore, research needs to be carried out to determine which MRI images are most predictive for detecting residual tumor.

Moreover, this study limited assessment and quantification of diagnostic value of iUS to B-mode images. Several recent studies report on the potential of more advanced iUS techniques like: Doppler imaging [35], [76], [77], elastosonography [63], [65] and Contrast-Enhanced Ultrasound (CEUS) [52], [66], [77]–[81]. Future research needs to show if more advanced iUS techniques have additional value in detecting residual tumor in pediatric neurosurgery.

## Conclusion:

This study demonstrated that iUS has good diagnostic value in intraoperatively detecting brain tumors before and after debulking. Regarding pre-debulking volume analysis, a high correlation (R=0.996) was found between tumor volume on preoperative MRI and iUS images. Furthermore, a good similarity was found between the two modalities, shown by a median DSC of 0.71 (IQR: 0.11) and a median HD 95th percentile of 4.61 mm (IQR: 2.06 mm).

Regarding the post-debulking volume analysis, this study demonstrated that iUS achieved a sensitivity of 100% and specificity of 80% in accurately detecting residual tumor volume. However, this study showed that accurate tumor residual volume estimation with iUS is not always feasible. Residual tumor volume and position estimates on iUS are less comparable to iMRI due to imaging artifacts and a decrease in spatial accuracy of IGS. However, a median HD $95^{th}$ percentile smaller than 1 cm was achieved. This was considered clinically relevant, since iUS can direct the surgeon's attention to areas suspect for residual tumor in a large resection cavity. Based on our findings, iUS is considered a valuable addition to the neurosurgical armamentarium and could be a good alternative if iMRI is not available.

# VII

# General discussion

Through the years many new technologies have been added to the surgical armamentarium to improve the surgical treatment and patient outcomes. With an increasing number of modalities with complex underlying physical principles, the complexity of the surgical procedure also increases. To assure an efficient, effective and safe implementation of a novel modality, adequate knowledge and experience is necessary. This can be a challenge given the variety of different surgical procedures and existing technical modalities. Therefore, introduction of new modalities requires flexibility and extensive training of the OR team. If this is not realized, a modality may become a burden on the surgical workflow, making a modality prone to being abandoned. Pediatric neurosurgery is no exception to this. However, unique challenges arise specific to pediatric oncological neurosurgery.

Pediatric neurosurgery is a very precise field that requires narrow surgical margins, resulting in lengthy and complex procedures. Adding advanced modalities to these procedures could easily become a burden if numerous available options are not fully understood and therefore not fully deployed. For efficiency purposes, a discrimination must be made between a modality qualifying as a must-have and a nice-to-have.

Chapter IV of this thesis focuses on the usage and user experience of all different OR modalities since their introduction to the novel Neuro OR suite in our center. We found that the optimal configuration is not easily obtained, because of the multifactorial character of surgeries. Nevertheless, we defined practical solutions and surgical guidelines, based on the outcomes of the evaluation questionnaires. A differentiation is made between procedures in prone and supine position, because we found that techniques need to be initialized differently for each position. Based on our findings, practical guidelines for technical modality usage per position are proposed. Besides, new research directions have been defined to further investigate the role of new modalities within the different procedures. Navigated intraoperative ultrasound is one of the new modalities that is studied in this thesis.

In chapter VI of this thesis, the diagnostic value of intraoperative ultrasound integrated with the neuronavigation was investigated before and after tumor debulking. To the best of our knowledge, this is the first study that quantifies the diagnostic value of navigated iUS compared to iMRI in the pediatric population.

Our study showed that tumor volumes on iUS and iMRI are highly correlated before debulking and a good Dice score and clinically relevant Hausdorff distances were found. Our findings demonstrate that iUS can be reliably used in determining the preoperative tumor volume based on iUS. Therefore, iUS is a reliable alternative for imaging the tumor when MRI images are made months in advance or have a poor image quality. It was also observed that the navigated iUS images could indicate the image registration accuracy and the degree of brain shift.

Moreover, our study demonstrated that residual tumor could be detected with iUS with a high diagnostic accuracy (89%). We found a sensitivity of 100% and specificity of 80%. We found a high sensitivity and a lower specificity as compared to previous studies [34], [54], [67], [73]. In our study, additional analysis have been carried out to quantify the visual congruency that was qualitatively described in other studies. Our findings show that iUS is a good alternative to iMRI in detecting residual tumor. Based on our results, if no residual tumor is seen on iUS, one may assume that there is also no residue visible on iMRI. However, if there is residue visible on iUS, the surgeon is advised to reinspect the resection cavity microscopically. Even though our findings showed a moderate Dice score and HD 95$^{th}$ percentile for residual tumor, iUS is still considered clinically relevant. With these metric values for overlap with iMRI, iUS can direct the surgeon's attention to the suspected focal areas without needing to manipulate the entire resection cavity. Besides, a good median absolute volume difference was found, indicating that iUS can still be reliably used for reduced tumor volumes. Nevertheless, this study and previous studies [34], [49], [74] recommend to remain cautious in removing residual tumor solely based on iUS information. Especially tumor volume estimation of smaller tumor remnants is complicated by image artifacts. However, the role of iUS should encompass consistently acquiring updates of the surgical field to monitor the progress of the resection. Early detection of residual tumor on iUS may affect the timing of the iMRI scan.

Besides its diagnostic value, iUS was considered to be a flexible, versatile and non-invasive modality that can be quickly applied during surgery at the surgeon's desire. It has a minor impact on the surgical workflow by adding 3 to 5 minutes per scanning session, whereas iMRI can take up to an hour per scanning session. Besides, iMRI is potentially more hazardous than iUS. Although interpretation of unnavigated iUS is more difficult, the images can still quickly provide the surgeon with additional information. These advantages make iUS a good alternative when iMRI is not available or accessible. Therefore, we would recommend every neurosurgical department to add navigated intraoperative ultrasound to their neurosurgical armamentarium.

### Future perspectives

In this graduation project, the usage of newly implemented advanced OR modalities in the novel Neuro OR suite has been evaluated. Which are all subject to future research to work towards further optimization of using advanced modalities in the surgical workflow. Intraoperative ultrasound was one of the advanced modalities that has been further researched in this work. The diagnostic value of navigated 2D B-mode imaging has been quantified. However, iUS is a versatile modality which may have more potential applications like Doppler and elastography imaging, that could be explored in future research.

Only when a technical modality is fully explored and understood it can be optimally applied in the surgical setting. In a highly innovative environment, new possibilities always need to be explored and existing modalities need to be evaluated to provide the best care possible.

A technical physician could play an important role in further exploring and innovating the OR of the future for the optimal implementation of technical modalities. Moreover, a technical physician can support the OR team in planning and applying technical modalities in the surgical procedures. In the future, the addition of a technical physician to the OR team may lead to increased surgical efficiency, effectiveness, and safety.

# VIII

# General conclusions

The first aim of this thesis was to evaluate the role of the technical modalities involved in pediatric neurosurgery in the hybrid Neuro OR suite. The second aim of this thesis was to quantify the diagnostic value of intraoperative ultrasound. For the first part, a survey research concerning user experience of surgical techniques was carried out. Practical challenges were identified and best practices were explored. In this thesis new guidelines concerning technical modality usage are proposed.

In the second part, the diagnostic value of navigated intraoperative ultrasound was evaluated. This study showed that iUS has a good diagnostic accuracy (89%) with a sensitivity of 100% and specificity of 80% in detecting residual brain tumor. Our work is the first in quantifying the diagnostic value of navigated iUS. We found that iUS a good predictor for preoperative tumor volume estimation, showing a high correlatoin with iMRI (R=0.996). A Dice similarity score of (0.71) and (0.61) was found for preoperative and postoperative tumor volume comparison, respectively. Besides, a median 95$^{th}$ percentile Hausdorff distance of 5.84 mm was found for the postoperative tumor volume comparison.

Although none of these metrics are considered excellent, iUS may still have an important role in clinical practice. The found metrics show that iUS could direct the surgeon's attention to areas suspect for residual tumor. Navigated iUS creates an additional check for tumor residual before starting an iMRI scanning session. If navigated iUS is available, implementation in the surgical procedure should always be considered. The modality will always provide the surgeon with additional information, while it poses almost no burden on the workflow. Besides, navigated iUS uses less time and resources compared to iMRI. Therefore, centers that do not have access to an iMRI should consider navigated iUS as a good alternative. Future research should be carried out to further explore the value of navigated iUS.

This thesis is the first work that assesses the role of different technical modalities in surgical procedures, working towards optimal clinical implementation. An elaborate overview of OR modalities and evaluation of the effectiveness in the process led to new insights in applying and innovating modalities. Improvement and innovation of treatment options supported by technical modalities for pediatric surgery requires knowledge and experience. Therefore, the role of an extra OR team member with a technical background should be investigated. This might realize more effective, efficient and safer usage of technical OR modalities, for further optimization of the treatment of children with brain tumors.

# IX

# Bibliography


[1] Y. T. Udaka and R. J. Packer, "Pediatric Brain Tumors," *Neurol. Clin.*, vol. 36, no. 3, pp. 533–556, Aug. 2018, doi: 10.1016/J.NCL.2018.04.009.

[2] R. Rudà *et al.*, "EANO guidelines for the diagnosis and treatment of ependymal tumors," *Neuro. Oncol.*, vol. 20, no. 4, pp. 445–456, Mar. 2018, doi: 10.1093/NEUONC/NOX166.

[3] A. K. Gnekow *et al.*, "SIOP-E-BTG and GPOH Guidelines for Diagnosis and Treatment of Children and Adolescents with Low Grade Glioma," *Klin. Padiatr.*, vol. 231, no. 3, pp. 107–135, 2019, doi: 10.1055/A-0889-8256.

[4] V. Srinivasan, M. Ghali, R. North, Z. Boghani, D. Hansen, and S. Lam, "Modern management of medulloblastoma: Molecular classification, outcomes, and the role of surgery," *Surg. Neurol. Int.*, vol. 7, no. Suppl 44, p. S1135, 2016, doi: 10.4103/2152-7806.196922.

[5] J. Zipfel *et al.*, "Surgical Management of Pre-Chiasmatic Intraorbital Optic Nerve Gliomas in Children after Loss of Visual Function-Resection from Bulbus to Chiasm," *Child. (Basel, Switzerland)*, vol. 9, no. 4, Apr. 2022, doi: 10.3390/CHILDREN9040459.

[6] F. Revilla-Pacheco *et al.*, "Extent of resection and survival in patients with glioblastoma multiforme: Systematic review and meta-analysis," *Medicine (Baltimore).*, vol. 100, no. 25, p. e26432, Jun. 2021, doi: 10.1097/MD.0000000000026432.

[7] N. Sanai, M. Y. Polley, M. W. McDermott, A. T. Parsa, and M. S. Berger, "An extent of resection threshold for newly diagnosed glioblastomas: Clinical article," *J. Neurosurg.*, vol. 115, no. 1, pp. 3–8, Jul. 2011, doi: 10.3171/2011.2.JNS10998.

[8] Y. Fujii *et al.*, "Threshold of the extent of resection for WHO Grade III gliomas: retrospective volumetric analysis of 122 cases using intraoperative MRI," *J. Neurosurg.*, vol. 129, no. 1, pp. 1–9, Jul. 2018, doi: 10.3171/2017.3.JNS162383.

[9] R. L. Siegel Mph *et al.*, "Cancer statistics, 2023," *CA. Cancer J. Clin.*, vol. 73, no. 1, pp. 17–48, Jan. 2023, doi: 10.3322/CAAC.21763.

[10] K. D. Miller *et al.*, "Brain and other central nervous system tumor statistics, 2021," *CA. Cancer J. Clin.*, vol. 71, no. 5, pp. 381–406, Sep. 2021, doi: 10.3322/CAAC.21693.

[11] S. Wilne, J. Collier, C. Kennedy, K. Koller, R. Grundy, and D. Walker, "Presentation of childhood CNS tumours: a systematic review and meta-analysis," *Lancet Oncol.*, vol. 8, no. 8, pp. 685–695, Aug. 2007, doi: 10.1016/S1470-2045(07)70207-3.

[12] J. T. Low *et al.*, "Primary brain and other central nervous system tumors in the United States (2014-2018): A summary of the CBTRUS statistical report for clinicians," *Neuro-Oncology Pract.*, vol. 9, no. 3, pp. 165–182, May 2022, doi: 10.1093/NOP/NPAC015.

[13] I. F. Pollack, "Brain Tumors in Children," *https://doi.org/10.1056/NEJM199412013312207*, vol. 331, no. 22, pp.

1500–1507, Dec. 1994, doi: 10.1056/NEJM199412013312207.

[14] "Midsagittal section of the brain: anatomy | Kenhub." https://www.kenhub.com/en/library/anatomy/midsagittal-section-of-the-brain (accessed Aug. 09, 2023).

[15] J. Knight and O. De Jesus, "Tonsillar Herniation," *StatPearls*, Feb. 2023, Accessed: Jul. 28, 2023. [Online]. Available: https://www.ncbi.nlm.nih.gov/books/NBK562170/.

[16] "glioblastoma_extent_of_resection [Neurosurgery Wiki]." https://operativeneurosurgery.com/doku.php?id=glioblastoma_extent_of_resection (accessed Aug. 03, 2023).

[17] R. Reisch, A. Stadie, R. A. Kockro, and N. Hopf, "The Keyhole Concept in Neurosurgery," *World Neurosurg.*, vol. 79, no. 2, p. S17.e9-S17.e13, Feb. 2013, doi: 10.1016/J.WNEU.2012.02.024.

[18] "Telovelar Approach | The Neurosurgical Atlas." https://www.neurosurgicalatlas.com/volumes/cranial-approaches/telovelar-approach (accessed Aug. 03, 2023).

[19] H. Bhatt, M. I. Bhatti, C. Patel, and P. Leach, "Paediatric posterior fossa tumour resection rates in a small volume centre: the past decade's experience," *https://doi.org/10.1080/02688697.2020.1859085*, vol. 35, no. 4, pp. 451–455, 2020, doi: 10.1080/02688697.2020.1859085.

[20] "Posterior Interhemispheric Transcallosal Intervenous/Paravenous Variant | The Neurosurgical Atlas." https://www.neurosurgicalatlas.com/volumes/cranial-approaches/third-ventricular-approaches/posterior-interhemispheric-transcallosal-intervenous-paravenous-variant (accessed Aug. 03, 2023).

[21] S. Anetsberger, P. Gonzalez-Lopez, Y. Elsawaf, A. G. Lucifero, S. Luzzi, and S. K. Elbabaa, "Interhemispheric Approach," *Acta Biomed.*, vol. 92, no. S4, 2022, doi: 10.23750/ABM.V92IS4.12801.

[22] "Pterional Craniotomy | The Neurosurgical Atlas." https://www.neurosurgicalatlas.com/volumes/cranial-approaches/pterional-craniotomy (accessed Aug. 03, 2023).

[23] M. T. Foster *et al.*, "Reporting morbidity associated with pediatric brain tumor surgery: are the available scoring systems sufficient?," *J. Neurosurg. Pediatr.*, vol. 27, no. 5, pp. 556–565, Feb. 2021, doi: 10.3171/2020.9.PEDS20556.

[24] C. Catsman-Berrevoets and Z. Patay, "Cerebellar mutism syndrome," *Handb. Clin. Neurol.*, vol. 155, pp. 273–288, Jan. 2018, doi: 10.1016/B978-0-444-64189-2.00018-4.

[25] "Spatial Transformation Matrices." https://www.brainvoyager.com/bv/doc/UsersGuide/CoordsAndTransforms/SpatialTransformationMatrices.html (accessed Jul. 11, 2023).

[26] F. Maes, D. Loeckx, D. Vandermeulen, and P. Suetens, "Image registration using mutual information," *Handb. Biomed. Imaging Methodol. Clin. Res.*, pp. 295–308, Jan. 2015, doi: 10.1007/978-0-387-09749-7_16/FIGURES/1.

[27] M. A. Mongen and P. W. A. Willems, "Current accuracy of surface matching compared to adhesive markers in patient-to-image registration," *Acta Neurochir. (Wien).*, vol. 161, no. 5, pp. 865–870, Mar. 2019, doi: 10.1007/S00701-019-03867-8/FIGURES/4.

[28] J. Wach, M. Banat, V. Borger, H. Vatter, H. Haberl, and S. Sarikaya-Seiwert, "Intraoperative MRI-guided Resection in Pediatric Brain Tumor Surgery: A Meta-analysis of Extent of Resection and Safety Outcomes," *J. Neurol. Surgery, Part A Cent. Eur. Neurosurg.*, vol. 82, no. 1, pp. 64–74, Jan. 2021, doi: 10.1055/S-0040-1714413/ID/JR202624RE-43.

[29] A. F. Choudhri, A. Siddiqui, P. Klimo, and F. A. Boop, "Intraoperative MRI in pediatric brain tumors," *Pediatr. Radiol. 2015 453*, vol. 45, no. 3, pp. 397–405, Sep. 2015, doi: 10.1007/S00247-015-3322-Z.

[30] M. Giordano *et al.*, "Intraoperative magnetic resonance imaging in pediatric neurosurgery: safety and utility," *J.*

*Neurosurg. Pediatr.*, vol. 19, no. 1, pp. 77–84, Jan. 2017, doi: 10.3171/2016.8.PEDS15708.

[31] U. Yeole, V. Singh, A. Mishra, S. Shaikh, P. Shetty, and A. Moiyadi, "Navigated intraoperative ultrasonography for brain tumors: a pictorial essay on the technique, its utility, and its benefits in neuro-oncology," *Ultrasonography*, vol. 39, no. 4, pp. 394–406, Oct. 2020, doi: 10.14366/USG.20044.

[32] M. Smits, "Update on neuroimaging in brain tumours," *Curr. Opin. Neurol.*, vol. 34, no. 4, pp. 497–504, Aug. 2021, doi: 10.1097/WCO.0000000000000950.

[33] I. J. Gerard, M. Kersten-Oertel, J. A. Hall, D. Sirhan, and D. L. Collins, "Brain Shift in Neuronavigation of Brain Tumors: An Updated Review of Intra-Operative Ultrasound Applications," *Front. Oncol.*, vol. 10, p. 1, Feb. 2020, doi: 10.3389/FONC.2020.618837.

[34] D. C. D. A. Bastos *et al.*, "Challenges and Opportunities of Intraoperative 3D Ultrasound With Neuronavigation in Relation to Intraoperative MRI," *Front. Oncol.*, vol. 11, p. 1463, May 2021, doi: 10.3389/FONC.2021.656519/BIBTEX.

[35] B. Saß, M. Pojskic, D. Zivkovic, B. Carl, C. Nimsky, and M. H. A. Bopp, "Utilizing Intraoperative Navigated 3D Color Doppler Ultrasound in Glioma Surgery," *Front. Oncol.*, vol. 11, p. 3122, Aug. 2021, doi: 10.3389/FONC.2021.656020/BIBTEX.

[36] I. J. Gerard, M. Kersten-Oertel, K. Petrecca, D. Sirhan, J. A. Hall, and D. L. Collins, "Brain shift in neuronavigation of brain tumors: A review," *Med. Image Anal.*, vol. 35, pp. 403–420, Jan. 2017, doi: 10.1016/J.MEDIA.2016.08.007.

[37] P. U. Bidkar, A. Thakkar, N. Manohar, and K. S. Rao, "Intraoperative neurophysiological monitoring in paediatric neurosurgery," *Int. J. Clin. Pract.*, vol. 75, no. 8, p. e14160, Aug. 2021, doi: 10.1111/IJCP.14160.

[38] L. Ma and B. Fei, "Comprehensive review of surgical microscopes: technology development and medical applications," *https://doi.org/10.1117/1.JBO.26.1.010901*, vol. 26, no. 1, p. 010901, Jan. 2021, doi: 10.1117/1.JBO.26.1.010901.

[39] L. L., "The stereotaxic method and radiosurgery of the brain.," *Acta Chir Scand.*, p. 102(4), 1951.

[40] E. A. Spiegel, H. T. Wycis, M. Marks, and A. J. Lee, "Stereotaxic apparatus for operations on the human brain," *Science (80-. ).*, vol. 106, no. 2754, pp. 349–350, Oct. 1947, doi: 10.1126/SCIENCE.106.2754.349/ASSET/596394F7-2B82-4FFE-9AA0-BBCEA0AFA11C/ASSETS/SCIENCE.106.2754.349.FP.PNG.

[41] D. A. Orringer, A. Golby, and F. Jolesz, "Neuronavigation in the surgical management of brain tumors: Current and future trends," *Expert Rev. Med. Devices*, vol. 9, no. 5, pp. 491–500, Sep. 2012, doi: 10.1586/ERD.12.42.

[42] M. Rivera, S. Norman, R. Sehgal, and R. Juthani, "Updates on Surgical Management and Advances for Brain Tumors," *Curr. Oncol. Rep.*, vol. 23, no. 3, pp. 1–9, Mar. 2021, doi: 10.1007/S11912-020-01005-7/METRICS.

[43] M. Luo *et al.*, "A comprehensive model-assisted brain shift correction approach in image-guided neurosurgery: a case study in brain swelling and subsequent sag after craniotomy," p. 4, Mar. 2019, doi: 10.1117/12.2512763.

[44] R. M. Comeau, A. F. Sadikot, A. Fenster, and T. M. Peters, "Intraoperative ultrasound for guidance and tissue shift correction in image-guided neurosurgery," *Med. Phys.*, vol. 27, no. 4, pp. 787–800, Apr. 2000, doi: 10.1118/1.598942.

[45] G. J. Dohrmann and J. M. Rubin, "History of Intraoperative Ultrasound in Neurosurgery," *Neurosurg. Clin. N. Am.*, vol. 12, no. 1, pp. 155–166, Jan. 2001, doi: 10.1016/S1042-3680(18)30074-3.

[46] A. E. Powles, D. J. Martin, I. T. Wells, and C. R. Goodwin, "Physics of ultrasound," *Anaesth. Intensive Care Med.*, vol. 19, no. 4, pp. 202–205, Apr. 2018, doi: 10.1016/J.MPAIC.2018.01.005.

[47] M. K. Feldman, S. Katyal, and M. S. Blackwood, "US Artifacts1," *https://doi.org/10.1148/rg.294085199*, vol. 29, no. 4, pp. 1179–1189, Jul. 2009, doi: 10.1148/RG.294085199.

[48] A. Šteňo, J. Buvala, V. Babková, A. Kiss, D. Toma, and A. Lysak, "Current Limitations of Intraoperative Ultrasound in Brain Tumor Surgery," *Front. Oncol.*, vol. 11, p. 851, Mar. 2021, doi: 10.3389/FONC.2021.659048/BIBTEX.

[49] A. Šteňo, J. Buvala, and J. Šteňo, "Large Residual Pilocytic Astrocytoma After Failed Ultrasound-Guided Resection: Intraoperative Ultrasound Limitations Require Special Attention," *World Neurosurg.*, vol. 150, pp. 140–143, Jun. 2021, doi: 10.1016/J.WNEU.2021.03.138.

[50] A. Martegani, L. Mattei, and L. Aiani, "US physics, basic principles, and clinical application," *Intraoperative Ultrasound Neurosurg. From Stand. B-mode to Elastosonography*, pp. 9–17, Mar. 2016, doi: 10.1007/978-3-319-25268-1_2/COVER.

[51] M. Del Bene, F. DiMeco, and G. Unsgård, "Editorial: Intraoperative Ultrasound in Brain Tumor Surgery: State-Of-The-Art and Future Perspectives," *Front. Oncol.*, vol. 11, p. 4523, Nov. 2021, doi: 10.3389/FONC.2021.780517/BIBTEX.

[52] L. Dixon, A. Lim, M. Grech-Sollars, D. Nandi, and S. Camp, "Intraoperative ultrasound in brain tumor surgery: A review and implementation guide," *Neurosurg. Rev.*, vol. 45, no. 4, pp. 2503–2515, Aug. 2022, doi: 10.1007/S10143-022-01778-4/FIGURES/6.

[53] Y. Hou, Y. Li, Q. Li, Y. Yu, and J. Tang, "Full-course resection control strategy in glioma surgery using both intraoperative ultrasound and intraoperative MRI," *Front. Oncol.*, vol. 12, p. 4503, Aug. 2022, doi: 10.3389/FONC.2022.955807/BIBTEX.

[54] Y. Hou and J. Tang, "Advantages of Using 3D Intraoperative Ultrasound and Intraoperative MRI in Glioma Surgery," *Front. Oncol.*, vol. 12, p. 2743, Jun. 2022, doi: 10.3389/FONC.2022.925371/BIBTEX.

[55] N. Sewberath Misser, B. Van Zaane, J. E. N. Jaspers, H. Gooszen, and J. Versendaal, "Implementing Medical Technological Equipment in the OR: Factors for Successful Implementations," *J. Healthc. Eng.*, vol. 2018, 2018, doi: 10.1155/2018/8502187.

[56] J. Misser, Navin Sewberath; Jasper, Joris; van Zaane, Bas; Gooszen, Hein; Versendaal, "Evaluation of an implementation protocol for digitization and devices in Operating Rooms," Accessed: Nov. 24, 2022. [Online]. Available: https://www.researchgate.net/publication/352778566_Evaluation_of_an_implementation_protocol_for_digitization_and_devices_in_Operating_Rooms.

[57] N. S. Misser, J. Jaspers, B. van Zaane, H. Gooszen, and J. Versendaal, "Transforming operating rooms: factors for successful implementations of new medical equipment," *31st Bled eConference Digit. Transform. Meet. Challenges, BLED 2018*, pp. 279–290, 2018, doi: 10.18690/978-961-286-170-4.18.

[58] M. Lauer *et al.*, "Neurotoxicity of subarachnoid Gd-based contrast agent accumulation: a potential complication of intraoperative MRI?," *Neurosurg. Focus*, vol. 50, no. 1, p. E12, Jan. 2021, doi: 10.3171/2020.10.FOCUS20402.

[59] E. Mazzucchi *et al.*, "Intraoperative Integration of Multimodal Imaging to Improve Neuronavigation: A Technical Note," *World Neurosurg.*, vol. 164, pp. 330–340, Aug. 2022, doi: 10.1016/J.WNEU.2022.05.133.

[60] M. A. Mongen and P. W. A. Willems, "Current accuracy of surface matching compared to adhesive markers in patient-to-image registration," *Acta Neurochir. (Wien).*, vol. 161, no. 5, pp. 865–870, Mar. 2019, doi: 10.1007/S00701-019-03867-8/FIGURES/4.

[61] K. G. Abdullah, D. Lubelski, P. G. P. Nucifora, and S. Brem, "Use of diffusion tensor imaging in glioma resection," *Neurosurg Focus*, vol. 34, no. 4, p. E1, Apr. 2013, doi: 10.3171/2013.1.focus12412.

[62] D. C. Vanderweyen *et al.*, "The role of diffusion tractography in refining glial tumor resection," *Brain Struct. Funct. 2020 2254*, vol. 225, no. 4, pp. 1413–1436, Mar. 2020, doi: 10.1007/S00429-020-02056-Z.

[63] S. Cepeda *et al.*, "Comparison of Intraoperative Ultrasound B-Mode and Strain Elastography for the Differentiation of Glioblastomas From Solitary Brain Metastases. An Automated Deep Learning Approach for Image Analysis," *Front. Oncol.*, vol. 10, p. 3322, Feb. 2021, doi: 10.3389/FONC.2020.590756/BIBTEX.

[64] F. Prada *et al.*, "Contrast-enhanced MR Imaging versus Contrast-enhanced US: A Comparison in Glioblastoma Surgery by Using Intraoperative Fusion Imaging," *https://doi.org/10.1148/radiol.2017161206*, vol. 285, no. 1, pp. 242–249, May 2017, doi: 10.1148/RADIOL.2017161206.

[65] F. Prada *et al.*, "Multiparametric Intraoperative Ultrasound in Oncological Neurosurgery: A Pictorial Essay," *Front. Neurosci.*, vol. 16, p. 881661, Apr. 2022, doi: 10.3389/FNINS.2022.881661/BIBTEX.

[66] M. Hwang, C. E. Barnewolt, J. Jüngert, F. Prada, A. Sridharan, and R. A. Didier, "Contrast-enhanced ultrasound of the pediatric brain," *Pediatr. Radiol. 2021 5112*, vol. 51, no. 12, pp. 2270–2283, Feb. 2021, doi: 10.1007/S00247-021-04974-4.

[67] A. Carai *et al.*, "Intraoperative Ultrasound-Assisted Extent of Resection Assessment in Pediatric Neurosurgical Oncology," *Front. Oncol.*, vol. 11, Apr. 2021, doi: 10.3389/FONC.2021.660805.

[68] C. R. Wirtz *et al.*, "The benefit of neuronavigation for neurosurgery analyzed by its impact on glioblastoma surgery," *http://dx.doi.org/10.1080/01616412.2000.11740684*, vol. 22, no. 4, pp. 354–360, 2016, doi: 10.1080/01616412.2000.11740684.

[69] A. A. Taha and A. Hanbury, "Metrics for evaluating 3D medical image segmentation: Analysis, selection, and tool," *BMC Med. Imaging*, vol. 15, no. 1, pp. 1–28, Aug. 2015, doi: 10.1186/S12880-015-0068-X/TABLES/5.

[70] J. A. Moliterno, T. R. Patel, and J. M. Piepmeier, "Neurosurgical approach," *Cancer J.*, vol. 18, no. 1, pp. 20–25, Jan. 2012, doi: 10.1097/PPO.0B013E3183243F6E3.

[71] J. S. Young, R. A. Morshed, S. L. Hervey-Jumper, and M. S. Berger, "The surgical management of diffuse gliomas: Current state of neurosurgical management and future directions," *Neuro. Oncol.*, Jul. 2023, doi: 10.1093/NEUONC/NOAD133.

[72] C. de Quintana-Schmidt *et al.*, "Neuronavigated Ultrasound in Neuro-Oncology: A True Real-Time Intraoperative Image," *World Neurosurg.*, vol. 157, pp. e316–e326, Jan. 2022, doi: 10.1016/J.WNEU.2021.10.082.

[73] P. Shetty, U. Yeole, V. Singh, and A. Moiyadi, "Navigated ultrasound-based image guidance during resection of gliomas: practical utility in intraoperative decision-making and outcomes.," *Neurosurg. Focus*, vol. 50, no. 1, pp. 1–10, Jan. 2021, doi: 10.3171/2020.10.FOCUS20550.

[74] S. Culleton *et al.*, "Imaging pitfalls in paediatric posterior fossa neoplastic and non-neoplastic lesions," *Clin. Radiol.*, vol. 76, no. 5, pp. 391.e19-391.e31, May 2021, doi: 10.1016/J.CRAD.2020.12.011.

[75] C. Giussani *et al.*, "Intraoperative MRI versus intraoperative ultrasound in pediatric brain tumor surgery: is expensive better than cheap? A review of the literature," *Child's Nerv. Syst. 2022 388*, vol. 38, no. 8, pp. 1445–1454, May 2022, doi: 10.1007/S00381-022-05545-0.

[76] M. Ivanov, S. Wilkins, I. Poeata, and A. Brodbelt, "Intraoperative ultrasound in neurosurgery - A practical guide," *Br. J. Neurosurg.*, vol. 24, no. 5, pp. 510–517, Oct. 2010, doi: 10.3109/02688697.2010.495165.

[77] F. Prada *et al.*, "Identification of residual tumor with intraoperative contrast-enhanced ultrasound during glioblastoma resection," *Neurosurg. Focus*, vol. 40, no. 3, p. E7, Mar. 2016, doi: 10.3171/2015.11.FOCUS15573.

[78] G. M. Della Pepa *et al.*, "Contrast enhanced ultrasound (CEUS) applications in neurosurgical and neurological settings – New scenarios for brain and spinal cord ultrasonography. A systematic review," *Clin. Neurol. Neurosurg.*, vol. 198, p. 106105, Nov. 2020, doi: 10.1016/J.CLINEURO.2020.106105.

[79] G. M. Della Pepa *et al.*, "5-Aminolevulinic Acid and Contrast-Enhanced Ultrasound: The Combination of the Two Techniques to Optimize the Extent of Resection in Glioblastoma Surgery," *Neurosurgery*, vol. 86, no. 6, pp. E529–E540, Jun. 2020, doi: 10.1093/NEUROS/NYAA037.

[80] F. Prada *et al.*, "Identification of residual tumor with intraoperative contrast-enhanced ultrasound during glioblastoma resection.," *Neurosurg. Focus*, vol. 40, no. 3, Mar. 2016, doi: 10.3171/2015.11.FOCUS15573.

[81] J. H. Squires and M. Beth McCarville, "Contrast-Enhanced Ultrasound in Children: Implementation and Key Diagnostic Applications," *https://doi.org/10.2214/AJR.21.25713*, vol. 217, no. 5, pp. 1217–1230, Apr. 2021, doi: 10.2214/AJR.21.25713.

# X

# Appendices

# Complementarity of OR techniques in pediatric oncological

Questionnaire is to be filled out after ***every*** pediatric oncological neurosurgical procedure, **IF** any advanced OR techniques listed below in this questionnaire are used. Language: Dutch or English

Filled out questionnaires should be returned to K. Klein Gunnewiek, Master student Technical Medicine:
E-mail: k.kleingunnewiek@prinsesmaximacentrum.nl

## General information:

**Initials Surgeon:** _____

**Date of surgery:** _____

**Patient Number:** _____

**Overall impression of OR technique usage:**
(How was the interplay of modalities?)

_____

**Technical problems:**

☐ None

☐ Yes, namely: _____

**Planned Surgical Goal:**

☐RS-0 ☐RS-1 ☐RS-2 ☐RS-3

**Accomplished Surgical Goal:**

☐RS-0 ☐RS-1 ☐RS-2 ☐RS-3

## Technical information:

| **Was the technique necessary to accomplish the goal?**<br>1-Strongly disagree, 2-Disagree, 3-Neutral, 4-Agree, 5-Strongly agree | | | | | | | *Please specify explanation in every case.*<br>*If applicable: include information about phase during surgery* |
|---|---|---|---|---|---|---|---|
| | **1** | **2** | **3** | **4** | **5** | **N/A** | **Explanation:** |
| **Planning:** | | | | | | | |
| Image Fusion: | ☐ | ☐ | ☐ | ☐ | ☐ | ☐ | |
| Image Registration:<br>☐iMRI☐Surface☐Fiducial | ☐ | ☐ | ☐ | ☐ | ☐ | ☐ | |
| **Acquisition:** | | | | | | | |
| iMRI: | ☐ | ☐ | ☐ | ☐ | ☐ | ☐ | |
| Ultrasound:<br>Navigated: ☐ Yes ☐No | ☐ | ☐ | ☐ | ☐ | ☐ | ☐ | |
| Neuromonitoring: | ☐ | ☐ | ☐ | ☐ | ☐ | ☐ | |
| Other: | ☐ | ☐ | ☐ | ☐ | ☐ | ☐ | |

PLEASE TURN PAGE TO CONTINUE FILLING IN THE QUESTIONNAIRE

Technical information:

| **Was the technique necessary to accomplish the goal?**<br>1-Strongly disagree, 2-Disagree, 3-Neutral, 4-Agree, 5-Strongly agree | | | | | | | *Please specify explanation in every case.*<br>*If applicable: include information about phase during surgery* |
|---|---|---|---|---|---|---|---|
| | **1** | **2** | **3** | **4** | **5** | **N/A** | **Explanation:** |
| **Navigation:** | | | | | | | |
| Navigation Pointer: | ☐ | ☐ | ☐ | ☐ | ☐ | ☐ | |
| Cirq: | ☐ | ☐ | ☐ | ☐ | ☐ | ☐ | |
| Navigated Microscope:<br>(Tracking motion) | ☐ | ☐ | ☐ | ☐ | ☐ | ☐ | |
| **Visualization:** | | | | | | | |
| Microscope:<br>☐Kinevo ☐Pentero | ☐ | ☐ | ☐ | ☐ | ☐ | ☐ | |
| Endoscope:<br>☐Qevo ☐Other:_____ | ☐ | ☐ | ☐ | ☐ | ☐ | ☐ | |
| Exoscope: | ☐ | ☐ | ☐ | ☐ | ☐ | ☐ | |
| Head-Up Display:<br>(Projection in Microscope) | ☐ | ☐ | ☐ | ☐ | ☐ | ☐ | |

Additional information:

**Aspects learnt during this procedure:**_____

_____

_____

_____

_____

_____

**Aspects to change in future procedures:**_____

_____

_____

_____

_____

**Filled out questionnaires should be returned to K. Klein Gunnewiek, Master student Technical Medicine:**
**E-mail: k.kleingunnewiek@prinsesmaximacentrum.nl**

## Appendix B: Example of navigated iUS in the intraoperative setting

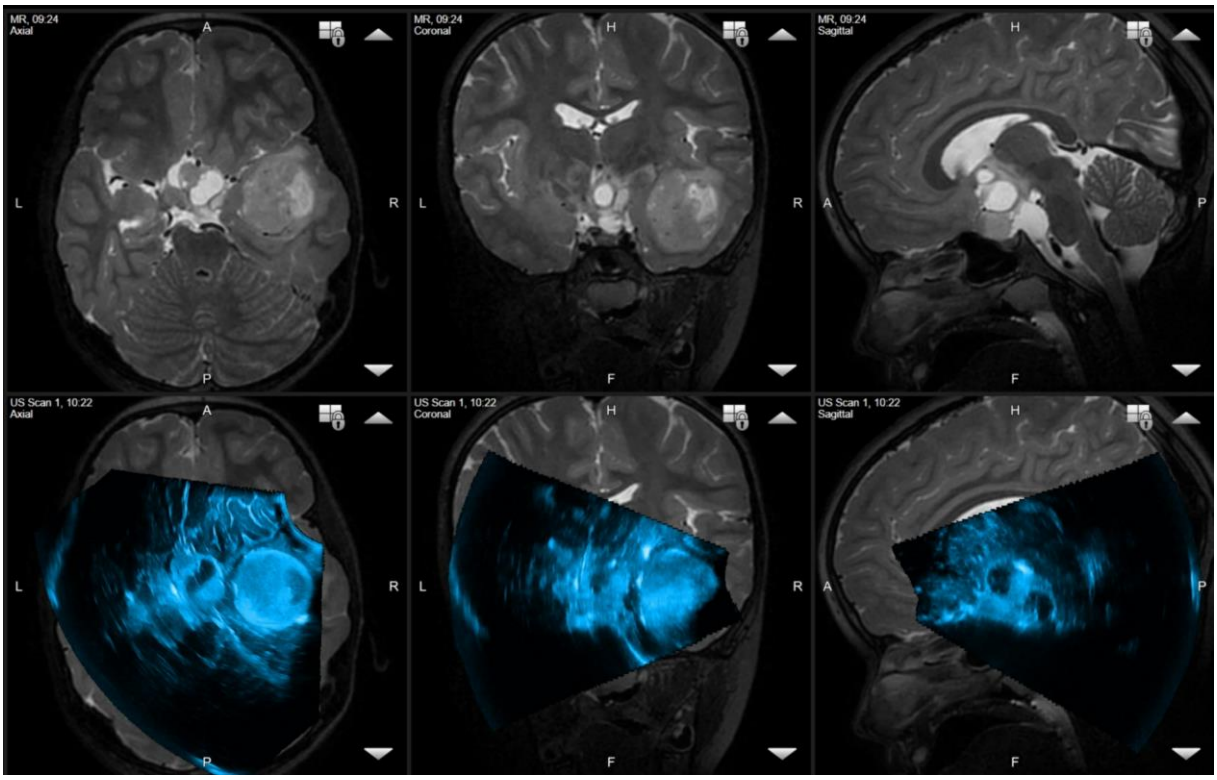

Appendix C: Instructions for acquisition of iUS swipe:

## Acquisition Protocol Assessment of Intraoperative Ultrasonic Imaging

This protocol describes the steps to be taken to answer the research questions regarding iUS applicability. The protocol is divided in three different acquisition moments, consecutively performed during surgery. The timing of each moment is described below. Every acquisition requires a three dimensional navigated US volume to be reconstructed within the Brainlab software, referred to as swipe. The protocol for performing a swipe will be similar for every acquisition moment, and is therefore explained only once.

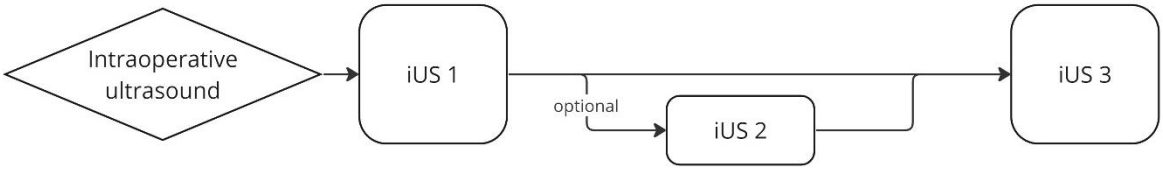


*Figure 2: Workflow consecutive US acquisition moments*

- *iUS 1:* Swipe is made after trepanation, but before dura opening.
- *iUS2:* Additional swipes are made dependent on surgical desire, during tumor debulking.
- *iUS3:* Shortly before the patient is prepared for an iMRI scanning session, a swipe of the cavity is made. This will be repeated for every scanning session.

**Preparation:**

1. Activate the Ultrasound Navigation module in Brainlab once the BK5000 machine has been started. A neurosurgical standard scanning protocol needs to be chosen.
2. Estimate an initial US depth based on preoperative planning and activate auto-gain.
3. Cover the transducer in a sterile sheath with either gel or saline solution between the cover and the transducer; while removing air bubbles.
4. Mount the navigation array with the reflective spheres on the transducer. Check if the navigation software detects the transducer.

**Protocol for a US Swipe:**

1. Prepare the region to assure best scan results, which includes:
    a. Remove excessive blood, especially blood cloths
    b. If possible, position the patient such that the craniotomy is the highest point, to avoid fluid leakage
    c. Fill the cavity with a sterile saline solution and wait 10-20 seconds allowing air bubbles to dissipate.
2. Check if auto-gain is activated on the BK5000 machine and if the Ultrasound Navigation module is activated in the Brainlab software before scanning. Also, check if a reasonable initial depth has been chosen to visualize the ROI.
3. Bring the transducer in the camera viewing field, keeping the reflective spheres pointing towards the camera as much as possible. Check if the software registers the transducer.
4. Place the transducer in the craniotomy and start orienting the area of interest, starting with either coronal or sagittal positioning of the transducer. Try keeping the transducer in one of these anatomical planes during the rest of the acquisition.

5. Try to locate the tumor and visualize it properly. The gain, focus and depth might need to be changed.
6. Once the tumor has been located and properly visualized, scanning should be started by pressing scan US in the Brainlab software:


7. Bring the transducer in a position capturing the outermost part of the tumor, with sufficient additional surrounding tissue. Important landmarks like ventricles and falx need to be taken into consideration.
8. Start scanning by pressing the transducer's button twice.
9. Move the transducer in a constant linear fashion during approx. 10 seconds, as shown in the figure below. The transducer will produce a sound while moving.
    a. While moving, point the tracking frame as much to the camera as possible.
    b. **Do not move** the transducer over the **same area twice.**


*Figure 3: Workflow US Volume Acquisition. Transducer is viewed from aside. The scanning plane aligns with the sagittal plane.*

10. Once done, press the button once.
11. The reconstruction will be checked for correctness. If an additional swipe is needed, please restart at step 7.
12. Time stamps are noted on the form to distinguish US1 from 2 and 3.

**End of acquisition and data export:**

1. The measured volumes are automatically saved along with the other imaging data.
2. The volumes need to be exported for further analysis.

## Appendix D: MRI acquisition protocol

The iMRI acquisition protocol consisted of four sequences for anatomical information, three T1 weighted sequences and one T2 weighted sequence. A magnetization-prepared rapid gradient-echo (MPRAGE) sequences is included for a wide field of view, acquiring the fiducials required for automatic registration. Then two sequences are included for anatomical purposes, with a higher resolution; one contrast enhanced and one without contrast. The contrast sequence is run last, allowing acquisition of scans without contrast.

T1-MPRAGE image is scanned with a wide field of view for Brainlab Automatic Registration

- TE = 2.165 ms
- TR = 4.63 ms
- FOV in voxel spacing: [352 352 250] with resolution of [0.99 0.99 1] results in FOV in mm spacing of 350 x 350 x 250 mm
- Flip angle 6 degrees

T1 MPRAGE normal

- TE 3.28 ms
- TR: 6.89 ms
- FOV in voxel spacing: [528 528 256] with resolution of [0.436 0.436 0.6] results in FOV in mm spacing of 230 x 230 x 150 mm
- Flip angle 6 degrees

T2 3D:

- TE 280 ms
- TR 3 s
- FOV in voxel spacing: [512 512 360] with resolution of [0.449 0.449 0.5] results in FOV in mm spacing of 230 x 230 x 180 mm
- Flip angle 90 degrees

T1 Gd C+:

- TE 3.295 ms
- TR 7.02 ms
- FOV in voxel spacing: [528 528 256] with resolution of [0.436 0.436 0.6] results in FOV in mm spacing of 230 x 230 x 150 mm
- Flip angle 6 degrees

# Form for Qualitative Assessment of Intraoperative Ultrasound Usage

Form to be filled out to assess surgical interpretation and additional value of ultrasound intraoperatively.
To be returned to K. Klein Gunnewiek | k.kleingunnewiek@prinsesmaximacentrum.nl

## General information:

**Initials Surgeon:** _____

**Date of surgery:** _____

**Patient Number:** _____

**Technical problems:**
☐ None ☐ Yes, namely:_____

## iUS1: 3D reconstruction of swipe **before** opening dura mater

Time stamp: ☐

Appearance of Tumor with Auto-gain enabled: ☐ Hyperechoic ☐ Iso-echoic ☐ Hypoechoic

Is the 3D reconstruction visually congruent with the preoperative imaging?

☐ Yes ☐ No Comments: _____

Informative in Navigation/ Localization of anatomical landmarks and tumor?

☐ Yes ☐ No Comments: _____

## *Optional*: iUS2B: 3D reconstruction of swipe(s) **during** resection process

Time stamps: ☐ ☐

Overall displacement of tissue creates: *Shrinkage/Expansion of cavity*

Showing tumor residual?

☐ Yes ☐ No Comments: _____

Informative in updating neuronavigation intraoperatively?

☐ Yes ☐ No Comments: _____

## iUS3: 3D reconstruction of swipe(s) **before every** iMRI scan session

Time stamps: ☐ ☐

Estimation of residual tumor percentage on iUS image(s): ____% (optional: ____%)

Identifiable artifacts?

☐ Yes ☐ No Comments: _____

Additional Comments: _____

## Appendix F: Example of fusion tree

The fusion tree describes the relationship between scans relative to one another. The check marks shows which scans are fused and which scan is a parent and which is a child. This visualizes the order and direction of transformation.

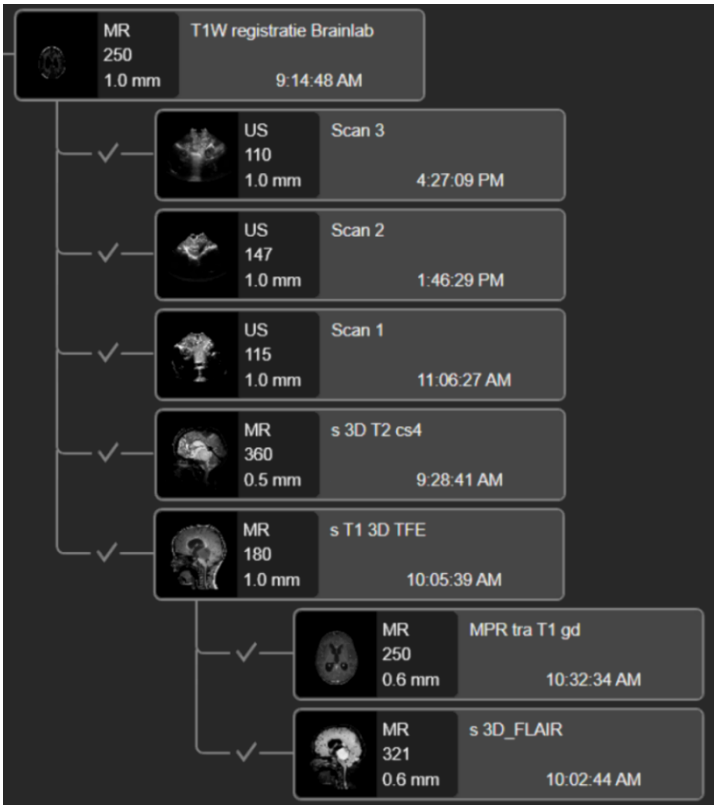

## Appendix G: Outlier in contrast ratio

The case below illustrates the outlier in the contrast ratio data. The lesion was hyperintense on both T1w images with and without contrast. However, it shows hypointensity of iUS images; suggesting that the lesion contains an oily-like substance.

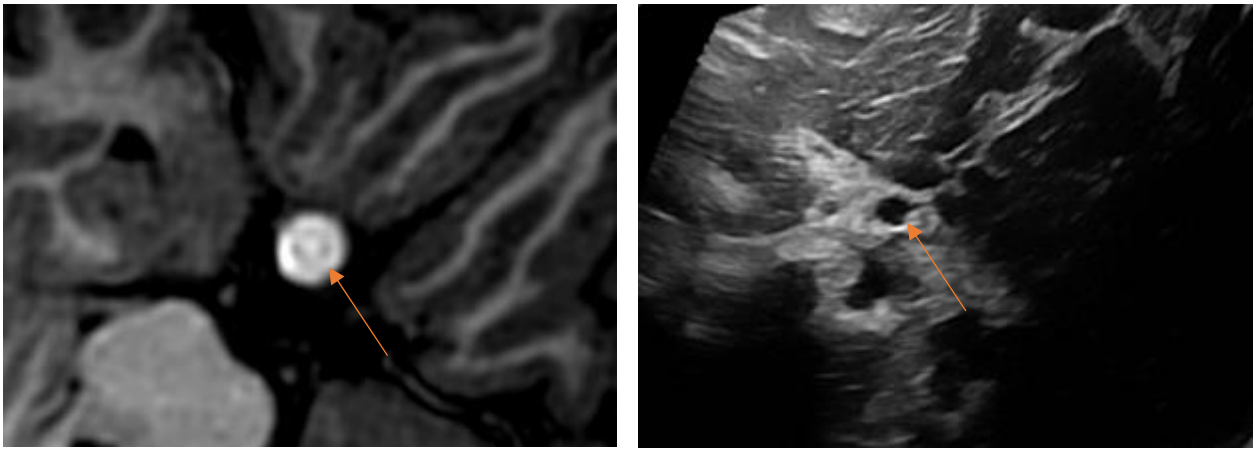

## Appendix H: Boxplot of DSC for corrected and uncorrected volumes

Due to fusion and registration errors, the positional information has not been saved correctly in four cases. A manual correction was done to align landmarks on both MRI and iUS. The group has been separately evaluated if the manual correction could have improved the overall DSC. The boxplots below show that the DSC that were found are within the range for uncorrected iUS1. For iUS3, the DSC range of the corrected (n=4) is lower than the uncorrected (n=3). This rejects the hypothesis that the correction has improved the DSC of the group as a whole.

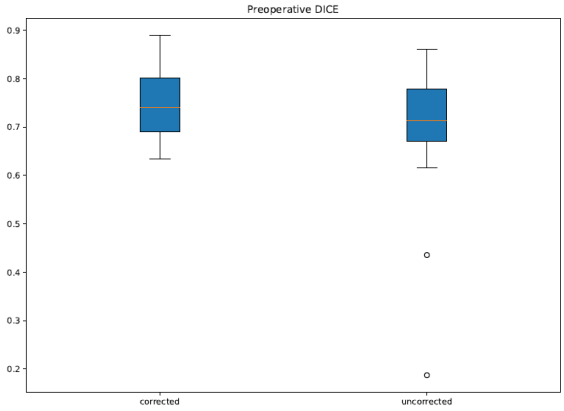


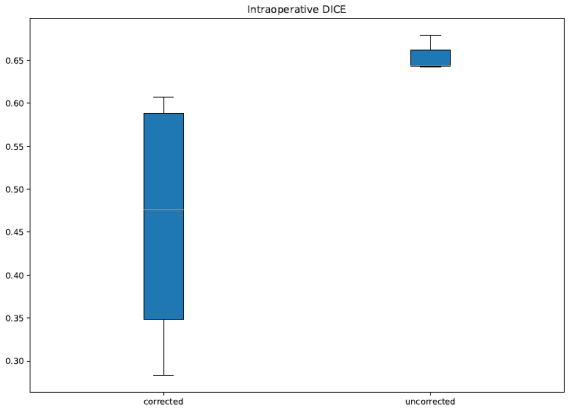

## Appendix J: Research proposal iUS

Below, different work packages are defined as new research directions to explore further usage of iUS. These draft ideas were to be used in writing a grant proposal, which was not further worked out during my M3 due to time constraints.

***Research Plan:***

*Workpackage 1: To determine the sensitivity and specificity of intraoperative ultrasound imaging compared to intraoperative MR imaging in detecting residual tumor volume.*

This research focusses on assessing the performance of iUS in identifying residual tumor tissue. Obtaining additional information regarding residual tumor may lead to safely increasing the extent of resection, therewith increasing prognostic benefits. iMRI is able to define residual tumor, however iUS could potentially reduce scanning time or be a substitute to MRI. In this research, before every iMRI scanning session, an iUS swipe will be acquired and the images will be fused and compared with the MR images regarding residual tumor. A volumetric comparison will be done in which DICE similarity measures and Hausdorf distances are quantitative measures. Besides, the images will be qualitatively assessed. The iUS images are interpreted by surgeon for tumor presence, the iMR images by the radiologist. This will create a dichotomous outcome, either tumor is present or not, allowing calculation of sensitivity and specificity of iUS compared to iMRI.

*Workpackage 2: To investigate the accuracy of US-based rigid patient-to-image registration and its qualitative benefits during resection procedure (especially posterior fossa)*

Fifty percent of pediatric brain tumors are located infratentorially, for which patients are positioned prone for surgery. In prone position, there are no anatomical landmarks easily visible for the optic tracking camera, which impedes registration based on surface matching. Since the conventional patient-to-image registration is difficult, the navigation is often discarded or not initialized. Automatic registration based on fixed fiducials scanned with iMRI is an alternative, however this method is time consuming and not widely accessible. Since navigation has shown to have major additional value in neurosurgery, another registration method is proposed in this research. By using navigated intraoperative ultrasound, the patient-to-image registration may be performed based on iUS imaging and its congruency with preoperative MRI. The performance will be assessed by comparison of iUS-based patient-to-image registration with iMRI-based patient-to-image registration. If the iUS-based registration shows to be sufficiently accurate in initializing the neuronavigation, iMRI automatic registration could be replaced in future for certain procedures.

*Workpackage 3: Diagnostic value of iUS and spatial accuracy of navigated iUS*

- *3A: To investigate the diagnostic value of iUS (B-mode in combination with elasto-sonography).*
- *3B: To determine the spatial accuracy of navigated iUS for localizing tumor compared to registered preoperative MRI (gold standard)*

While planning the surgical procedure and strategy, preoperative MR imaging is used by the surgeon. In the OR, neuronavigation can be additionally used to plan the craniotomy. However, any additional information regarding the tumor is only obtained when the tumor is revealed. iUS may inform the surgeon additionally about the location, size, morphology and pathology before opening of the dura. Additional information may change the surgical approach and goals, which could potentially optimize the surgical workflow. If additional iUS images show the location of the tumor reliably, the information can be used to determine surgical approach. Besides, obtaining information regarding the tumor type could change surgical resection goals. Before the dura is opened, an iUS swipe will be made to visualize the tumor. The echogenicity will be quantitatively determined by obtaining the mean and standard deviation of the relative intensity within the tumor tissue. Moreover, elasto-sonography will be used with the same approach to obtain mechanical tissue properties,

adding information to the echogenicity. Mechanical differences of tumor with tissue may visualize tumors that are iso-echogenic. Other more qualitative measures will be reported upon by the surgeons. These measures will be compared to the histopathological outcome. The correlation between echogenicity and histopathology will be assessed. Regarding spatial accuracy, the tumor will be segmented on both iMRI and iUS, and DICE coefficients and Hausdorff distances will be calculated to assess congruency.

*Workpackage 4:*

- *4A: To investigate whether arterial blood flow through the circle of Willis as measured by intraoperative Doppler US is correlated to cerebral perfusion as measured by Arterial Spin Labeling intraoperative MRI.*
- *4B: To investigate whether the intraoperative administration of papaverine changes the blood flow through the circle of Willis.*

During tumor debulking, manipulation of major cerebral arteries may result in vasospasms. This could cause local hypoperfusion and therewith increase the risk of postoperative complications. Obtaining additional information regarding cerebral perfusion may indicate if intraoperative administration of vasodilating agents might be necessary, or to change surgical approach. iUS doppler is a quick and easy applicable modality to measure flow and velocity in vessels, obtaining immediate information upon which the surgeon can act. Besides, the efficacy of vasodilating agents may be assessed by doppler US. The flow through the MCA or ACA will be measured right before every iMRI scanning session in which an ASL sequence is included. The correlation between flow doppler and ASL cerebral perfusion will be researched. Moreover, if papaverine is used as a vasodilating agent, the blood flow will be measured right before and after administration to quantify flow differences. If doppler shows to be predictive in estimating cerebral perfusion, the surgeon can use iUS to get a swift interpretation of the perfusion and act upon it.

*Workpackage 5: To develop an iUS-based elastic image registration algorithm.*

This workpackage will be researched in close collaboration with Brainlab AG. The institute will acquire and annotate data for Brainlab to develop a software package together which makes elastic image registration possible. Brain shift occurring during surgery, particularly in the posterior fossa region, decreases the navigational accuracy. A method for updating the navigation is by rigid transformation of the imaging data. However, this does not take the non-linear deformations into account, resulting in less precise navigation correction. Elastic deformation can overcome this problem by transforming the images locally to update to the most recent situation. Collapse of the soft brain tissue due to fluid leakage, gravitational forces and tumor debulking results in non-linear shift. It would be ideal if the scans could be locally adjusted for the differences compared to the preoperative setting.

*Workpackage 6: To evaluate the impact of technical innovations in the OR on the mental workload of the surgeon.*

In recent years, numerous novel techniques have been added to the neurosurgical armamentarium. Adding new tools also requires additional knowledge and also is an investment of time to truly understand the application of the techniques. If techniques are not applied correctly or are not well-understood, they could become a burden on the surgical processes and impede the workflow. In this case the additional time, therapeutic or economic benefits will not be experienced and surgeons may tend to work around the techniques, while trying to achieve the surgical goal. In this workpackage we would like to research the impact of adding highly complex techniques in a highly complex surgical environment on the surgical workflow. The workflow might be impeded when the techniques pose a major weight on the mental workload of the surgeon. These results will be evaluated with questionnaires which assess the user-experience and the mental workload of the surgeon during a surgical procedure. Hopefully, this will provide new insights in how to implement and integrate new technical innovations in a highly complex environment, which might impact the way in which new techniques are handled in practice.